

Figure 13.31 An illustration of a possible backscatter plot from a fiber under test [Ref. 76].

A number of optical time domain reflectometers are commercially available for operation both in the shorter and longer wavelength regions. The former instruments emit a series of short (10 to 100 ns), intense optical pulses (100 to 500 mW) from which the backscattered light is received, analysed and displayed on an oscilloscope, or plotted on a chart recorder. A typical example of a high performance OTDR is shown in Figure 13.32. This flexible instrument employs plug-in units to enable it to operate in both the longer wavelength region (at 1.31 μm and 1.55 μm), as well as the shorter wavelength window (0.85 μm). The longer wavelength units produce pulse widths in the range 100 ns to 10 μs , the latter pulses providing one-way dynamic ranges of 34 dB and 30 dB at wavelengths of 1.31 μm and 1.55 μm respectively. Hence, when using the device with low loss single-mode fiber, measurements can be made at distance in excess of 150 km with a resolution of up to 10 cm. It must be noted, however, that the accuracy of these distance measurements is around ± 1 m.

A number of themes have been pursued over recent years in relation to OTDR performance. These include the enlargement of the device dynamic range, the enhancement of the device resolution, the reduction of noise levels intrinsic to

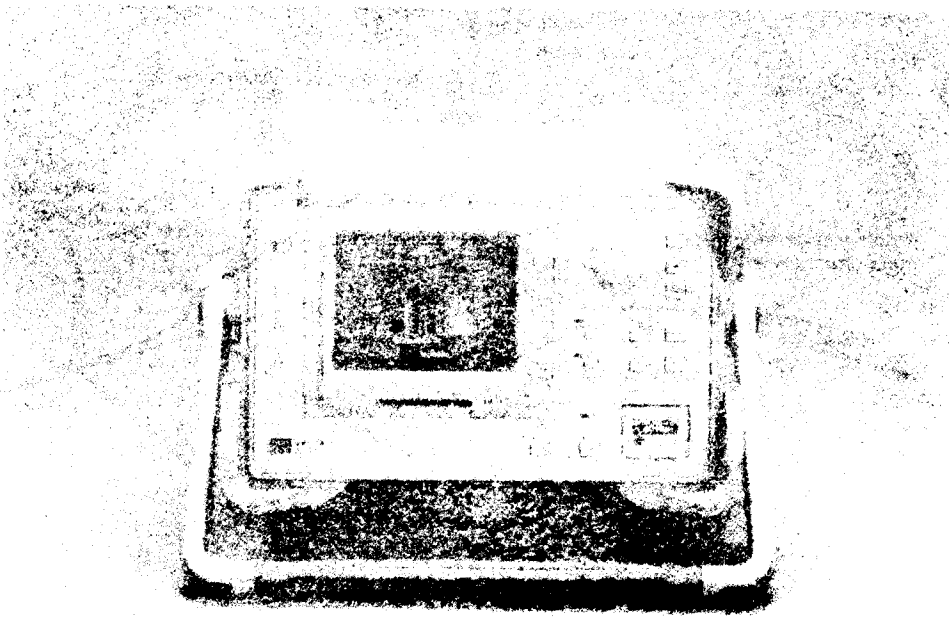


Figure 13.32 The Anritsu MW9040A optical time domain reflectometer. Courtesy of Anritsu Europe Limited.

single-mode fibers and the increase in the user friendliness of the equipment [Ref. 80]. Significant improvements have been obtained in the former two device performance characteristics with a range of strategies including the use of higher input optical power levels, decreasing the minimum detectable optical power and employing narrower pulse widths.

For example, one strategy which has proved successful is the use of a photon counting technique [Ref. 81] in which the backscattered photons are detected digitally. In this method the avalanche photodiode is operated in a Geiger tube breakdown mode [Ref. 82] by biasing the device above its normal operating voltage where it can detect a single photon. The photon counting technique has demonstrated significantly improved receiver sensitivity (i.e. -7 dB) than the best analog system at a wavelength of $1.3 \mu\text{m}$. Moreover, a resolution of up to 1.5 cm with high sensitivity (3×10^{-10} W) has been reported when operating at a wavelength of $0.85 \mu\text{m}$ using a single photon detecting APD at room temperature [Ref. 83].

Single-mode fiber OTDRs exhibit an additional problem over multimode devices, namely, polarization noise. In general, the state of polarization of the backscattered light differs from that of the laser pulse coupled into the fiber at the input end and is dependent on the distance of the backscattering fiber element from the input fiber

end. This results in an amplitude fluctuation in the backscattered light known as polarization noise. Interestingly, this same phenomenon can be employed to measure the evolution of the polarization in the fiber with the so-called polarization optical time domain reflectometer (POTDR) [Ref. 43]. However, in a conventional single-mode OTDR reduction of the polarization noise is necessary using a polarization independent acousto-optic deflector (see Section 10.6.2) or, more usually, a polarization scrambler [Ref. 80].

Problems

13.1 Describe what is meant by 'equilibrium mode distribution' and 'cladding mode stripping' with regard to transmission measurements in optical fibers. Briefly outline methods by which these conditions may be achieved when optical fiber measurements are performed.

13.2 Discuss with the aid of a suitable diagram the cut-back technique used for the measurement of the total attenuation in an optical fiber. Indicate the differences in the apparatus utilized for spectral loss and spot attenuation measurement.

A spot measurement of fiber attenuation is performed on a 1.5 km length of optical fiber at a wavelength of 1.1 μm . The measured optical output power from the 1.5 km length of fiber is 50.1 μW . When the fiber is cut back to a 2 m length, the measured optical output power is 385.4 μW . Determine the attenuation per kilometre for the fiber at a wavelength of 1.1 μm .

13.3 Briefly outline the principle behind the calorimetric methods used for the measurement of absorption loss in optical fibers.

A high absorption optical fiber was used to obtain the plot of $(T_\infty - T_t)$ (on a logarithmic scale) against time shown in Figure 13.33(a). The measurements were achieved using a calorimeter and thermocouple experimental arrangement. Subsequently, a different test fiber was passed three times through the same

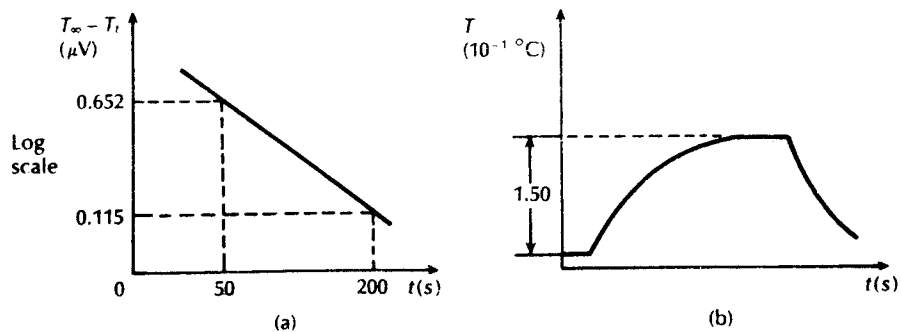


Figure 13.33 Fiber absorption for measurements for Problem 13.3: (a) plot of $(T_\infty - T_t)$ against time for a high absorption fiber; (b) the heating and cooling curve for the test fiber.

calorimeter before further measurements were taken. Measurements on the test fiber produced the heating and cooling curve shown in Figure 13.33(b) when a constant 76 mW of optical power, at a wavelength of 1.06 μm , was passed through it. The constant C for the experimental arrangement was calculated to be $2.32 \times 10^4 \text{ J }^\circ\text{C}^{-1}$. Calculate the absorption loss in decibels per kilometre, at a wavelength of 1.06 μm , for the fiber under test.

- 13.4** Discuss the measurement of fiber scattering loss by describing the use of two common scattering cells.

A Nd:YAG laser operating at a wavelength of 1.064 μm is used with an integrating sphere to measure the scattering loss in an optical fiber sample. The optical power propagating within the fiber at the sphere is 98.45 μW and 5.31 nW of optical power is scattered within the sphere. The length of fiber in the sphere is 5.99 cm. Determine the optical loss due to scattering for the fiber at a wavelength of 1.064 μm in decibels per kilometre.

- 13.5** Fiber scattering loss measurements are taken at a wavelength of 0.75 μm using a solar cell cube. The reading of the input optical power to the cube is 7.78 V with a gain setting of 10^5 . The corresponding reading from the scattering cell which incorporates a 4.12 cm length of fiber is 1.56 V with a gain setting of 10^9 . Previous measurements of the total fiber attenuation at a wavelength of 0.75 μm gave a value of 3.21 dB km⁻¹. Calculate the absorption loss for the fiber at a wavelength of 0.75 μm in decibels per kilometre.

- 13.6** Discuss with the aid of suitable diagrams the measurement of dispersion in optical fibers. Consider both time and frequency domain measurement techniques.

Pulse dispersion measurements are taken on a multimode graded index fiber in the time domain. The 3 dB width of the optical output pulses from a 950 m fiber length is 827 ps. When the fiber is cut back to a 2 m length the 3 dB width of the optical output pulses becomes 234 ps. Determine the optical bandwidth for a kilometre length of the fiber assuming Gaussian pulse shapes.

- 13.7** Pulse dispersion measurements in the time domain are taken on a multimode and a single-mode step index fiber. The results recorded are:

	Input pulse width (3 dB)	Output pulse width (3 dB)	Fiber length (km)
(a) Multimode fiber	400 ps	31.20 ns	1.13
(b) Single-mode fiber	200 ps	425 ps	2.35

Calculate the optical bandwidth over 1 kilometre for each fiber assuming Gaussian pulse shapes.

- 13.8** Compare and contrast the major techniques employed to obtain a measurement of the refractive index profile for an optical fiber. In particular suggest reasons why the refracted near field method has been adopted as the reference test method by the EIA.
- 13.9** The fraction of light reflected at an air-fiber interface r can be obtained from the Fresnel formulae of Eq. (5.1) and for small changes in refractive index:

$$\frac{\delta r}{r} = \left(\frac{4}{n_1^2 - 1} \right) \delta n_1$$

where n_1 is the fiber core refractive index at the point of reflection. Show that the fractional change in the core refractive index $\delta n_1/n_1$ may be expressed in terms of the

fractional change in the reflection coefficient $\delta r/r$ following:

$$\frac{\delta n_1}{n_1} = \left(\frac{r^2}{1-r} \right) \frac{\delta r}{r}$$

Hence, show that for a step index fiber with n_1 of 1.5, a 5% change in r corresponds to only a 1% change in n_1 .

- 13.10** Describe, with the aid of suitable diagrams, the reference test methods which are utilized to determine the effective cutoff wavelength in single-mode fiber.
- 13.11** Compare and contrast two simple techniques used for the measurement of the numerical aperture of optical fibers.

Numerical aperture measurements are performed on an optical fiber. The angular limit of the far field pattern is found to be 26.1° when the fiber is rotated from a centre zero point. The far field pattern is then displayed on a screen where its size is measured as 16.7 cm. Determine the numerical aperture for the fiber and the distance of the fiber output end face from the screen.

- 13.12** Describe, with the aid of a suitable diagram, the shadow method used for the on-line measurement of the outer diameter of an optical fiber.

The shadow method is used for the measurement of the outer diameter of an optical fiber. A fiber outer diameter of $347 \mu\text{m}$ generates a shadow pulse of $550 \mu\text{s}$ when the rotating mirror has an angular velocity of 3 rad s^{-1} . Calculate the distance between the rotating mirror and the optical fiber.

- 13.13** Define the mode-field diameter (MFD) in a single-mode fiber and indicate how this parameter relates to the spot size.

Discuss the techniques which are commonly employed to measure the MFD by either direct or indirect methods. Comment on their relative attributes and drawbacks.

- 13.14** Outline the major design criteria of an optical fiber power meter for use in the field. Suggest any problems associated with field measurements using such a device.

Convert the following optical power meter readings to numerical values of power: 25 dBm, -5.2 dBm , $3.8 \text{ dB}\mu$.

- 13.15** Describe what is meant by optical time domain reflectometry. Discuss how the technique may be used to take field measurements on optical fibers. Indicate the advantages of this technique over other measurement methods to determine attenuation in optical fibers.

A backscatter plot for an optical fiber link provided by OTDR is shown in Figure 13.34. Determine:

- (a) the attenuation of the optical link for the regions indicated *A*, *B* and *C* in decibels per kilometre.
- (b) the insertion loss of the joint at the point *X*.

- 13.16** Discuss the sensitivity of OTDR in relation to commercial reflectometers. Comment on an approach which may lead to an improvement in the sensitivity of this measurement technique.

The Rayleigh scattering coefficient for a silica single-mode step index fiber at a wavelength of $0.80 \mu\text{m}$ is 0.46 km^{-1} . The fiber has a refractive index of 1.6 and a numerical aperture of 0.14. When a light pulse of 60 ns duration at a wavelength of $0.80 \mu\text{m}$ is launched into the fiber, calculate the level in decibels of the backscattered light compared with the Fresnel reflection from a clean break in the fiber. It may be assumed that the fiber is surrounded by air.

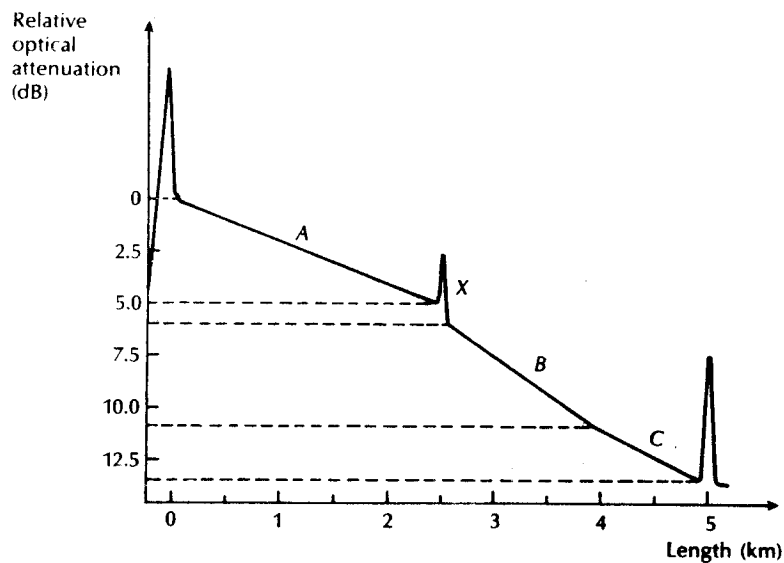


Figure 13.34 The backscatter plot for the optical link of Problem 13.15.

Answers to numerical problems

- | | | | |
|------|------------------------------------|-------|--|
| 13.2 | 5.92 dB km ⁻¹ | 13.11 | 0.44, 17.0 cm |
| 13.3 | 1.77 dB km ⁻¹ | 13.12 | 21.0 cm |
| 13.4 | 3.91 dB km ⁻¹ | 13.14 | 316.2 mW, 302 μW, 2.40 μW |
| 13.5 | 1.10 dB km ⁻¹ | 13.15 | (a) 2.0 dB km ⁻¹ , 3.0 dB km ⁻¹ ,
2.5 dB km ⁻¹ ; |
| 13.6 | 525.9 MHz km | | (b) 1.0 dB |
| 13.7 | (a) 15.9 MHz km,
(b) 7.3 GHz km | 13.16 | -37.3 dB |
| 13.9 | 1.0% | | |

References

- [1] CCITT. Recommendation G.652, 'Characteristics of a single-mode fiber cable', CCITT document Fascicle III.2, pp. 272–291, 1986.
- [2] M. Tateda, T. Horiguchi, M. Tokuda and N. Uchida, 'Optical loss measurement in graded index fiber using a dummy fiber', *Appl. Opt.*, **18**(19), pp. 3272–3275, 1979.
- [3] M. Eve, A. M. Hill, D. J. Malyon, J. E. Midwinter, B. P. Nelson, J. R. Stern and J. V. Wright, 'Launching independent measurements of multimode fibres', *2nd European Conference on Optical Fiber Communication* (Paris), pp. 143–146, 1976.
- [4] M. Ikeda, Y. Murakami and C. Kitayama. 'Mode scrambler for optical fibres' *Appl. Opt.*, **16**(4), pp. 1045–1049, 1977.

- [5] S. Seikai, M. Tokuda, K. Yoshida and N. Uchida, 'Measurement of baseband frequency response of multimode fibre by using a new type of mode scrambler', *Electron. Lett.*, **13**(5), pp. 146–147, 1977.
- [6] F. P. Kapron, 'Fiber-optic test methods', in *Fiber Optics Handbook for Engineers and Scientists*, F. C. Allard (Ed.), McGraw-Hill, pp. 4.1–4.54, 1990.
- [7] FOTP-50. Light launch conditions for long length graded-index optical fiber spectral attenuation measurements.
- [8] J. P. Dakin, W. A. Gambling and D. N. Payne, 'Launching into glass-fibre waveguide', *Opt. Commun.*, **4**(5), pp. 354–357, 1972.
- [9] FOTP-46. Spectral attenuation measurement for long-length graded-index optical fibers.
- [10] FOTP-78. Spectral attenuation cutback measurement for single-mode fibers.
- [11] FOTP-53. Attenuation by substitution measurement – for multimode graded-index optical fibers or fiber assemblies used in long length communication systems.
- [12] K. I. White, 'A calorimetric method for the measurement of low optical absorption losses in optical communication fibres', *Opt. Quantum Electron.*, **8**, pp. 73–75, 1976.
- [13] K. I. White and J. E. Midwinter, 'An improved technique for the measurement of low optical absorption losses in bulk glass', *Opto-electronics*, **5**, pp. 323–334, 1973.
- [14] A. R. Tynes, 'Integrating cube scattering detector', *Appl. Opt.*, **9**(12), pp. 2706–2710, 1970.
- [15] F. W. Ostermayer and W. A. Benson, 'Integrating sphere for measuring scattering loss in optical fiber waveguides', *Appl. Opt.*, **13**(8), pp. 1900–1905, 1974.
- [16] S. de Vito and B. Sordo, 'Misura di attenuazione e diffusione in fibre ottiche multimodo', *LXXV Riunione AEI*, Rome, 15–21 Sept. 1974.
- [17] J. P. Dakin, 'A simplified photometer for rapid measurement of total scattering attenuation of fibre optical waveguides', *Opt. Commun.*, **12**(1), pp. 83–88, 1974.
- [18] L. G. Cohen, P. Kaiser and C. Lin, 'Experimental techniques for evaluation of fiber transmission loss and dispersion', *Proc. IEEE*, **68**(10), pp. 1203–1208, 1980.
- [19] S. D. Personick, 'Baseband linearity and equalization in fiber optic digital communication systems', *Bell Syst. Tech. J.*, **52**(7), pp. 1175–1194, 1973.
- [20] D. Gloge, E. L. Chinnock and T. P. Lee, 'Self pulsing GaAs laser for fiber dispersion measurement', *IEEE J. Quantum Electron.*, **QE-8**, pp. 844–846, 1972.
- [21] FOTP-51. Pulse distortion measurement of multimode glass fiber information transmission capacity.
- [22] F. Krahn, W. Meininghaus and D. Rittich, 'Measuring and test equipment for optical cable', *Phillips Telecomm. Rev.*, **37**(4), pp. 241–249, 1979.
- [23] FOTP-168. Chromatic dispersion measurement of multimode graded-index and single-mode optical fibers by spectral group delay measurement in the time domain.
- [24] I. Kokayashi, M. Koyama and K. Aoyama, 'Measurement of optical fibre transfer functions by swept frequency technique and discussion of fibre characteristics', *Electron. Commun. Jpn*, **60-C**(4), pp. 126–133, 1977.
- [25] FOTP-30. Frequency domain measurement of multimode optical fiber information transmission capacity.
- [26] FOTP-169. Chromatic dispersion measurement of single-mode fibers by phase-shift method.
- [27] W. E. Martin, 'Refractive index profile measurements of diffused optical waveguides', *Appl. Opt.*, **13**(9), pp. 2112–2116, 1974.

- [28] H. M. Presby, W. Mammel and R. M. Derosier, 'Refractive index profiling of graded index optical fibers', *Rev. Sci. Instr.*, **47**(3), pp. 348–352, 1976.
- [29] B. Costa and G. De Marchis, 'Test methods (optical fibres)', *Telecomm. J. (Engl. Ed.) Switzerland*, **48**(11), pp. 666–673, 1981.
- [30] L. C. Cohen, P. Kaiser, J. B. MacChesney, P. B. O'Conner and H. M. Presby, 'Transmission properties of a low-loss near-parabolic-index fiber', *Appl. Phys. Lett.*, **26**(8), pp. 472–474, 1975.
- [31] L. C. Cohen, P. Kaiser, P. D. Lazay and H. M. Presby, 'Fiber characterization', in S. E. Miller and A. G. Chynoweth (Eds.), *Optical Fiber Telecommunications*, pp. 343–400, Academic Press, 1979.
- [32] M. E. Marhic, P. S. Ho and M. Epstein, 'Nondestructive refractive index profile measurement of clad optical fibers', *Appl. Phys. Lett.*, **26**(10), pp. 574–575, 1975.
- [33] P. L. Chu, 'Measurements in optical fibres', *Proc. IEEE Australia*, **40**(4), pp. 102–114, 1979.
- [34] M. J. Adams, D. N. Payne and F. M. E. Sladen, 'Correction factors for determination of optical fibre refractive-index profiles by near-field scanning techniques', *Electron. Lett.*, **12**(11), pp. 281–283, 1976.
- [35] FOTP-43. Output near-field radiation pattern measurement of optical waveguide fibers.
- [36] A. J. Ritger, 'Bandwidth improvement in MCVD multimode fibers by fluorine etching to reduce centre dip', *Eleventh European Conf. on Optical Commun.*, pp. 913–916, 1985.
- [37] F. E. M. Sladen, D. N. Payne and M. J. Adams, 'Determination of optical fibre refractive index profile by near field scanning technique', *Appl. Phys. Lett.*, **28**(5), pp. 255–258, 1976.
- [38] K. W. Raine, J. G. N. Baines and D. E. Putland, 'Refractive index profiling – state of the art', *J. of Lightwave Technol.*, **7**(8), pp. 1162–1169, 1989.
- [39] FOTP-44. Refractive index profile, refracted ray method.
- [40] A. H. Cherin, *An Introduction to Optical Fibers*, McGraw-Hill, 1983.
- [41] K. I. White 'Practical application of the refracted near-field technique for the measurement of optical fiber refractive index profiles', *Opt. and Quantum Electron.*, **11**(2), pp. 185–196, 1979.
- [42] W. J. Stewart, 'Optical fiber and preform profiling technology', *J. of Quantum Electron.*, **QE-18**(10), pp. 1451–1466, 1982.
- [43] E.-G. Neuman, *Single-Mode Fibers: Fundamentals*, Springer-Verlag, 1988.
- [44] D. B. Payne, M. H. Reeve, C. A. Millar and C. J. Todd, 'Single-mode fiber specification and system performance', *Symp. Opt. Fiber Meas. NBS spec. publ.*, **683**, pp. 1–5, 1984.
- [45] FOTP-80. Cutoff wavelength of uncabled single-mode fiber by transmitted power.
- [46] R. Srivastava and D. L. Franzen, 'Single-mode optical fiber characterization', *National Bureau of Standards Report*, pp. 1–101, July 1985.
- [47] D. L. Franzen, 'Determining the effective cutoff wavelength of single-mode fibers: an interlaboratory comparison', *J. of Lightwave Technol.*, **LT-3**, pp. 128–134, 1985.
- [48] C. A. Millar, 'Comment: fundamental mode spot-size measurement in single-mode optical fibers', *Electron. Lett.*, **18**, pp. 395–396, 1982.
- [49] FOTP-170. Cable cutoff wavelength of single-mode fiber by transmitted power.
- [50] FOTP-177. Numerical aperture of graded-index optical fiber.
- [51] D. L. Franzen, M. Young, A. H. Cherin, E. D. Head, M. J. Hackert, K. W. Raine

- and J. G. N. Baines, 'Numerical aperture of multimode fibers by several methods: resolving differences', *J. of Lightwave Technol.*, **7**(6), pp. 896-901, 1989.
- [52] W. A. Gambling, D. N. Payne and H. Matsumura, 'Propagation studies on single-mode phosphosilicate fibres' *2nd European Conference on Optical Fiber Communication* (Paris), pp. 95-100, 1976.
- [53] F. T. Stone, 'Rapid optical fibre delta measurement by refractive index tuning', *Appl. Opt.*, **16**(10), pp. 2738-2742, 1977.
- [54] L. G. Cohen and P. Glynn, 'Dynamic measurement of optical fibre diameter', *Rev. Sci. Instrum.*, **44**(12), pp. 1745-1752, 1973.
- [55] H. M. Presby, 'Refractive index and diameter measurements of unclad optical fibres', *J. Opt. Soc. Am.*, **64**(3), pp. 280-284, 1974.
- [56] P. L. Chu, 'Determination of diameters and refractive indices of step-index optical fibres', *Electron. Lett.*, **12**(7), pp. 150-157, 1976.
- [57] H. M. Presby and D. Marcuse, 'Refractive index and diameter determinations of step index optical fibers and preforms', *Appl. Opt.*, **13**(12), pp. 2882-2885, 1974.
- [58] D. Smithgall, L. S. Wakins and R. E. Frazee, 'High-speed noncontact fibre-diameter measurement using forward light scattering', *Appl. Opt.*, **16**(9), pp. 2395-2402, 1977.
- [59] FOTP-58. Core diameter measurement of graded-index optical fibers.
- [60] M. Artiglia, G. Coppa, P. DiVita, M. Potenza and A. Sharma, 'Mode field diameter measurements in single-mode optical fibers', *J. of Lightwave Technol.*, **7**(8), pp. 1139-1152, 1989.
- [61] FOTP-165. Single-mode fiber, measurement of mode field diameter by near-field scanning.
- [62] FOTP-164. Single-mode fiber, measurement of mode field diameter by far-field scanning.
- [63] K. Petermann, 'Constraints for the fundamental mode spot size for broadband dispersion-compensated single-mode fibres', *Electron. Lett.*, **19**, pp. 712-714, 1983.
- [64] FOTP-167. Mode field diameter measurement-variable aperture in the far field.
- [65] FOTP-174. Mode field diameter of single-mode optical fiber by knife-edge scanning in the far field.
- [66] J. Streckert, 'New method for measuring the spot size of single-mode fibers', *Opt. Lett.*, **5**, pp. 505-506, 1980.
- [67] M. L. Dakss, 'Optical-fiber measurements', in E. E. Basch (Ed.), *Optical-Fiber Transmission*, H. W. Sams & Co., pp. 133-178, 1987.
- [68] J. Streckert, 'A new fundamental mode spot size definition usable for non-Gaussian and noncircular field distributions', *J. of Lightwave Technol.*, **LT-3**, pp. 328-331, 1985.
- [69] FOTP-107. Return loss.
- [70] F. Krahn, W. Meininghaus and D. Rittich, 'Field and test measurement equipment for optical cables', *Acta Electronica*, **23**(3), pp. 269-275, 1979.
- [71] R. Olshansky, M. G. Blankenship and D. B. Keck, 'Length-dependent attenuation measurements in graded-index fibres', *Proceedings of 2nd European Conference on Optical Communication* (Paris), pp. 111-113, 1976.
- [72] M. K. Barnoski and S. M. Jensen, 'Fiber waveguides: a novel technique for investigating attenuation characteristics', *Appl. Opt.*, **15**(9), pp. 2112-2115, 1976.
- [73] S. D. Personick, 'Photon probe, an optical fibre time-domain reflectometer', *Bell Syst. Tech. J.*, **56**(3), pp. 355-366, 1977.

834 *Optical fiber communications: principles and practice*

- [74] E. G. Newman, 'Optical time domain reflectometer: comment', *Appl. Opt.*, **17**(11), p. 1675, 1978.
- [75] M. K. Barnoski and S. D. Personick, 'Measurements in fiber optics', *Proc. IEEE*, **66**(4), pp. 429–440, 1978.
- [76] J. D. Archer, *Manual of Fibre Optics Communication*, STC Components Group, UK, 1981.
- [77] FOTP-59. Measurement of fiber point defects using an OTDR.
- [78] FOTP-60. Measurement of fiber or cable length using an OTDR.
- [79] FOTP-61. Measurement of fiber or cable attenuation using an OTDR.
- [80] M. Tateda and T. Horiguchi, 'Advances in optical time-domain reflectometry', *J. of Lightwave Technol.*, **7**(8), pp. 1217–1224, 1989.
- [81] P. Healey, 'Optical time domain reflectometry by photon counting', *6th European Conference on Optical Communication* (UK), pp. 156–159, 1980.
- [82] P. P. Webb *et al.*, 'Single photon detection with avalanche photodiodes', *Bull. Am. Phys. Soc. II*, **15**, p. 813, 1970.
- [83] C. G. Bethea, B. F. Levine, S. Cova and G. Ripamonti, 'High-resolution, high sensitivity optical time-domain reflectometer', *Opt. Lett.*, **13**(3), pp. 233–235, 1988.

Applications and future developments

- 14.1 Introduction
 - 14.2 Public network applications
 - 14.3 Military applications
 - 14.4 Civil, consumer and industrial applications
 - 14.5 Optical sensor systems
 - 14.6 Computer applications
 - 14.7 Local area networks
- References
-

14.1 Introduction

In order to appreciate the many areas in which the application of lightwave transmission via optical fibers may be beneficial, it is useful to review the advantages and special features provided by this method of communication. The primary advantages obtained using optical fibers for line transmission were discussed in Section 1.3 and may be summarized as follows:

- (a) enormous potential bandwidth;
- (b) small size and weight;
- (c) electrical isolation;
- (d) immunity to interference and crosstalk;
- (e) signal security;

- (f) low transmission loss;
- (g) ruggedness and flexibility;
- (h) system reliability and ease of maintenance;
- (i) potential low cost.

Although this list is very impressive, it is not exhaustive and several other attributes associated with optical fiber communications have become apparent as the technology has developed. Perhaps the most significant are the reduced power consumption exhibited by optical fiber systems in comparison with their metallic cable counterparts and their ability to provide for an expansion in the system capability, often without fundamental and costly changes to the system configuration. For instance, a system may be upgraded by simply changing from an LED to an injection laser source, by replacing a $p-i-n$ photodiode with an APD detector, or alternatively by operating at a longer wavelength without replacing the fiber cable.

The use of fibers for optical communication does have some drawbacks in practice. Hence to provide a balanced picture these disadvantages must be considered. They are:

- (a) the fragility of the bare fibers;
- (b) the small size of the fibers and cables which creates some difficulties with splicing and forming connectors;
- (c) some problems involved with forming low loss T-couplers;
- (d) some doubt in relation to the long-term reliability of optical fibers in the presence of moisture (effects of stress corrosion – see Section 4.7);
- (e) an independent electrical power feed is required for any electronic repeaters;
- (f) new equipment and field practices are required;
- (g) testing procedures tend to be more complex.

A number of these disadvantages are not just inherent in optical fiber systems but are always present at the introduction of a new technology. Furthermore, both continuing developments and experience with optical fiber systems are generally reducing the other problems.

The combination of the numerous attributes and surmountable problems makes optical fiber transmission a very attractive proposition for use within national and international telecommunication networks (PTT applications). To date applications for optical fiber systems in this area have proved the major impetus for technological developments in the field. The technology has progressed from what may be termed first generation systems using multimode step index fiber and operating in the shorter wavelength region (0.8 to 0.9 μm), to second generation systems utilizing multimode graded index fiber operating in both the shorter and longer wavelength regions (0.8 to 1.6 μm). Furthermore, fully engineered third generation systems incorporating single-mode fiber predominantly for operation in the longer wavelength region (1.1 to 1.6 μm) have been installed and are operating in the public telecommunications network. In addition many alternative fiber

systems applications have become apparent in other areas of communications where often first and second generation systems provide an ideal solution. Also the growing utilization of optical fiber systems has stimulated tremendous research efforts towards enhanced fiber design. This has resulted in improvement of the associated optoelectronics as well as investigation of 'passive' optics which are likely to provide an advance in the current 'state of the art' of optical fiber communications together with an expansion in its areas of use. Hence, what may be termed fourth generation systems are already close to realization being concerned with both coherent transmission (see Chapter 12) and integrated optics (see Sections 10.5 to 10.9) The potential for fifth generation systems is also apparent. For example, these could involve the development of fluoride glass fibers for very long-haul mid-infrared transmission (see Section 3.7) [e.g. Ref. 1] or the continuing advances in relation to soliton propagation [e.g. Ref. 2]. These latter investigations seek to utilize nonlinear pulse propagation in optical fibers to provide greatly increased channel capacity whilst exhibiting compatibility with integrated optical systems which function in a nonlinear environment.

In this chapter we consider current and potential applications of optical fiber communication systems together with some likely future developments. The discussion is primarily centred around application areas including the public network, military, civil, consumer and industrial which are dealt with in Sections 14.2 to 14.4.

This is followed in Section 14.5 with a description of the continuing developments associated with optical sensor systems which are becoming a major application area. Computer applications are then outlined in Section 14.6 prior to a more detailed discussion in Section 14.7 of the application and developments of optical fiber communications technology within the expanding field of local area networks.

14.2 Public network applications

The public telecommunications network provides a variety of applications for optical fiber communication systems. It was in this general area that the suitability of optical fibers for line transmission first made an impact. The current plans of the major PTT administrations around the world feature the installation of increasing numbers of optical fiber links as an alternative to coaxial and high frequency pair cable systems. In addition it is indicated [Ref. 3] that administrations have largely abandoned plans for millimetric waveguide transmission (see Section 1.1) in favour of optical fiber communications.

14.2.1 Trunk network

The trunk or toll network is used for carrying telephone traffic between major conurbations. Hence there is generally a requirement for the use of transmission systems which have a high capacity in order to minimize costs per circuit. The

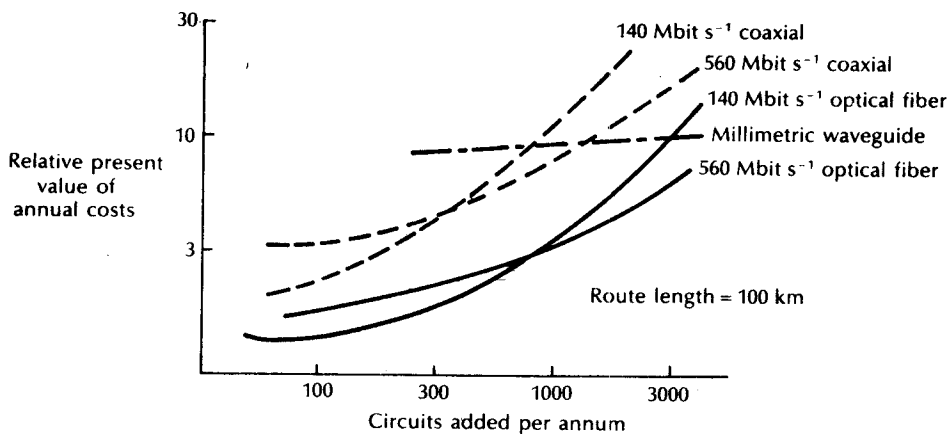


Figure 14.1 Relative present value cost comparison of different high capacity line transmission media. Reproduced with permission of the International Telecommunication Unit (ITU), Geneva, Switzerland, from C. J. Lilly, 'The application of optical fibers in the trunk network', *ITU Telecommunication Journal*, 49-11/1982, p. 109.

transmission distance for trunk systems can vary enormously from under 20 km to over 300 km, and occasionally to as much as 1000 km. Therefore transmission systems which exhibit low attenuation and hence give a maximum distance of unrepeated operation are the most economically viable. In this context optical fiber systems with their increased bandwidth and repeater spacings offer a distinct advantage. This may be observed from Figure 14.1 [Ref. 4] which shows a cost comparison of different high capacity line transmission media. It may be observed that optical fiber systems show a significant cost advantage over coaxial cable systems and compete favourably with millimetric waveguide systems at all but the highest capacities. It may also be noted that only digital systems are compared. This is due to the advent of the fully integrated digital public network which invariably means that the majority of trunk routes will employ digital transmission systems. The above media cost observations were confirmed by a more recent study [Ref. 5] which focuses on the interoffice or junction network (see Section 14.2.2). In this application area the use of twisted pair copper cable can prove more expensive than optical fiber.

The speed of operation of most digital trunk optical fiber systems is at present based on the principal digital hierarchies for Europe and North America which were shown in Table 11.1. Proprietary systems (where one contractor supplies the complete system in order to minimize interface problems) operating at 34 Mbit s⁻¹ and 140 Mbit s⁻¹ were installed in the trunk network in the UK on low and high growth rate trunk routes, respectively, in the late 1970s. In the main these systems operate in the 0.85 to 0.9 μm wavelength region using injection laser sources via graded index fiber to silicon APD detectors with repeater spacings of between 8 and

10 km. A typical system power budget for a 140 Mbit s^{-1} system operating over 8 km of multimode graded index fiber at a wavelength of $0.85 \mu\text{m}$ is shown in Table 14.1 [Ref. 6]. The mean power launched from the laser into the fiber may be improved by over 3 dB using lens coupling rather than the butt launch indicated.

High radiance LED sources emitting at $1.3 \mu\text{m}$ were also used with multimode graded index fiber in proprietary trunk systems operating at both 34 Mbit s^{-1} and 140 Mbit s^{-1} , most notably in a link between London and Birmingham which is 205 km in length. Field trials of single-mode fiber systems operating in the longer wavelength region demonstrated repeaterless transmission at 565 Mbit s^{-1} over 62 km at $1.3 \mu\text{m}$ and 140 Mbit s^{-1} over 91 km at $1.5 \mu\text{m}$ [Ref. 7]. These field trials were followed by the installation of proprietary long wavelength single-mode systems utilizing PIN-FET hybrid receivers between Luton and Milton Keynes, a distance of 27.3 km, and over 52 km between Liverpool and Preston [Ref. 8].

Subsequently the deployment of both 140 and 565 Mbit s^{-1} single-mode fiber systems has taken place in the UK trunk network at an operating wavelength of $1.3 \mu\text{m}$ and with repeater spacings in the range 30 to 60 km [Ref. 9, 10]. Together with the more recent deployment of 565 Mbit s^{-1} systems operating at $1.55 \mu\text{m}$, it meant that by 1990 some 70% of the UK long-haul traffic was conveyed by fiber systems [Ref. 11].

Typical optical power budgets for high performance 565 Mbit s^{-1} single-mode fiber systems operating at the 1.3 and $1.55 \mu\text{m}$ transmission wavelength are provided in Table 14.2. At the former wavelength a Fabry-Perot injection laser source is utilized, whilst a distributed feedback laser is employed at the $1.55 \mu\text{m}$ wavelength. In addition, the systems are considered using both $p-i-n$ photodiode and APD receivers where in the latter case the receiver sensitivity at both

Table 14.1 A typical optical power budget for a 140 Mbit s^{-1} trunk system operating over 8 km of multimode graded index fiber at a wavelength of $0.85 \mu\text{m}$

Mean power launched from the laser transmitter (butt coupling)	-4.5 dBm
APD receiver sensitivity at 140 Mbit s^{-1} (BER 10^{-9})	-48.0 dBm
Total system margin	43.5 dB
Cabled fiber loss ($8 \times 3 \text{ dB km}^{-1}$)	24.0 dB
Splice losses ($9 \times 0.3 \text{ dB each}$)	2.7 dB
Connector loss ($2 \times 1 \text{ dB each}$)	2.0 dB
Dispersion-equalization penalty	6.0 dB
Safety margin	7.0 dB
Total system loss	41.7 dB
Excess power margin	1.8 dB

Table 14.2 Optical power budgets for 565 Mbit s⁻¹ single-mode fiber trunk systems operating at 1.3 and 1.55 μm

Transmitter type	F-P laser 1.3 μm		DFB laser 1.55 μm	
	<i>p-i-n</i>	APD	<i>p-i-n</i>	APD
Receiver type				
Mean power launched from laser transmitter (dBm)	0	0	-3	-3
Receiver sensitivity (dBm)	-32	-39	-33	-40
Total system margin (dB)	32	39	30	37
Connector loss (2 \times 1 dB)	2	2	2	2
Penalties (dB)	3	3.5	3	3.5
Ageing and temperature margin (dB)	2	2.5	3	3.5
Design margin (dB)	3	3	3	3
Safety margin (dB)	5	5.5	6	6.5
Maximum repeater spacing (km)	55	70	95	125
Cabled fiber loss (dB km ⁻¹)	0.4	0.4	0.2	0.2
Total cable loss (dB)	22	28	19	25
Total system loss (dB)	32	39	30	37

wavelengths is increased by some 7 dB. The allocation for penalties does not just result from chromatic dispersion but also from laser chirp and extinction ratio penalties, together with reflection noise, jitter and component tolerances. Moreover, it may be observed that the safety margin is separated into an ageing and temperature component as well as a design margin to ensure satisfactory system performance. This latter factor should take account of any cable repairs required over the lifetime of the system operation.

The maximum repeater spacing (or unrepeated transmission distance) for each of the systems is given in bold in Table 14.2 which enables the total cabled fiber loss to be determined using the loss per kilometre figure. This latter parameter, which represents good quality silica fiber cable, also incorporates the splice losses. It may be observed that the total system losses correspond to the total system margins in all cases and hence excess power margins are not present. However, this is to be expected as the power budgets are calculated using the maximum repeater spacing. It is interesting to note that in the UK public network a 30 km unrepeated transmission distance is quite sufficient since it is the maximum spacing between existing surface stations and hence power feed points. This removes any requirement for the installation of a metallic conductor for power feed within the system, as well as allowing any repeaters to be installed above ground in a protected internal environment. Benefits gained include significantly reduced system costs along with additional reliability and ease of maintenance.

In the early 1980s the preferred transmission rate for multimode optical fiber

trunk systems based on the 1.5 Mbit s^{-1} digital hierarchy (i.e. North America) was 45 Mbit s^{-1} . This was largely due to the fact that much higher growth rates were required for the high speed systems operating at 274 Mbit s^{-1} and above. It was indicated [Ref. 12] that these high speed systems were more appropriate to very long-haul trunk routes (up to 6400 km) where repeater spacings in excess of 25 km were required. However, since 1984 there has been rapid deployment of single-mode fiber systems in the trunk network, typically operating at the $1.3 \mu\text{m}$ transmission wavelength with repeater spacings around 40 km and bit rates in the range 400 to 600 Mbit s^{-1} [Ref. 13]. This change was stimulated by the nearly two orders in magnitude in bit rate-distance product provided by these single-mode systems over the earlier 45 Mbit s^{-1} multimode fiber systems, together with their potential for substantial upgrade in the future. More recently, however, interest in North America has focused on the synchronous optical network developments discussed in Section 14.2.5.

Work is in progress in Europe, North America and Japan associated with the development of the advanced transmission techniques for IM/DD optical fiber systems described in Section 11.9 for use in trunk networks. Furthermore, the deployment of optical amplifiers in this area of the telecommunication network following the developments discussed in Section 11.10 is likely in the near future. In the longer term the incorporation of coherent optical systems within trunk networks would appear assured, in particular considering the field demonstrations outlined in Section 12.8. Nevertheless it must be noted that the coherent technology is still largely experimental and therefore its deployment may well be gradual rather than rapid, dictated by commercial considerations in relation to the benefits that may be obtained on specific routes.

14.2.2 Junction network

The junction or interoffice network usually consists of routes within major conurbations over distances of typically 5 to 20 km. However, the distribution of distances between switching centres (telephone exchanges) or offices in the junction network of large urban areas varies considerably for various countries as indicated in Figure 14.2 [Ref. 15]. It may be observed from Figure 14.2 that the benefits of long unrepeated transmission distances offered by optical fiber systems are not as apparent in the junction network due to the generally shorter link lengths. Nevertheless optical fiber junction systems are often able to operate using no intermediate repeaters whilst alleviating duct congestion in urban areas.

In Europe optical fiber systems with transmission rates of 8 Mbit s^{-1} , and for busy routes 34 Mbit s^{-1} , have found favour in the junction network. A number of proprietary systems predominantly operating at 8 Mbit s^{-1} using both injection laser and LED sources via multimode graded index fiber to APD detectors are in operation in the UK with repeater spacings between 7.5 and 12 km. A typical optical power budget for such a system operating at a wavelength of $0.88 \mu\text{m}$ over 12 km is shown in Table 14.3 [Ref. 6]. It may be noted that the mean power

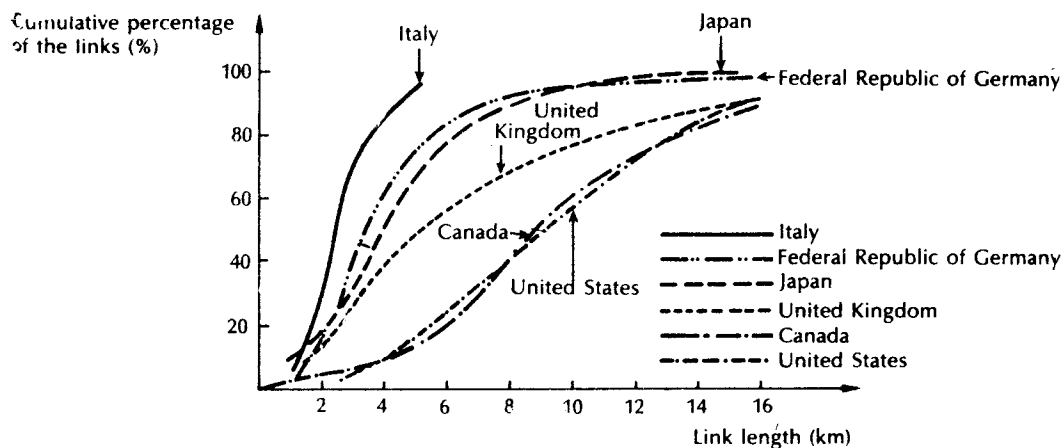


Figure 14.2 Distribution of distances between switching centres in metropolitan areas. Reproduced with permission of the International Telecommunications Union (ITU), Geneva, Switzerland, from O. Cottatelucci, F. Lombardi and G. Pellegrini, 'The Application of optical fibers in the junction network', *ITU Telecommunication Journal*, 49-11/1982, p. 101.

launched from the laser is reduced below the level obtained with similar dimensioned multimode graded index fiber in the optical power budget shown in Table 14.1. This is due to the lower duty factor when using a $2B3B$ code on the 8 Mbit s^{-1} system in comparison with a $7B8B$ code used on the 140 Mbit s^{-1} system (see Section 11.6.7).

Table 14.3 Typical optical power budget for a junction system operating at a wavelength of $0.88 \mu\text{m}$, a transmission rate of 8 Mbit s^{-1} and an unrepeated distance of 12 km

Mean power launched from the laser transmitter	-6.0 dBm
Receiver sensitivity at 8 Mbit s^{-1} and a wavelength of $0.88 \mu\text{m}$ (BER 10^{-9})	-63.0 dBm
Total system margin	57.0 dB
Cabled fiber loss ($12 \times 3.5 \text{ dB km}^{-1}$)	42.0 dB
Splice losses ($13 \times 0.3 \text{ dB}$)	3.9 dB
Connector losses ($2 \times 1 \text{ dB}$)	2.0 dB
Dispersion-equalization penalty	0 dB
Safety margin	7.0 dB
Total system loss	54.9 dB
Excess power margin	2.1 dB

In North America, 6 Mbit s^{-1} systems offer flexibility whereas 45 Mbit s^{-1} systems prove suitable for junction traffic requirements of crowded areas. However, economic studies for the United States have indicated that 45 Mbit s^{-1} systems are the most economic choice for the initial service [Ref. 15]. Hence a significant number of commercial 45 Mbit s^{-1} junction systems have been installed. These operate in the shorter wavelength region utilizing injection laser sources, multimode graded index fiber and APD detectors with repeater spacings up to 7.5 km. In addition, several experimental 32 Mbit s^{-1} junction systems have been in operation in Japan since 1980. These systems, which utilize both injection laser and LED sources to APD detectors, have repeater spacings up to 21 km.

Since 1986 PTTs and telephone companies have been installing single-mode fiber in the junction network. This is particularly the case in the United Kingdom and North America [Ref. 16]. These systems using single-mode injection lasers operating at $1.3 \mu\text{m}$ where the fiber attenuation is in the range 0.4 to 0.5 dB (see Table 14.2) offer the potential for substantial upgrades to cater for the perceived future service requirements of the interoffice networks. In addition, the operation of LEDs with single-mode fiber could prove attractive in these as well as in future local access network (see Section 14.2.3) applications.

An aspect of the interoffice network which has been stimulated by the proliferation of local area networks (LANs) (see Section 14.7) is the requirement for

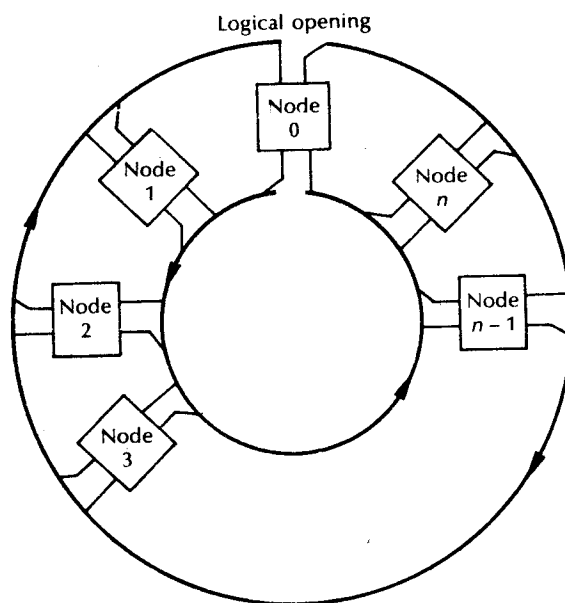


Figure 14.3 Distributed queue dual bus (DQDB) MAN architecture arranged as a physical ring structure.

the interconnection of such networks in the geographically separated area of the junction network. This had led to investigation and standardization discussions associated with packet-based communications over the metropolitan area. Such metropolitan area networks (MANs) are being developed for use in the interconnection of LANs, whilst also potentially providing voice and video services [Refs. 16–18]. Early proposals from the IEEE 802.6 committee suggested a distance optimization of a 50 km diameter network (in order to match the dimensions of typical large metropolitan areas) using a slotted ring architecture.

The emerging standard for MANs, however, is the distributed queue dual bus (DQDB) architecture developed by a subsidiary of Telecom Australia [Refs. 18, 19]. The topology utilizes a dual loop of the transmission medium (nominally optical fiber) that can be arranged in a physical ring but is, in fact, a logical bus. This looped-bus configuration, which is shown in Figure 14.3, eliminates the need to remove data from the medium, as must be done with ring networks. The DQDB MAN employs asynchronous transfer mode (ATM) multiplexing and switching (see Section 14.2.3) in order to provide bandwidth on demand and to efficiently handle bursty traffic. Nevertheless, the MAN standard is compatible with the synchronous optical network developments (see Section 14.2.5) in that it will directly interface with the 155 Mbit s^{-1} level in the synchronous hierarchy. In addition, there is continuing interest in the use of ring topologies operating at high speed with synchronous time division multiplexing for application in the future interoffice networks [Ref. 20].

14.2.3 Local access network

The local access network or subscriber loop connects telephone subscribers to the local switching centre or office. Possible network configurations are shown in Figure 14.4 and include a ring, tree and star topology from the local switching centre. In a ring network (Figure 14.4(a)) any information fed into the network by a subscriber passes through all the network nodes and hence a number of transmission channels must be provided between all nodes. This may be supplied by a time division multiplex system utilizing a broadband transmission medium. In this case only information addressed to a particular subscriber is taken from the network at that subscriber node. The tree network, which consists of several branches as indicated in Figure 14.4(b), must also provide a number of transmission channels on its common links.* However, in comparison with the ring network it has the advantage of greater flexibility in relation to topological enlargement. Nevertheless in common with the ring network, the number of subscribers is limited by the transmission capacity of the links used.

In contrast, the star network (Figure 14.3(c)) provides a separate link for every subscriber to the local switching centre. Hence the amount of cable required is

* The tree network may be considered as a multiple bus network in which access to the local switching centre from a node requires the use of a common bus link. In this context the bus topology is sometimes referred to as the base configuration.

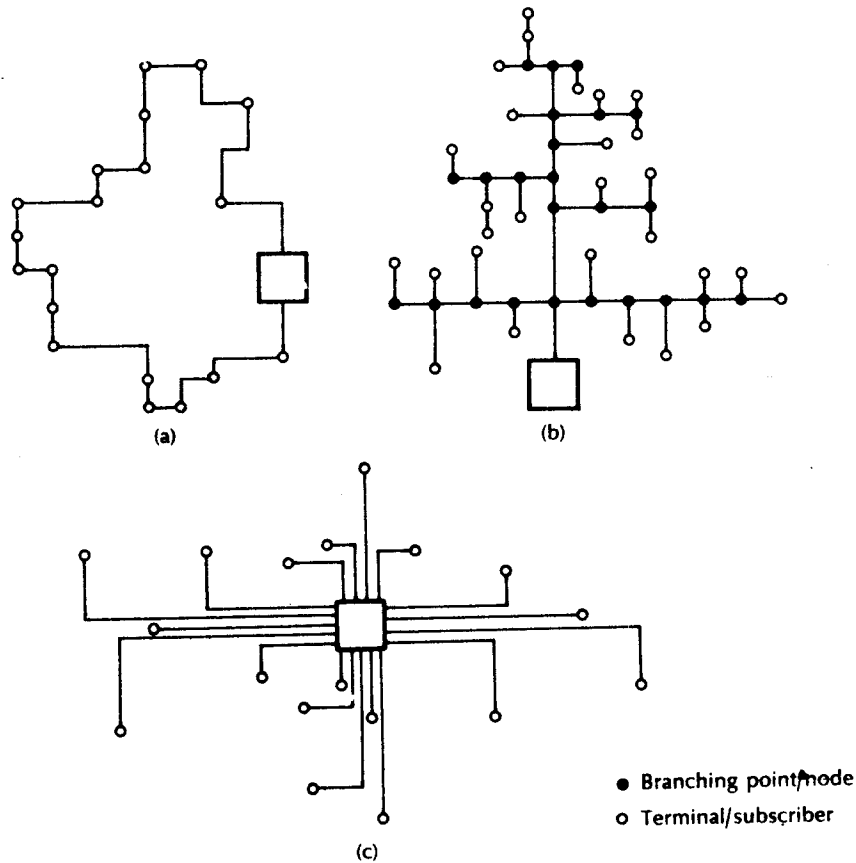


Figure 14.4 Local access network configurations: (a) ring network; (b) tree network; (c) star network.

considerably increased over the ring or tree network, but is offset by enhanced reliability and availability for the subscribers. In addition, simple subscriber equipment is adequate (i.e. no TDM) and network expansion is straightforward. Thus virtually all local and rural telephone networks utilize a star configuration based on copper conductors (twisted pair) for full duplex (bothway) speech transmission. There is substantial interest in the possibility of replacing the existing narrowband local access network twisted pairs with optical fibers. These can also be utilized in the star configuration to provide wideband services (videophone, television, stereo hi-fi, facsimile, data, etc.) to the subscriber together with the narrowband speech channel. Alternatively the enhanced bandwidth offered by optical fibers will allow the use of ring or tree configurations in local and rural networks. This would reduce the quantity of fiber cable required for subscriber

loops. However, investigations indicate [Ref. 21] that the cable accounts for only a small fraction of the total network cost. Furthermore, it is predicted that the cost of optical fiber cable may be reduced towards the cost of copper twisted pairs with the large production volume required for local access networks.

Small scale field trials of the use of optical fibers in local access networks have been carried out in several countries including France (the Biarritz project [Ref. 22]), Japan (the Yokosuta field trial [Ref. 21]), Canada (the Elie rural field trial [Ref. 23]) and Germany (BIGFON – wideband integrated fiber optic local telecommunications network; a total of ten projects in seven towns [Ref. 21]). These field trials utilized star configurations providing a full range of wideband services to each subscriber through the use of both analog and digital signals on optical fibers.

In the United Kingdom a small Fibrevision (Cable TV) network was installed in Milton Keynes using a switched star configuration [Refs. 24, 25]. This led to the implementation of a cable TV fiber switched star network (SSN) by British Telecom in the Westminster Cable TV franchise area [Ref. 26]. Using the experience gained on that project, British Telecom have designed a modified switched star network which incorporates telephony services to take single-mode fiber through the local access network to the subscriber premises. This active network is known as the broadband integrated distributed star (BIDS), a schematic of which is provided in Figure 14.5 [Ref. 27]. Broadband signals are collected at the headend and then transmitted to a number of hub-sites on $1.3\ \mu\text{m}$ single-mode fiber super-primary links. Each fiber is capable of carrying up to 16 TV channels using analog FM modulation (see Section 11.7.5) to the hub-site which would normally be located at the local telephone exchange. This allows for the interface of the telephony services from the telecommunications network, these being transmitted over a $140\ \text{Mbit s}^{-1}$ single-mode fiber primary link to a broadband access point (BAP). Similarly, the broadband services are carried to the BAP on primary fiber links. Finally, secondary single-mode fiber links are employed to transmit the telephony and data services plus two TV channels to the subscriber or customer premises.

An alternative strategy developed by British Telecom involves the use of a passive optical network (PON). Unlike the BIDS network this development is aimed at a staged approach from the initial provision of telephony and other low bit rate services whilst allowing the subsequent upgrading to the distribution of broadband services. The initial concept of telephony on a passive optical network (TPON) is illustrated in Figure 14.6(a) [Ref. 28]. In this case one single-mode fiber operating at $1.3\ \mu\text{m}$ is fed from the local telephone exchange and fanned out via passive optical splitters or tree couplers (see Section 5.6.2) at cabinet and distribution point (DP) positions in order to feed a number of individual subscribers. Each TPON system is designed to provide up to 128 fiber feeds to network terminating equipment (NTE) in customer premises. Time division multiplexing is employed at a rate of $20\ \text{Mbit s}^{-1}$ for the telephony services over the broadcast fiber network to the NTEs. The ongoing transmission to the customer premises is provided by a time division multiple access scheme operated at each NTE which associates the appropriate bits of information into assigned time slots.

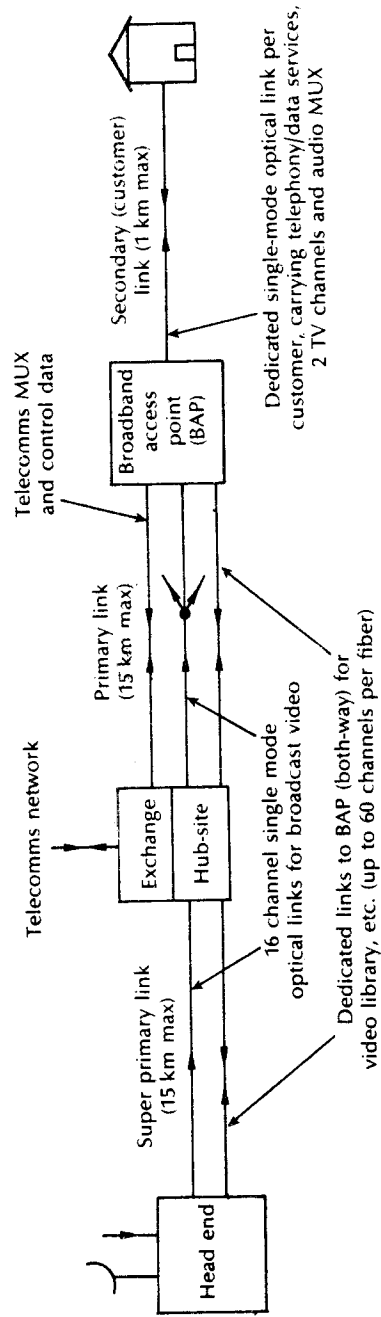


Figure 14.5 Broadband integrated distributed star (BIDS) network.

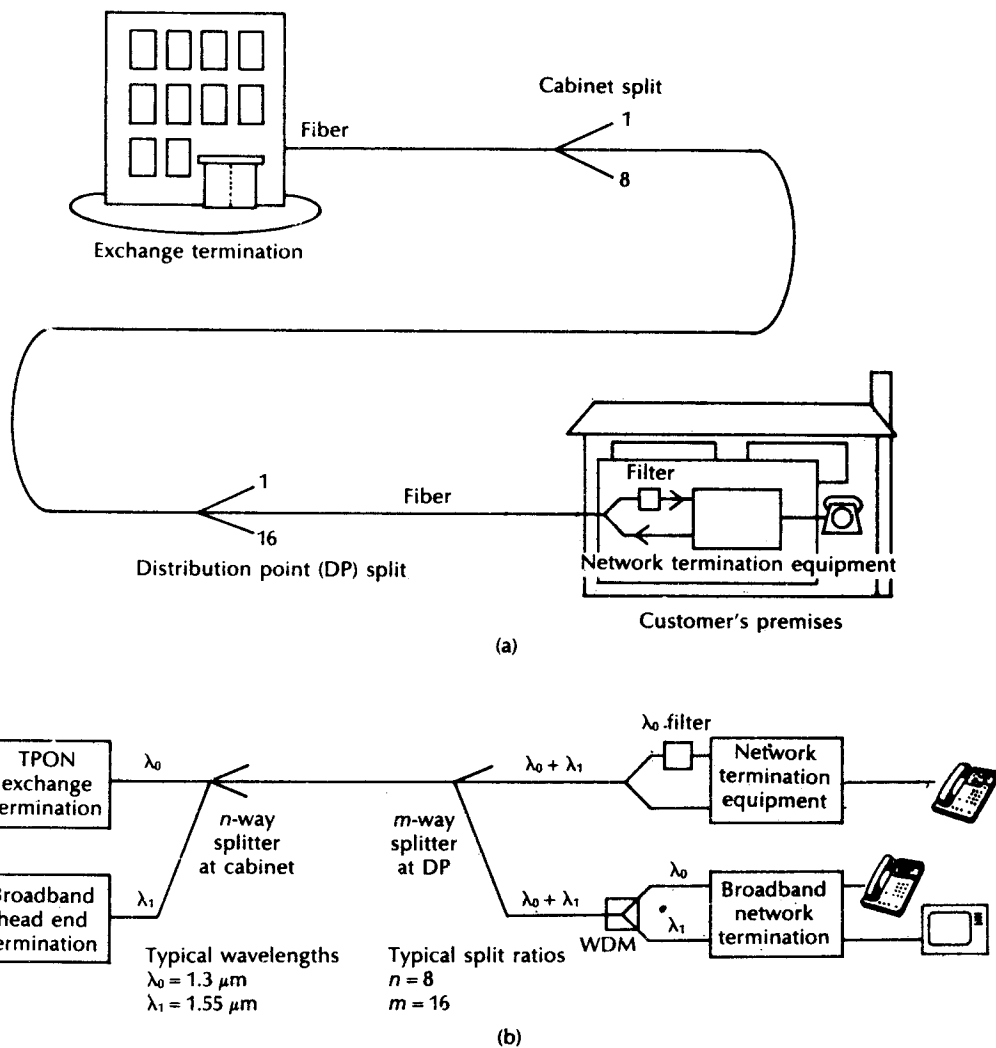


Figure 14.6 Passive optical local access network: (a) telephony on a passive optical network (TPON) configuration; (b) broadband passive optical network (BPON) upgrade.

The enhancement to incorporate broadband services or the broadband passive optical network (BPON) is shown in Figure 14.6(b) [Ref. 29]. It may be observed that the broadband services are carried over the same fiber network architecture but at a different signal wavelength (e.g. $1.55 \mu\text{m}$). This use of wavelength division multiplexing (see Section 11.9.3) allows the equivalent of between sixteen and thirty-two TV channels to be transmitted on each additional wavelength signal when analog subcarrier multiplexing (see Section 11.9.2) is employed. For example,

a multiplex of thirty-two video modulated carriers can be assembled at the broadband headend in the frequency band 950 MHz to 1.75 GHz for downstream transmission to the customer premises on the 1.55 μm wavelength signal.

British Telecom is conducting a field trial for the above networks at Bishops Stortford, Essex in the United Kingdom over the period 1990 to 1993 [Refs. 30 to 32]. It is envisaged that some 400 residential customers together with twenty-eight businesses will be provided with both telephony and broadband services employing either the BIDS or TAPON/BPON systems. Initially, the broadband services provided will be broadcast TV and stereo audio but upgrades to include high-fidelity telephony, video, a video library and high definition TV are planned.

In the United States various trials for the deployment of optical fiber in the local access network have been undertaken. For example, Southern Bell have provided CATV on multimode graded index fiber to just over 250 subscribers at Hunter's Creek, Orlando, Florida [Ref. 33]. This trial has been followed by a more ambitious project to provide basic Integrated Services Digital Network (ISDN), together with CATV, on single-mode fiber to residences at Heathrow, a development north of Orlando. The ISDN terminology describes the end to end digital connectivity with a standard set of interfaces for integrated services delivery. Hence the basic or narrowband ISDN service is intended to provide subscribers with access to two 64 kbits s^{-1} digital circuit switched channels* and a 16 kbits s^{-1} packet switched channel. † Broadband ISDN (BISDN) which can offer transmission rates in the hundreds of Mbit s^{-1} region is also the subject of standardization [Refs. 34, 35] which should facilitate the worldwide compatibility of broadband services such as switched access TV, videophone, high quality audio and multimedia desktop teleconferencing. Nevertheless, it is likely that such services would require optical fiber (and, in particular, single-mode fiber) within the local access network.

A double active star access network topology using fiber is finding application in the United States. It is based on the digital loop carrier (DLC) systems which are often employed to provide gain in the feeder segment of the US local access network, as illustrated in Figure 14.7 [Ref. 35]. The DLC remote node (RN) contains active electronics that provide battery, overvoltage protection, ringing, signalling, coding, hybrid and testing (BURSCHT) functions. Initially, optical fiber was employed in the feeder segment of such systems but more recently the SLC Series 5 Carrier System‡ has used a physical/logical star topology in both the feeder and distribution segments to extend the fiber to the subscriber premises [Ref. 36]. In this case the remote node electronics have been modified such that the BURSCHT functions are removed from the RN to the distant terminal (DT) which may be at or near the subscriber premises.

An alternative local access network architecture which is also finding some application in the United States is supplied by Raynet. It is based on a physical

* Known as B-channels which may be utilized for speech transmission.

† Known as D-channel which may be employed for data transmission.

‡ This system is marketed by AT&T.

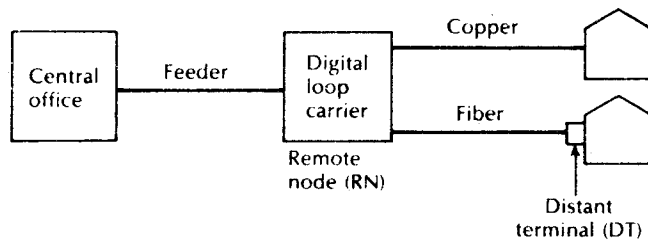


Figure 14.7 AT&T SLC Series 5 local access network architecture.

bus/logical star topology in the distribution segment using active service points, as shown in Figure 14.8 [Ref. 35]. The Raynet fiber bus system utilizes an office interface unit (OIU) at the central office (CO) or remote node (RN) which interfaces with eight 1.5 Mbit s^{-1} digital lines and two protection lines from a central office switch. These are transmitted/received on two-unidirectional fiber buses that carry digitized voice signals, together with signalling information to several subscriber interface units (SIU), each of which supports eight subscriber lines. The SIUs are designed to be placed at or near the subscriber premises such that the copper conductors are only employed over short distances. It may be noted that in comparison with the AT & T SLC Series 5 Carrier System, the Raynet bus architecture reduces the quantity of fiber required in the feeder and distribution segments of the local access network but it increases the number of locations containing active electronics.

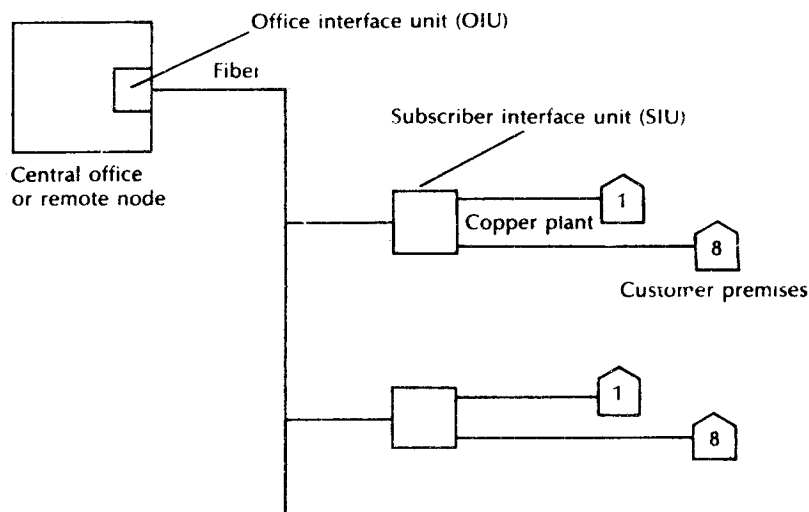


Figure 14.8 Raynet fiber bus system for the local access network.

A passive fiber access network architecture using a double star topology has been demonstrated by Bellcore [Ref. 37]. It is called the Passive Photonic Loop (PPL) and is based on the LAMB DANET system (see Section 11.9.3) which is a very high capacity multiwavelength optical network. The PPL architecture is shown in Figure 14.9 and it employs wavelength division multiplexing techniques to support over twenty wavelength channels. It may be observed from Figure 14.9 that WDM is used between the central office and the remote node (or service access point), which allows a single feed fiber to be shared by a number of channels. Dedicated optical fiber links then connect the RN or SAP to the subscriber premises. Hence the PPL comprises a physical star/logical star topology in both the feeder and distribution segments of the local access network.

Following the LAMB DANET concept, each subscriber is assigned two unique wavelengths, one for upstream transmission and one for downstream transmission. Therefore, information to be transmitted to a particular subscriber is modulated onto the assigned downstream wavelength signal at the central office and then wavelength multiplexed onto the feeder fiber. This wavelength channel is demultiplexed at the remote node and then passed down the required distribution fiber. Thus the subscriber receives the required wavelength signal and no further filtering is necessary at the subscriber premises. The PPL system has been demonstrated experimentally, employing commercially available as well as custom specified components [Ref. 37]. Some twenty channels were operated in the $1.55 \mu\text{m}$ wavelength band to provide support for ten subscribers. The length of the feeder fiber employed was 9.7 km and the distribution fibers varied in length between 2.2 and 3.3 km. Finally, bidirectional transmission with a bit error rate of less than 10^{-9} when operating at both 600 and 1200 Mbit s^{-1} was obtained.

Although standards relating to the synchronous optical network (SONET) have been adopted (see Section 14.2.5), it is apparent that some broadband services and in particular bursty traffic are not easily accommodated by SONET alone. Hence an alternative packetized multiplexing and switching technique called asynchronous transfer mode (ATM) has been investigated for carrying information within the

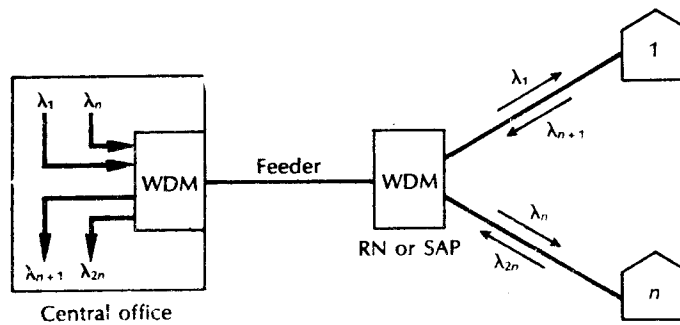


Figure 14.9 Passive photonic loop (PPL) local access network architecture.

SONET payload [Ref. 35]. A particular focus of these activities has concerned the local access network [Ref. 38]. For example, work in this area in the United Kingdom has resulted in the development of ATM operation on a passive optical network [Ref. 39]. Hence, the so called APON system allows a 155 Mbit s^{-1} ATM data stream to be distributed over the shared access PON architectures.

Finally, coherent transmission techniques are also under investigation for the provision of the future optical access network. In particular, coherent optical FDM systems and networks (see Section 12.8.2) offer the potential for many thousands of separate channels within each of the long wavelength windows. Although this powerful attribute of coherent transmission is regarded as offering tremendous potential for future subscriber distribution networks, it is almost certain that initial deployments of optical fiber in the access network will focus on the aforementioned intensity modulation/direct detection technology and that the coherent optical subscriber loop will not be a commercial reality for some time.

14.2.4 Submerged systems

Undersea cable systems are an integral part of the international telecommunications network. They find application on shorter routes especially in Europe. On longer routes, such as across the Atlantic, they provide route diversity in conjunction with satellite links. The number of submerged cable routes and their capacities are steadily increasing and hence there is a desire to minimize the costs per channel. In this context digital optical fiber communication systems appear to offer substantial advantages over current analog FDM and digital PCM coaxial cable systems. High capacity coaxial cable systems require high quality, large diameter cable to overcome attenuation, and still allow repeater spacings of around 5 km. By comparison, it was predicted [Ref. 40] that single-mode optical fiber systems operating at 1.3 or $1.55 \mu\text{m}$ will provide repeated spacings of 25 to 50 km and eventually even longer.

Research and development of single-mode fiber submerged cable systems is progressing in a number of countries including the United Kingdom, France, the United States and Japan. A successful field trial of a 140 Mbit s^{-1} system was carried out by STC Submarine Systems in Loch Fyne, Scotland in 1980 using a 9.5 km cable length, including a single PCM repeater [Ref. 41]. In the same year a 10 km field trial cable was installed by NTT along the Izu coast in Japan [Ref. 40]. Component reliability together with deep sea cable structure and strength are considered the major problems. These problems were gradually addressed and overcome, however, resulting in the installation of Optican 1 (Tenerife to Gran Canaria), United Kingdom–Belgium 5 (Broadstairs to Ostend), Kynsu to Okinawa, and Honshu to Hokkaido [Ref. 42]. The first two of these short-haul submerged systems, each operating at 280 Mbit s^{-1} per fiber pair, were deployed in 1985 and 1986 respectively. The latter two, which transmit at 400 Mbit s^{-1} on each fiber pair, being installed by NTT.

In 1988 the first generation of repeater transoceanic optical fiber systems was brought into service. This included TAT-8 (United States and France), TPC-3 (Hawaii to Japan) and HAW-4 (California to Japan) [Ref. 43]. These single-mode fiber systems operate at a wavelength of $1.3\ \mu\text{m}$ with a transmission capacity of $560\ \text{Mbit s}^{-1}$ (two fibers at $280\ \text{Mbit s}^{-1}$ each) and with repeater spacings of approximately 50 km [Ref. 44]. Furthermore, two more $1.3\ \mu\text{m}$ single-mode transoceanic systems have been subsequently installed across the Atlantic (PTAT-1) and Pacific (NPC) oceans [Ref. 45]. Both of these systems contain three fibers (in each direction), each operating at a rate of $420\ \text{Mbit s}^{-1}$.

Second generation submerged systems transmitting at a wavelength of $1.55\ \mu\text{m}$ have been successfully demonstrated. For example, a repeaterless system with a span of 104 km was installed between Tainan and Peng-Hun, off Taiwan in 1988 [Ref. 46]. This system, which was equipped with distributed feedback lasers and avalanche photodiode receivers, operated at a transmission rate of $417\ \text{Mbit s}^{-1}$ on each fiber. In addition the UK-Netherlands 12 link using single-mode fiber operating at a wavelength of $1.55\ \mu\text{m}$ was installed in 1989 over an unrepeated distance of 155 km. However, the transmission rate per fiber was limited to $140\ \text{Mbit s}^{-1}$. The installation of the first, second generation transoceanic system was also completed in 1991. This TAT-9 system between the United States and Europe will also operate at the significantly higher transmission rate of $560\ \text{Mbit s}^{-1}$ per fiber with repeater spacings in excess of 100 km [Ref. 45]. Moreover, a further Pacific link (TPC-4) is planned to come into operation in 1992 which will also employ second generation technology at the $565\ \text{Mbit s}^{-1}$ data rate. These deployments of systems which are designed for an operational life of twenty-five years provide an indication of the reliability and maturity of the existing $1.55\ \mu\text{m}$ component technology.

The future perspective for submerged optical fiber communications, particularly in the medium- and long-haul range (i.e. distances above 250 km), suggests the use of optical amplifier technology with the present intensity modulation/direct detection systems (see Section 11.10) [Ref. 47]. It is apparent from recent demonstrations that distances up to 1000 km can be achieved using around ten amplifiers without the need for optical isolators or filters [Ref. 48]. In addition, it is likely that one area of early implementation for coherent optical systems (see Chapter 12) will be in undersea applications where the increased transmission distances afforded by this technology can be of great benefit. For example, KDD have already demonstrated $765\ \text{bit s}^{-1}$ coherent transmission over 90 km of submerged fiber cable [Ref. 11]. Moreover, in theory, distances of the order of 2000 km could be realized using coherent technology with concatenated optical amplifiers employing optical isolators.

For distances significantly in excess of 2000 km, however, it is suggested that the present second generation systems operating at a wavelength of $1.55\ \mu\text{m}$ and using electronic regenerators may well be continued with because further technology breakthroughs will be required to enable the use of optical amplifiers (either semiconductor or fiber devices) over such distances [Ref. 48]. The limitation is the

spontaneous emission at each amplifier, which is both random and signal related, that degrades the signal to noise ratio. Another feature of such systems is the very long interaction length over which dispersion and nonlinear effects can build up and cause distortion. Although these aspects of amplifier operation are under investigation, very-long-haul submarine communications without electronic repeaters may await the deployment of lower loss mid-infrared fiber types (see Section 3.7) within engineered systems. However, it should be noted that coherent transmission over a range of 2200 km at a rate of 2.5 Gbit s^{-1} using erbium doped fiber amplifiers has been demonstrated in the laboratory by NTT in Japan [Ref. 49].

14.2.5 Synchronous networks

The existing baseband digital transmission hierarchies for the telecommunication network in Europe and North America were provided in Table 11.1 (Section 11.5), together with discussion of the time division multiplexing strategy. A schematic of the way in which the European hierarchy is multiplexed up to the 140 Mbit s^{-1} rate from the constituent 2 Mbit s^{-1} (thirty channel) signals is shown in Figure 14.10(a). Difficulties arise, however, with this multiplexing strategy, which is currently adopted throughout the world, in that each 2 Mbit s^{-1} transmission circuit (taking the European example) has its own independent clock to provide for timing and synchronization. This results in slightly different frequencies occurring throughout a network and is referred to as pleisochronous* transmission. Although this strategy is well suited to the transport of bits it suffers a major drawback in that in order to multiplex the different levels (i.e. 2 to 8 to 34 to 140 Mbit s^{-1}) extra bits need to be inserted (bit stuffing) at each intermediate level so as to maintain pleisochronous operation.

The presence of bit stuffing in the existing pleisochronous digital hierarchy makes it virtually impossible to identify and extract an individual channel from within a high bit rate transmission link. Thus to obtain an individual channel the whole demultiplexing procedure through the various levels (Figure 14.10(a)) must be carried out. This process is both complex and uneconomic, particularly when considering future telecommunication networking requirements such as drop and insert where individual channels are extracted or inserted at particular stages. Moreover, a substantial saving in electronic hardware together with increased reliability could be achieved by having a straight, say 2 to 140 Mbit s^{-1} multiplexing/demultiplexing capability as illustrated in Figure 14.10(b) [Ref. 10].

It was therefore clear that a new fully synchronous digital hierarchy was required to enable the international telecommunications network to evolve in the optical fiber era. In particular, this would facilitate the add/drop of lower transmission rate channel groups from much larger higher speed groups without the need for banks of multiplexers and large, unreliable distribution frames.

* Corresponding signals are defined as pleisochronous if their significant instants occur at nominally the same rate, any variation being constrained within specific limits.

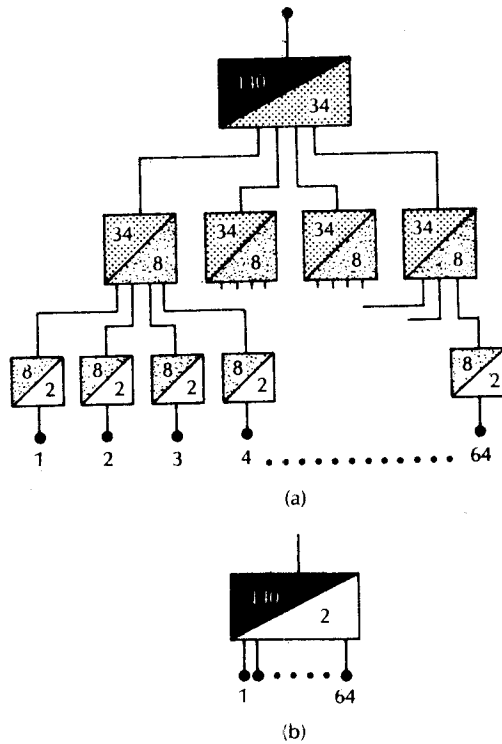


Figure 14.10 European multiplexing hierarchy: (a) existing pleisochronous structure; (b) synchronous multiplexing.

Furthermore, by the mid-1980s the lack of standards for optical networks had led to a proliferation of proprietary interfaces where transmission systems produced by one manufacturer would not necessarily interconnect with those from any other manufacturer such that the ability to mix and match different equipments was restricted. Hence standardization towards a synchronous optical network termed SONET commenced in the United States in 1985 [Ref. 51]. However, two key areas resulted in some modification to the original proposals. These were to make the standard operational in a pleisochronous environment and still retain its synchronous nature and to develop it into an international transmission standard in which the incompatibilities between the existing European and North American signal hierarchies could be resolved. In this latter context the CCITT began deliberation of the SONET concepts in 1986 which resulted in basic recommendations for a new synchronous digital hierarchy (SDH) in November 1988. These recommendations are now published [Refs. 52 to 54]. Prior to these recommendations the American National Standards Institute (ANSI) had issued draft standards relating to SONET [Ref. 55] but as a result of the extensive discussions

between the two standards authorities, the two hierarchies are effectively the same. Hence the synchronous optical network recommendations tend to be referred to as SONET in North America and SDH in Europe.

The SONET standard as ultimately developed by ANSI defines a digital hierarchy with a base rate of $51.840 \text{ Mbit s}^{-1}$, as shown in Table 14.4. The OC notation refers to the optical carrier level signal. Hence the base rate signal is OC-1. The STS level in brackets refers to a corresponding synchronous transport signal from which the optical carrier signal is obtained after scrambling (to avoid a long string of ones or zeros and hence enable clock recovery at receivers) and electrical to optical conversion.* Thus STS-1 is the basic building block of the SONET signal hierarchy. Higher level signals in the hierarchy are obtained by byte-interleaving (where a byte is eight bits) an appropriate number of STS-1 signals in a similar manner to that described for the European standard PCM system described in Section 11.5. This differs from the bit interleaving approach utilized in the existing North American digital hierarchy (see Table 11.1). The STS-1 frame structure shown in Figure 14.11 is precisely $125 \mu\text{s}$ and hence there are 8000 frames per second. This structure enables digital voice signal transport at 64 kbit s^{-1} (1 byte per $125 \mu\text{s}$) and the North American DS1-24 channel ($1.544 \text{ Mbit s}^{-1}$), as well as the European thirty channel ($2.048 \text{ Mbit s}^{-1}$) signals (see Table 11.1) to be accommodated. Other signals in the two hierarchies can also be accommodated. The basic STS 1 frame structure illustrated in Figure 14.11 comprises nine rows, each of 90 bytes which therefore provides a total of 810 bytes or 6480 bits per $125 \mu\text{s}$ frame. This results in the $51.840 \text{ Mbit s}^{-1}$ base rate mentioned above.

The first 3 bytes in each row of the STS-1 frame contain transport overhead bytes, leaving the remaining 783 bytes to be designated as the synchronous payload envelope (SPE). Apart from the first column (9 bytes) which is used for the path overhead, the remaining 774 bytes in the SPE constitute the SONET data payload.

Table 14.4 Levels of the SONET signal hierarchy

Level	Line rate (Mbit s^{-1})
OC-1 (STS-1)	51.840
OC-3 (STS-3)	155.520
OC-9 (STS-9)	466.560
OC-12 (STS-12)	622.080
OC-24 (STS-18)	1244.160
OC-36 (STS-36)	1866.240
OC-48 (STS-48)	2488.320

* STS-1 corresponds to OC-1 which is the lowest level optical signal used at the SONET equipment and network interface.

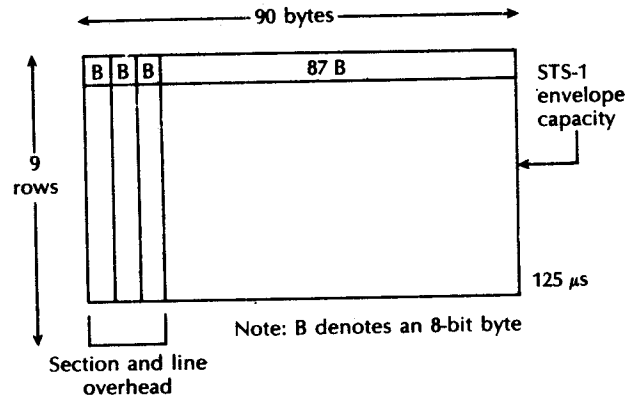


Figure 14.11 STS-1 frame structure.

The transport overhead bytes are utilized for functions such as framing, scrambling, error monitoring, synchronization and multiplexing whilst the path overhead within the SPE is used to provide end to end communication between systems carrying digital voice, video and other signals which are to be multiplexed onto the STS-1 signal. In the latter case a path is defined to end at a point at which the STS-1 signal is created or taken apart (i.e. demultiplexed) into its lower bit rate signals.

The STS-1 SPE does not have to be contained within a single frame; it may commence in one frame and end in another. A 'payload pointer' within the transport overhead is employed to designate the beginning of the SPE within that frame. This provides the flexibility required in order to accommodate different bit rates and a variety of services. Moreover, to accommodate sub-STS-1 signal rates a virtual tributary (VT) structure is defined comprising four rates: 1.728 Mbit s⁻¹ (VT 1.5); 2.304 Mbit s⁻¹ (VT 2); 3.456 Mbit s⁻¹ (VT 3); and 6.912 Mbit s⁻¹ (VT 6). For example, it may be observed that the 1.544 Mbit s⁻¹ and 2.048 Mbit s⁻¹ signal streams can each be mapped into a VT 1.5 and VT 2 respectively.

Finally, the higher order multiplexing of a number of STS-1 signals is obviously important in order to achieve the higher bit rates required for wideband services. The format of the STS-*N* signal frame is shown in Figure 14.12 which, as mentioned previously, is obtained by byte-interleaving *N* STS-1 signals. In this case the transport overhead bytes of each STS-1 (i.e. the first three single byte columns of each STS-1 signal shown in Figure 14.11) are frame aligned to create the 3*N* bytes of transport overhead, which is illustrated in Figure 14.12. However, the SPEs do not require alignment since the service payload pointers within the associated transport overhead bytes provide the location for the appropriate SPEs.

The synchronous digital hierarchy (SDH), as defined by the CCITT [Refs. 52 to 54], operates in the same manner as described above but differs in some of its terminology. In this case the 125 μs frame structure is referred to as a synchronous transport module (STM) and the base rate STM-1 is 155.520 Mbit s⁻¹ which

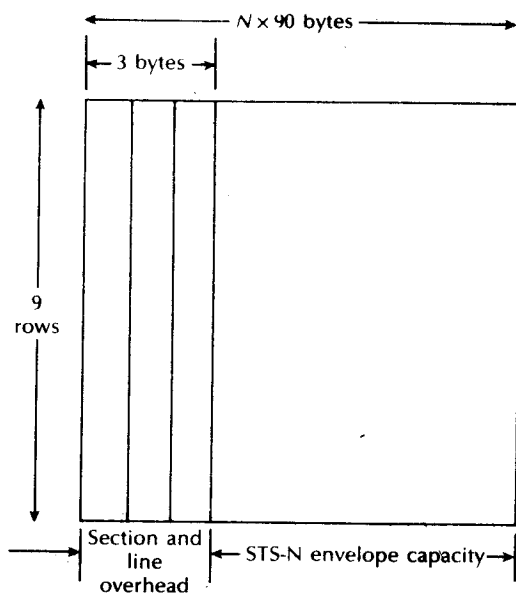


Figure 14.12 STS-N frame structure.

corresponds to OC-3 (STS-3), as may be observed from Table 14.5. Hence the European 140 (i.e. 139.264) Mbit s^{-1} pleisochronous signal can be mapped within an STM-1 signal when including a suitable overhead.

As would be expected, the higher level STM signals also correspond to SONET optical carrier rates as well as providing a match to appropriate multiples in the European pleisochronous hierarchy. Again, these higher levels are formed by simple byte interleaving. Tributaries are used to incorporate the signal rates below the STM-1 rate into the frame format where they may be located by means of pointers. Hence a $2.048 \text{ Mbit s}^{-1}$ channel can be readily identified within a $155.520 \text{ Mbit s}^{-1}$ stream. As with SONET this will allow a network of high capacity

Table 14.5 Corresponding levels and bit rates for SDH and SONET

SDH level	Line rate (Mbit s^{-1})	SONET level
STM-1	155.520	OC-3
STM-4	622.080	OC-12
STM-8	1244.160	OC-24
STM-12	1866.240	OC-36
STM-16	2488.320	OC-48

cross-connects to be established at nodes throughout the transmission network. Moreover, this facility will enable a managed network to efficiently route and distribute traffic between nodes, dropping off capacity to exchanges for traffic switching [Ref. 56].

14.3 Military applications

In these applications, although economics are important, there are usually other, possibly overriding, considerations such as size, weight, deployability, survivability (in both conventional and nuclear attack [Ref. 57]) and security. The special attributes of optical fiber communication systems therefore often lend themselves to military use.

14.3.1 Mobiles

One of the most promising areas of military application for optical fiber communications is within military mobiles such as aircraft, ships and tanks. The small size and weight of optical fibers provide an attractive solution to space problems in these mobiles which are increasingly equipped with sophisticated electronics. Also the wideband nature of optical fiber transmission will allow the multiplexing of a number of signals on to a common bus. Furthermore, the immunity of optical transmission to electromagnetic interference (EMI) in the often noisy environment of military mobiles is a tremendous advantage. This also applies to the immunity of optical fibers to lightning and electromagnetic pulses (EMP) especially within avionics. The electrical isolation, and therefore safety, aspect of optical fiber communications also proves invaluable in these applications, allowing routing through both fuel tanks and magazines.

The above advantages were demonstrated with preliminary investigations involving fiber bundles [Ref.3] and design approaches have included multiterminal data systems [Ref. 58] using single fibers, and use of an optical data bus [Ref. 59]. In the former case, the time division multiplex system allows ring or star configurations to be realized, or mixtures of both to create bus networks. The multiple access data highway allows an optical signal injected at any access point to appear at all other other access points. An example is shown in Figure 14.13 [Ref. 6] which illustrates the interconnection of six terminals using two 4×4 transmissive star couplers (see Section 5.6.2).

An experimental optical data bus was installed in the Mirage 4000 aircraft [Ref. 59]. However, significant problems were encountered with optical connection, fiber fragility and low light levels from the LED source. Nevertheless it was concluded that these drawbacks could be reduced by the use of spliced connections, star couplers rather than T-couplers and smaller diameter fibers (100 to 150 μm), which would make it possible to produce cables with smaller radii of curvature, and in which the fiber would be freer.

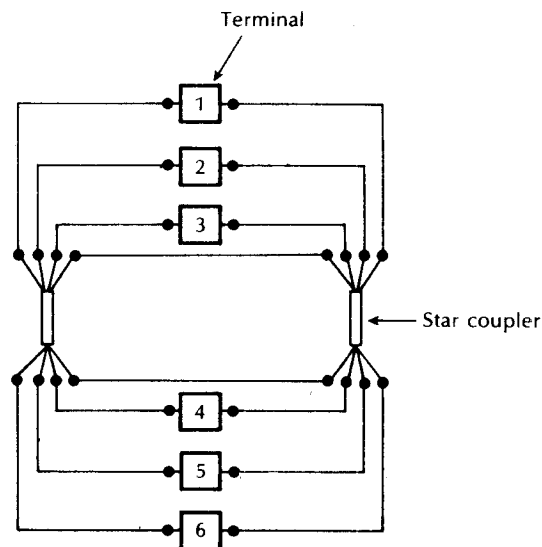


Figure 14.13 Multiple access bus showing the interconnection of six terminals using two four-way transmissive star couplers [Ref. 6].

Studies have also been carried out into the feasibility of using a 1 Mbit s^{-1} optical data bus for flight control, avionic weapons and internal data systems within a helicopter [Ref. 60]. In addition an optical fiber data highway has been installed in the Harrier GR5 aircraft, for operational use. It is incorporated between the communications, navigation and identification data converter located towards the rear of the aircraft and the amplifier control situated beneath the cockpit. The original system specification called for large core diameter plastic fiber for operation around 2.4 kbit s^{-1} [Ref. 60].

Moreover, a flight control system employing optical fibers for an airship has been demonstrated which provided a fly-by-light capability [Ref. 61]. In addition, the focus of investigations in this area has shifted towards the optical fiber realization of the universally accepted military data bus standard MIL-STD-1553B and the ways in which this may be applied within avionics applications [Ref. 62]. Finally, there is substantial interest in the application of optical fiber sensor systems (see Section 14.5) within mobiles (particularly aircraft to provide monitoring functions (e.g. [Ref. 63])). Moreover, these activities are not only confined to the military sphere but are also being pursued within civilian aircraft development.

14.3.2 Communication links

The other major area for the application of optical fiber communications in the military sphere includes both short and long distance communication links. Short

distance optical fiber systems may be utilized to connect closely spaced items of electronic equipment in such areas as operations rooms and computer installations. A large number of these systems have already been installed in military installations in the United Kingdom. These operate over distances from several centimetres to a few hundred metres at transmission rates between 50 bauds and 4.8 kbit s^{-1} [Ref. 60]. In addition a small number of 7 MHz video links operating over distances of up to 100 m are in operation. There is also a requirement for long distance communication between military installations which could benefit from the use of optical fibers. In both these cases advantages may be gained in terms of bandwidth, security and immunity to electrical interference and earth loop problems over conventional copper systems.

Other long distance applications include torpedo and missile guidance, information links between military vessels and maritime, and towed sensor arrays. In these areas the available bandwidth and long unrepeated transmission distances of optical fiber systems provide a solution which is not generally available with conventional technology. A fiber guided weapons system is illustrated in Figure 14.14 whereby a low loss, high tensile strength fiber is used to relay a video signal back to a control station to facilitate targeting by an operator. Such fiber guided anti-tank missiles (ATMS) have been demonstrated using LED sources and multimode fiber over a range of 5 to 10 km, with longer range systems employing single-mode fiber being under development [Ref. 64].

Investigations have also been carried out with regard to the use of optical fibers in tactical communication systems. In order to control sophisticated weapons systems in conjunction with dispersed military units there is a requirement for tactical command and control communications (often termed C^3). These communication systems must be rapidly deployable, highly mobile, reliable and have the ability to survive in military environments. Existing multichannel communication cable links employing coaxial cable or wire pairs do not always meet these requirements [Ref. 65]. They tend to be bulky, difficult to install (requiring long installation times), and are susceptible to damage. In contrast optical fiber cables offer special features which may overcome these operational

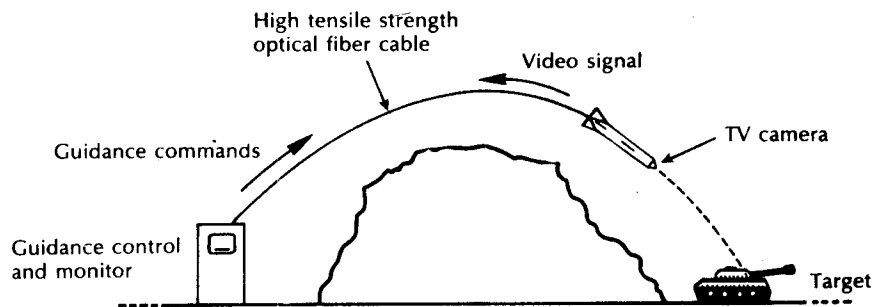


Figure 14.14 A fiber guided weapons system.

deficiencies. These include small size, light weight, increased flexibility, enhanced bandwidth, low attenuation removing the need for intermediate repeaters, and immunity to both EMI and EMP. Furthermore, optical fiber cables generally demonstrate greater ruggedness than conventional deployable cables, making them appear ideally suited for this application.

Optical fiber cables have been installed and tested within the Ptarmigan tactical communication system developed for the British Army [Ref. 66]. They may be utilized as a direct replacement for the HF quad cable system previously employed for the intranodal multichannel cable links within the system [Ref. 6]. The optical fiber element of the system comprises an LED source emitting at a wavelength of $0.9 \mu\text{m}$, graded index fiber and a APD detector. It is designed to operate over a range of up to 2 km at data rates of 256, 512 and 2048 kbit s^{-1} without the use of intermediate repeaters. The optical fiber cable assemblies are about half the weight of the HF quad cable, and are quick and easy to deploy in the field. Furthermore, special ruggedized expanded beam optical connectors (see Section 5.5) have been shown to be eminently suitable for use in conditions involving dust, dirt, rough handling and extreme climates. Successful integration of an optical fiber system into a more complex tactical communication system for use in the military environment has demonstrated its substantial operational and technical advantages over HF metallic cable systems.

In summary, it appears that confidence has grown in this technology such that its widescale use in military applications in the future will continue.

14.4 Civil, consumer and industrial applications

14.4.1 Civil

The introduction of optical fiber communication systems into the public network has stimulated investigation and application of these transmission techniques by public utility organizations which provide their own communication facilities over moderately long distances. For example these transmission techniques may be utilized on the railways and along pipe and electrical power lines. In these applications, although high capacity transmission is not usually required, optical fibers may provide a relatively low cost solution, also giving enhanced protection in harsh environments, especially in relation to EMI and EMP. Experimental optical fiber communication systems have been investigated within a number of organizations in Europe, North America and Japan. For instance, British Rail has successfully demonstrated a 2 Mbit s^{-1} system suspended between the electrical power line gantries over a 6 km route in Cheshire [Ref. 3]. Also, the major electric power companies have shown a great deal of interest with regard to the incorporation of optical fibers within the metallic earth of overhead electric power lines [Ref. 67].

It was indicated in Section 14.2.3 that optical fibers are eminently suitable for video transmission. Thus optical fiber systems are starting to find use in commercial

television transmission. These applications include short distance links between studio and outside broadcast vans, links between studios and broadcast or receiving aeriels, and close circuit television (CCTV) links for security and traffic surveillance. In addition, the implementation of larger networks for cable and common antenna television (CATV) has demonstrated the successful use of optical fiber communications in this area where it provides significant advantages, in terms of bandwidth and unrepeated transmission distance, over conventional video links.

One of the first commercial optical fiber video systems was installed in Hastings, UK, in 1976 by Rediffusion Limited for the transmission of television signals over a 1.4 km link for distribution to 34,000 customers. Another early optical fiber CATV field trial was the Hi-OVIS project carried out in Japan [Ref. 68]. The project involved the installation of an interactive video system, plus FM audio and digital data to 160 home subscribers and eight local studio terminals in various public premises. The system operated over a 6 km distribution cable consisting of thirty-six fibers plus additional branches to the various destination points; no repeaters were used in this entire network.

Various techniques have been utilized for video transmission including baseband intensity modulation, subcarrier intensity modulation (e.g. FM-IM), pulse analog techniques (e.g. PFM-IM) and digital pulse code modulation (PCM-IM). Generally, digital transmission is preferred on larger CATV networks as it allows time division multiplexing as well as greater unrepeated transmission distance [Ref. 70]. It also avoids problems associated with the nonlinearities of optical sources. An example of commercial digital video transmission is a 7.8 km optical fiber trunk system operating at 322 Mbits s^{-1} in London, Ontario, Canada [Ref. 71]. This system carries twelve video channels and twelve FM stereo channels along eight fibers installed in a 13 mm cable. A similar digital trunk system has been installed in a CATV network in Denmark [Ref. 72]. This link, using twelve fibers again operating over a distance of 7.8 km, has a capacity of eight channels and twelve FM stereo channels.

However, digital transmission of video signals is not always economic, owing to the cost and complexity of the terminal equipment. Hence, optical fiber systems using direct intensity modulation often provide an adequate performance for a relatively low system cost. For example, a block schematic of a long distance analog baseband video link for monitoring railway line appearances such as road crossings, tunnels and snowfall areas is shown in Figure 14.15 [Ref. 73]. Video signals from TV cameras installed at monitoring points *C* are gathered to the concentrating equipment through local transmission lines. These signals are then multiplexed in time, frequency or wavelength on to the main transmission line to the monitoring centre. An experimental optical fiber system operating at a wavelength of $1.32 \mu\text{m}$ using multimode graded index fiber and baseband intensity modulation was installed along a main line of the Japanese national railway [Ref. 73]. Successful video transmission over 16.5 km without intermediate repeaters was achieved, demonstrating the use of fiber systems for this application.

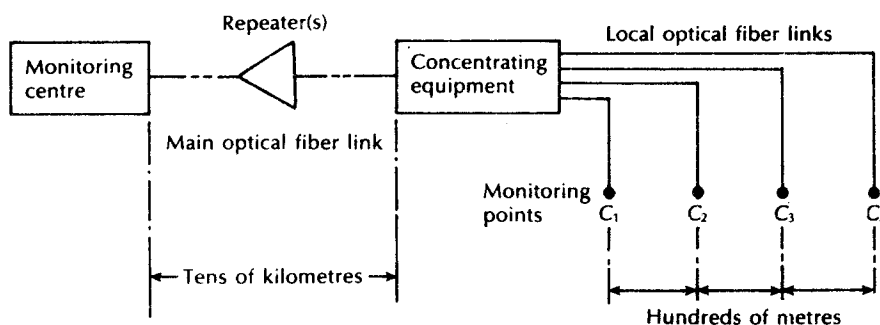


Figure 14.15 Block schematic of an optical fiber baseband video system for railway line monitoring [Ref. 73].

A similar CCTV monitoring system was implemented for the Kobe Mass Transit System, also in Japan [Ref. 74]. This system, which operates over shorter distances of between 300 m and 5 km, also uses analog intensity modulation together with wavelength division multiplexing of four TV channels at wavelengths of 730, 780, 837 and 879 nm on to multimode step index fiber.

The continuing interest in optical fiber video communications has more recently encompassed the use of subcarrier multiplexing (SCM) techniques. These developments have extended the maximum transmission distance without repeaters to over 100 km on single-mode fiber (see Section 11.9.2). Furthermore, the distribution of video signals is under investigation within the telecommunication local access network (see Section 14.2.3) and therefore there is a merging of the optical fiber network strategies that may be adopted in this area with those for the provision of cable TV.

In common with the military applications, other potential civil uses for optical fiber systems include short distance communications within buildings (e.g. broadcast and recording studios) and within mobiles such as aircraft and ships. However, a large market for optical fiber systems may eventually be within consumer applications.

14.4.2 Consumer

A major consumer application for optical fiber systems is within automotive electronics. Work is progressing within the automobile industry towards this end together with the use of microcomputers for engine and transmission control as well as control of convenience features such as power windows and seat controls. Optical fiber communication links in this area provide advantages of reduced size and weight together with the elimination of EMI. Furthermore, it is likely they will reduce costs by allowing for an increased number of control signals in the confined space presented by the steering column and internal transmission paths within the vehicle through multiplexing of signals on to a common optical highway.

Such techniques have been under investigation by General Motors for a number of years and a prototype system was reported [Ref. 75] to have demonstrated the feasibility in 1980. This system utilized a bundle of forty-eight high loss plastic fibers with a simple LED emitting in the visible spectrum. Further developments in the USA and elsewhere suggest that large core diameter (1 mm) single plastic fibers will be utilized in automobile multiplex systems within the passenger compartment, whereas glass fibers may be required to stand the high temperatures (120 °C) encountered in the engine compartment.

More recent work towards the replacement wiring harnesses in automobiles with multiplexed optical fiber data links has also been undertaken in a number of other centres [Refs. 76 to 78]. Several prototype systems have been demonstrated which provide, in addition to the usual control signals (e.g. lights), functions such as centralized locking, power windows and seats, and door lamps. The majority of these systems have employed large core diameter plastic fiber operating at low data rates and have sought to avoid the very high temperatures in the engine compartments. Nevertheless, the provision of optical sensing and monitoring functions (see Section 14.5) within the engine compartment is under investigation [Refs. 79, 80] and work progresses in the development of high temperature polymer fibers [Ref. 81]. In addition, prototype optical sensors for monitoring other automotive parameters such as road adhesion have been implemented [Ref. 82].

Other consumer applications are likely to include home appliances where, together with microprocessor technology, optical fibers may be able to make an impact in the 1990s. However, as with all consumer equipment, progress is very dependent on the instigation of volume production and hence low cost. This is a factor which appears to have delayed wider application of optical fiber systems in this area.

14.4.3 Industrial

Industrial uses for optical fiber communications cover a variety of generally on-premises applications within a single operational site. Hence in the past the majority of industrial applications have tended to fall within the following design criteria [Ref. 83]:

- (a) digital transmission at rates from d.c. to 20 Mbits⁻¹, synchronous or asynchronous, having compatibility with a common logic family (i.e. TTL or CMOS), being independent of the data format and with bit error rates less than 10⁻⁹;
- (b) analog transmission from d.c. to 10 MHz, exhibiting good linearity and low noise;
- (c) transmission distances from several metres up to a maximum of kilometres, although generally 1 km will prove sufficient;
- (d) a range of environments from benign to harsh, and often exhibiting severe electromagnetic interference from industrial machinery.

Optical fiber systems with performances to meet the above criteria are readily available at a reasonable cost. These systems offer reliable telemetry and control communications for industrial environments where EMI and EMP cause problems for metallic cable links. Furthermore, optical fiber systems provide a far safer solution than conventional electrical monitoring in situations where explosive or corrosive gases are abundant (e.g. chemical processing and petroleum refining plants). Hence the increasing automation of process control, which is making safe, reliable communication in problematical environments essential, is providing an excellent area for the application of optical fiber communication systems.

For example, optical fiber systems were successfully employed in nuclear testing applications in the United States by the Department of Energy. Two plasma diagnostic experiments developed by the Los Alamos Scientific Laboratory [Ref. 84] were carried out at the Nevada Test Site in Mercury, Nevada. These experiments utilized the unique properties of optical fibers to provide diagnostic capabilities which are not possible with coaxial cable systems. In the first experiment a wideband fiber system (1 GHz bandwidth) was used to record the wideband data from gamma ray sources. The second experiment, a neutron imaging system, provided a time and space resolution for a neutron source on a nanosecond time scale. The neutron source was attenuated and imaged through a pinhole on to an array of scintillator filaments, each of which was aligned to a single PCS fiber for transmission via a graded index fiber to a photomultiplier. A pulsed dye laser was used for system calibration. Both amplitude and overall timing calibration were achieved with an optical time domain reflectometer (see Section 13.10.1) being used regularly to record the fiber attenuation. It was estimated [Ref. 84] that this system provided a bandwidth advantage of at least a factor of 10 over coaxial cable, at approximately half the cost, and around one-fiftieth of the weight.

More recently the application of optical fiber communications systems within the industrial environment has grown to encompass two substantive technological areas, namely optical sensor systems and local area networks. These developments are discussed in Sections 14.5 and 14.7.2 respectively

14.5 Optical sensor systems

It was indicated in Section 14.4.3 that optical fiber transmission may be advantageously employed for monitoring and telemetry in industrial environments. The application of optical fiber communications to such sensor systems has stimulated much interest, especially for use in electrically hazardous environments where conventional monitoring is difficult and expensive. There is a requirement for the accurate measurement of parameters such as liquid level, flow rate, position, temperature and pressure in these environments which may be facilitated by optical fiber systems. Early work in this area featured electrical or electro-optical transducers along with optical fiber telemetry systems. A novel approach of this type involved a piezoelectric transducer which was used to apply local deformations

to a single fiber highway causing phase modulation of the transmitted signal [Ref. 86]. The unmodulated signal from the same optical source was transmitted via a parallel reference fiber to enable demodulation of the signals from various piezo-electric transducers located on the highway. This technique proved particularly useful when a number of monitoring signals were required at a central control point.

Electro-optical transducers together with optical fiber telemetry systems offer significant benefits over purely electrical systems in terms of immunity to EMI and EMP as well as intrinsic safety in the transmission to and from the transducer. However, they still utilize electrical power at the site of the transducer which is also often in an electrically problematical environment. Therefore much effort is currently being expended in the investigation and development of entirely optical sensor systems. These employ electrically passive optical transducer mechanisms which directly modulate the light for the optical fiber telemetry link.

The fundamental requirement of an electrically passive optical fiber sensor is the modulation of a light beam either directly or indirectly (e.g. with a mechanical linkage) by the measurand (e.g. pressure, temperature, flow velocity, displacement, vibration, strain, etc.) without recourse to electrical interfacing. Modulation of a light beam transmitted via a feed fiber takes place in the modulation zone of the generalized optical fiber sensor system depicted in Figure 14.16. The light beam can be modulated in five of its basic properties: namely, optical intensity, phase, polarization, wavelength and spectral distribution. Most fiber sensors employ the first three, although there is growing interest in the exploitation of the last two. Furthermore, it is possible to categorize the devices into two distinct groups based solely on their use of intensity or phase modulation respectively. This form of classification also largely separates the sensor systems in relation to the type of optical fiber and associated components required.

Optical fiber phase sensors generally utilize an interferometric approach necessitating the use of single-mode fiber and an optical source with spatial coherence (e.g. laser). Therefore, although these devices offer orders of magnitude increased sensitivity over conventional sensing mechanisms, they exhibit a requirement for somewhat sophisticated optical fiber components and optoelectronic devices. Alternatively, optical fiber intensity modulation sensors which may serve in less demanding applications often employ multimode fiber together with an incoherent light source (e.g. LED). These devices therefore tend to be simpler and easier to implement at lower cost.

Optical fiber sensors may be implemented as intrinsic or extrinsic devices. The former type is arranged such that the physical parameter to be sensed acts on the

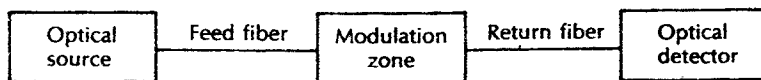


Figure 14.16 Basic optical fiber sensor system.

fiber itself to cause a change in the transmission characteristics. The latter type uses the fiber as a light guide to and from the sensor, which is configured to allow the measurand to change the coupling characteristics between the feed and return fiber (see Figure 14.16).

14.5.1 Phase and polarization fiber sensors

Very sensitive single-mode fiber passive optical phase sensors employ an interferometric approach, as illustrated in Figure 14.17(a). These devices cause interference of coherent monochromatic light propagating in a strained or temperature-varying fiber with light either directly from the laser source, or (as shown in Figure 14.17(a)) guided by a reference fiber isolated from the external influence. The effects of strain, pressure or temperature change give rise to differential optical paths by changing the fiber length, core diameter or refractive index with respect to the reference fiber. This provides a phase difference between the light emitted from the two fibers, giving interference patterns, as illustrated in Figure 14.17(a). Very accurate measurements of pressure or temperature may be obtained from these patterns. For example, using fused silica in such a two arm fiber interferometer, it can be shown that the temperature sensitivity is about $107 \text{ rad } ^\circ\text{C}^{-1} \text{ m}^{-1}$ [Ref. 87]. It should be noted that the interferometric sensor arrangement shown in Figure 14.17(a) is that of the Mach–Zehnder configuration [Ref. 89].

Another common single-mode fiber interferometric sensor which is finding widescale application is the fiber gyroscope [Ref. 90]. This device is based on the classical Sagnac ring interferometer, a fiber version of which is illustrated in Figure 14.17(b). In this device light entering the multiturn fiber coil is divided into two

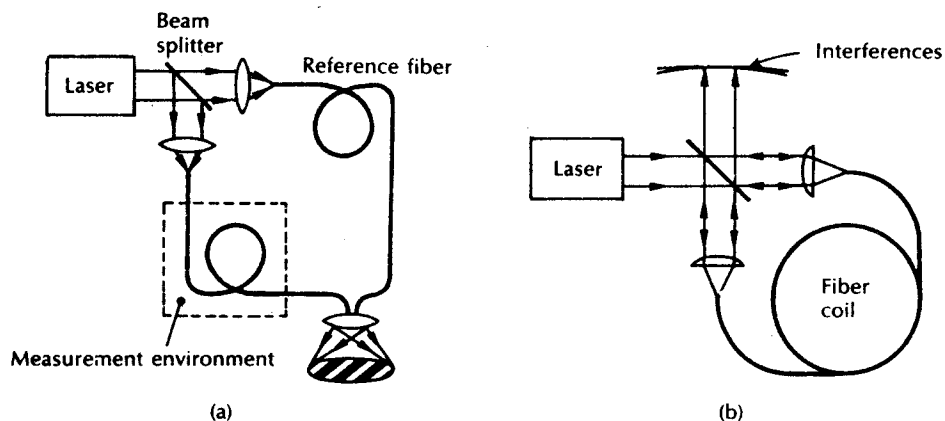


Figure 14.17 Single-mode fiber interferometric sensors: (a) a two arm interferometer (Mach–Zehnder); (b) ring interferometer with multiturn fiber coil (Sagnac).

counterpropagating waves which will return in phase after travelling along the same path in opposite directions. When the fiber coil is rotating about an axis perpendicular to the plane of the coil, however, then the path lengths between the counterpropagating waves differ. This difference produces a phase shift which in turn can be measured by interferometric techniques in order to obtain the rotation. A further interferometric sensor used to measure acoustic pressure which has attracted significant attention is the fiber hydrophone [Ref. 91].

Modulation of the polarization state of light within a fiber may also be utilized to take a physical measurement. A successful implementation of this technique is displayed in the Faraday rotation current monitor shown in Figure 14.18 [Ref. 92]. This device consists of a single polarization maintaining fiber (see Section 3.13.2) which passes up from earth to loop around the current-carrying conductor before passing back to earth. A He-Ne laser beam is linearly polarized and launched into the fiber which is then stripped of any cladding modes. The direction of polarization of the light in the fiber core is rotated by the longitudinal magnetic field around the loop, via the action of the Faraday magneto-optic effect [Ref. 93]. A Wollaston prism is used to sense the resulting rotation and resolves the emerging light into two orthogonal components. These components are separately detected with a photodiode prior to generation of a sum and difference signal of the two intensities (I_1 and I_2). The difference signal normalized to the sum give a parameter which is proportional to the polarization rotation ρ , following [Ref. 93]:

$$K\rho = \frac{I_1 - I_2}{I_1 + I_2} \quad (14.1)$$

where K is a constant which is dependent on the properties of the fiber. Hence a current measurement (either d.c. or a.c.) may be obtained which is independent of

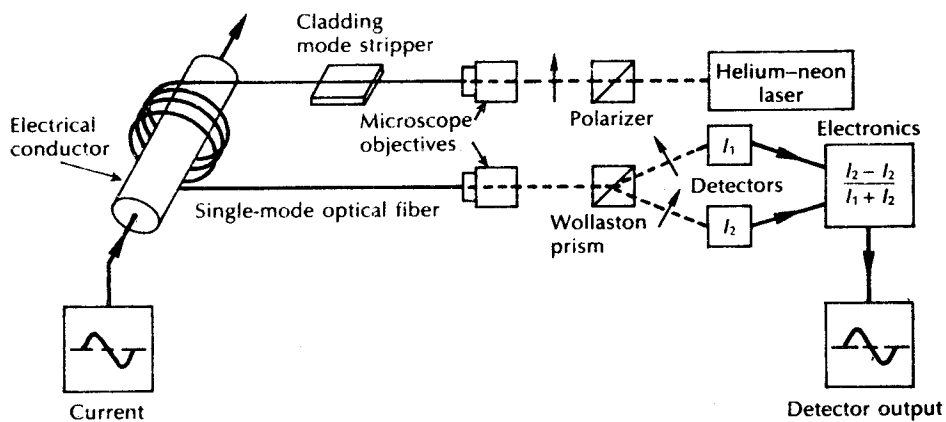


Figure 14.18 Single-mode optical fiber sensor for current measurement [Ref. 92].

the received light power. Finally, it should be noted that the phase and polarization sensors described in this section also constitute intrinsic single-mode fiber devices.

14.5.2 Intrinsic fiber sensors

A popular technique for the realization of an intrinsic multimode fiber sensor involves microbending of the fiber in the modulation region [Refs. 94, 95]. The sensing mechanism for this technique is shown in Figure 14.19(a). Deformation of the fiber on a small scale causes light to be coupled from the guided optical modes propagating in the fiber core into the cladding region where they are lost through radiation into the surrounding region. When the spatial wavelength of the deformation L is correctly chosen, the power coupled from the fiber into radiation modes is high, providing a very high sensitivity to pressure applied to the deformer in a direction perpendicular to the fiber core axis. Furthermore, if the deformation is caused by the measurand (e.g. pressure, vibration, sound, etc.), then the fluctuation in intensity of either the core or cladding light is directly proportional to the measurand for small deformations. Thus monitoring the fiber core or cladding allows detection of the measurand.

The configuration of a microbending fiber sensor for monitoring structural deformation developed by TRW (USA) is shown in Figure 14.19(b). The test data corresponding to this configuration is given in Figure 14.19(c) for a 1.4 mm spatial wavelength of 3 wavelengths [Ref. 94]. It must be noted, however, that a requirement of this sensor type is the removal of the cladding modes (by a cladding mode stripper) both immediately prior to, and after, the modulation zone. This prevents the occurrence of measurement errors from light which may be propagating in the cladding from the source as well as light coupling back from the cladding into the core after the modulation zone. Moreover, although fiber damage resulting from the deformation does not appear to be a severe problem, a settling-in period may be observed prior to the attainment of constant sensor characteristics [Ref. 94].

Also, in common with all fiber intensity modulation sensors, inaccuracies may occur due to source, detector and fiber cable instabilities. These, so-called, common-mode variations usually necessitate the transmission of a separate optical reference signal which is not modulated by the measurand. In this way any optical intensity variations can be removed from the returned measurand signal by comparison with the returned reference signal at the receive terminal. Various strategies have been demonstrated by which referencing for intensity modulation sensors may be achieved. These include: techniques which divide the transmitted optical signal in, or prior to, the modulation region in order to obtain a reference signal [Refs. 96, 97]; methods which employ two separate wavelength optical signals, one of which is modulated by the measurand and the other which acts as the reference signal [Refs. 98, 99]; and a balanced bridge arrangement that produces two return optical signals which allow any intensity variations on the measurand signal to be eradicated [Ref. 100]. It should be noted, however, that the

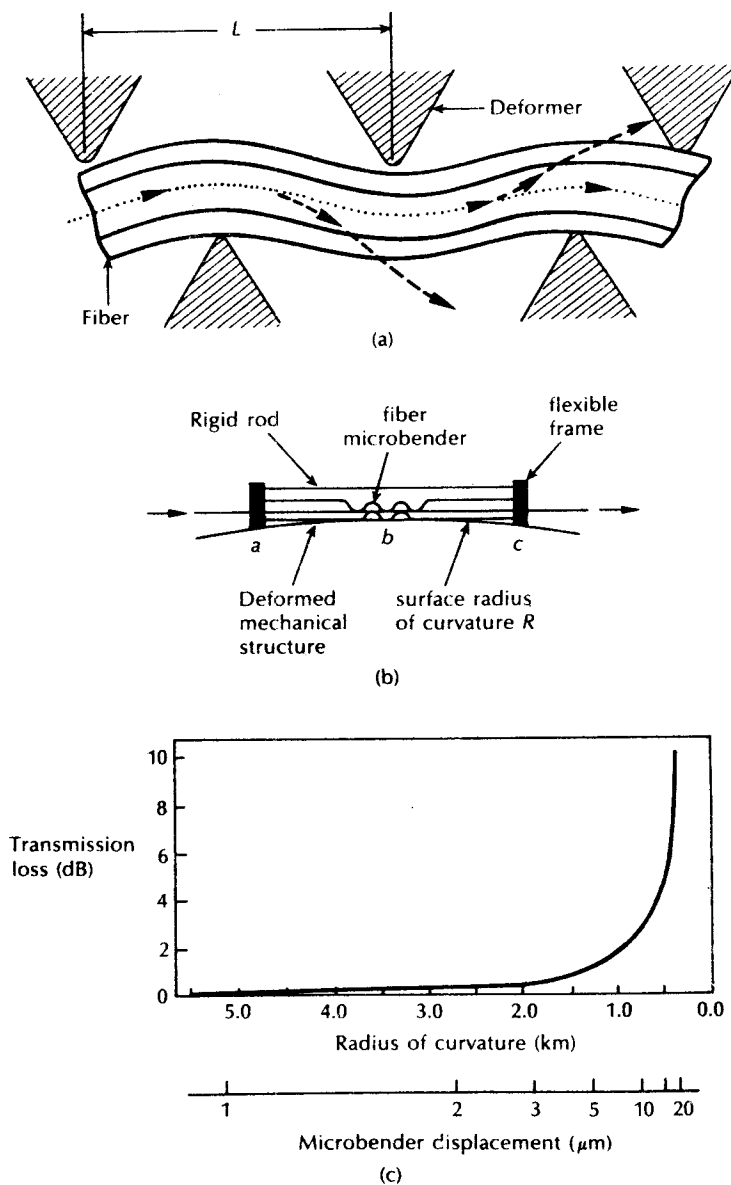


Figure 14.19 Fiber microbending sensor: (a) sensing mechanism; (b) a structure; (c) test data from (b). Reproduced with permission from S. K. Yao and C. K. Asawa, 'Microbending fiber optic sensing', *Proc. SPIE, Int. Soc. Opt. Eng.*, 412, p. 9, 1983.

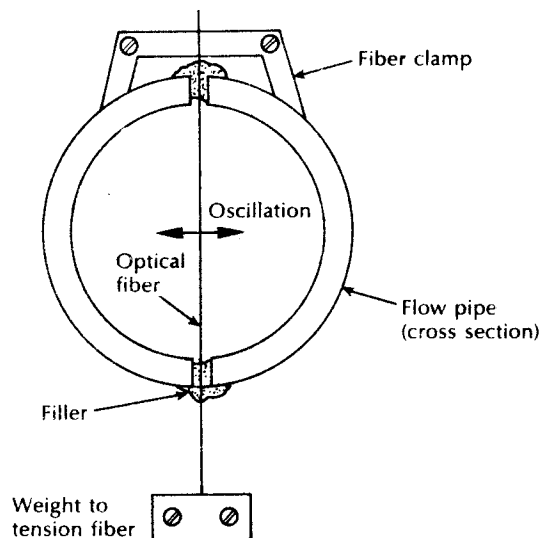


Figure 14.20 An optical fiber flow meter [Ref. 101].

first two techniques have been applied to specific extrinsic sensor mechanisms (see Section 14.5.3), whereas the latter method provides a more universal strategy.

Figure 14.20 shows an intrinsic optical fiber flow sensor mechanism. In this device a multimode optical fiber is inserted across a pipe such that the liquid flows past the transversely stretched fiber. The turbulence resulting from the fiber's presence causes it to oscillate at a frequency roughly proportional to the flow rate. This results in a corresponding oscillation in the mode power distribution within the fiber giving a similarly modulated intensity profile at the optical receiver. The technique has been used to measure flow rates from 0.3 to 3 m s^{-1} [Ref. 101]. However, it cannot measure flow rates below those at which turbulence occurs.

14.5.3 Extrinsic fiber sensors

Numerous extrinsic optical fiber sensor mechanisms have been proposed and investigated [Refs. 91, 95, 102, 103], but to date relatively few practical commercial devices have emerged. A technique which has been realized as a commercial product is illustrated in Figure 14.21 [Ref. 103]. This shows the operation of a simple optical fluid level switch. When the fluid, which has a refractive index greater than the glass forming the optical dipstick, reaches the chamfered end, total internal reflection ceases and the light is transmitted into the fluid. Hence an indication of the fluid level is obtained at the optical detector. Although this system is somewhat crude and will not provide a continuous measurement of a fluid level, it is simple and safe for use with flammable liquids.

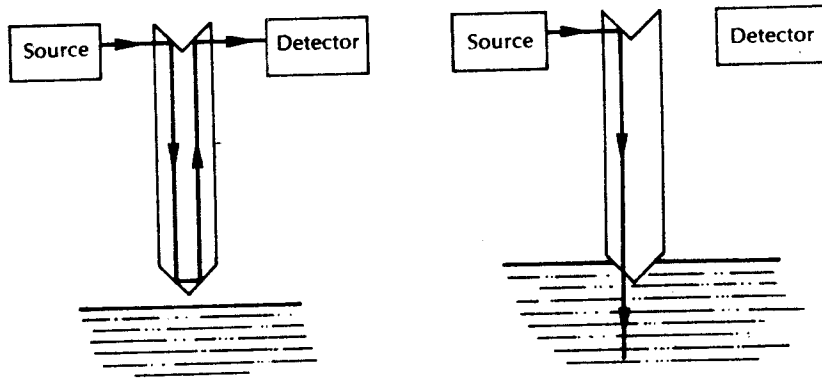


Figure 14.21 Optical fluid level detector.

Intensity modulation of the transmitted light beam is utilized in the extrinsic reflective or fonic optical sensor shown in Figure 14.22(a) to give a measurement of displacement [Ref. 104]. Light reflected from the target is collected by a return fiber(s) and is a function of the distance between the fiber ends and the target. Hence the position or displacement of the target may be registered at the optical detector. Furthermore, the sensitivity of this sensor may be improved by placing the axes of the feed and return fiber at an angle to one another and to the target [Ref. 105]. Unfortunately, this technique exhibits the drawback mentioned previously with regard to the stability of the optical components which is a feature of intensity

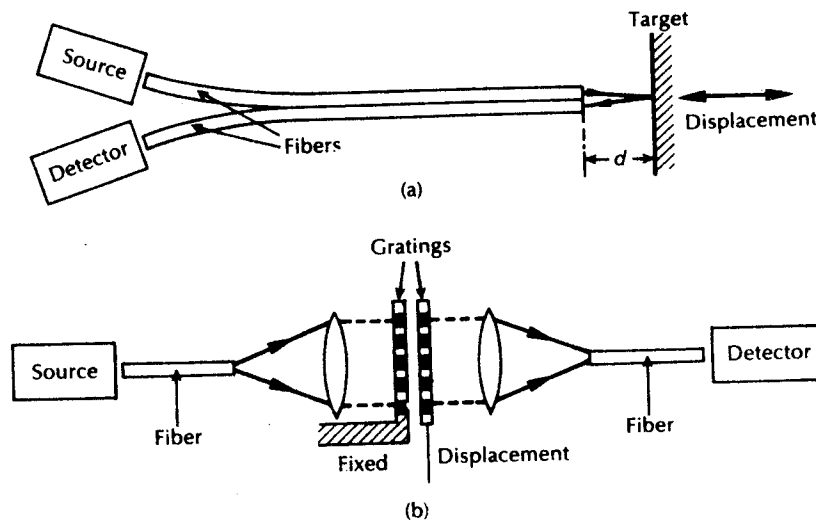


Figure 14.22 Optical displacement sensors: (a) reflective or fonic sensor; (b) Moiré fringe modulation sensor.

modulated fiber sensors. Nevertheless, it lends itself to the optical sensor referencing techniques described in Section 14.5.2.

A method of overcoming the above drawback with optical fiber intensity modulation sensors is to use a digital measurement technique. Such a technique is shown in Figure 14.22(b) whereby the measurement of displacement is obtained using a Moiré fringe modulator [Ref. 95]. In this case the opaque lined gratings produce dark Moiré fringes. Transverse movement of one grating with respect to the other causes the fringes to move up or down. Thus a count of the fringes as the gratings are moved provides a measurement of displacement. The fringe counting is independent of instabilities within the system components which affect the optical intensity. However, mechanical vibrations may severely affect the measurement accuracy and prove difficult to eradicate. Also there are problems involved with loss of count if, for any reason, optical power to the sensor is interrupted.

A multimode fiber sensor which provides measurement of pressure is illustrated in Figure 14.23(a). In this device the photoelastic effect induced by mechanical stress on a photoelastic material (e.g. piezo-optic glass, polyurethane, epoxy resin)

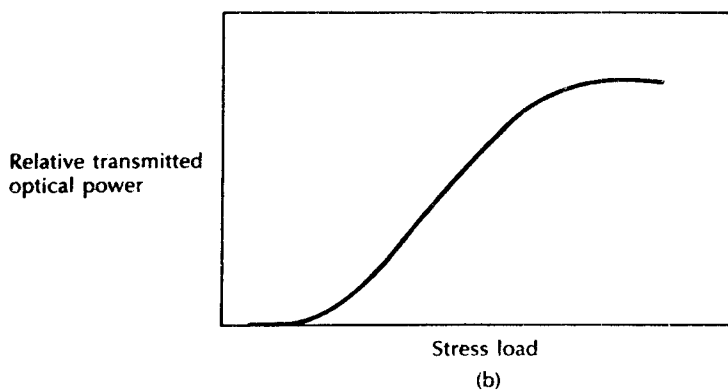
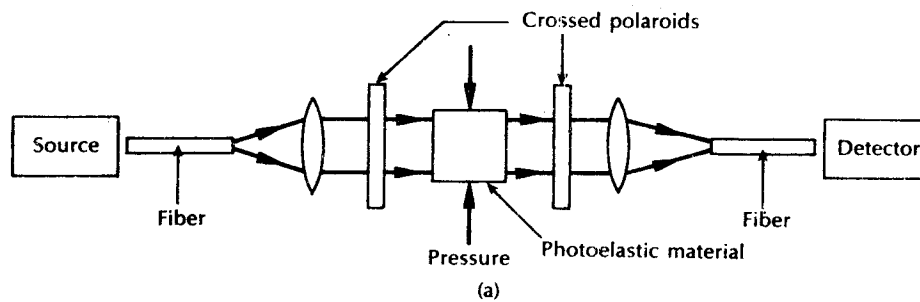


Figure 14.23 Photoelastic pressure sensor: (a) schematic structure; (b) response characteristic.

is utilized to rotate the optical polarization between a pair of crossed polarizers [Refs. 95, 103]. The phenomenon known as birefringence occurs with the application of mechanical stress to the transparent isotropic material, whereby it becomes optically anisotropic giving a variation in transmitted light through the sensor. The response of the sensor is typically sinusoidal, as illustrated in Figure 14.23(b), and a resolution of 10^{-4} of full range has been demonstrated [Ref. 103]. An advantage of this technique is that the stress may be induced directly without the need for an intermediate mechanism (e.g. pressure to displacement). A drawback, however, is that the birefringence exhibited by photoelastic materials is often temperature-dependent, making measurement of a single parameter difficult.

Another technique which has been adopted for commercial exploitation is utilized in the 'Fluoroptic' temperature sensor [Ref. 102]. This device, which is illustrated in Figure 14.24, uses a form of wavelength modulation which occurs when incoherent light is transmitted along a large core (multimode) fiber to a phosphorescent material. The light excites the rare earth phosphor which emits a number of lines at different wavelengths. Two of these spectral lines (in this case at wavelengths of 540 nm and 630 nm) are selected using filters in the receiver. The ratio of intensities of these chosen lines is a single valued function of the temperature of the phosphor. Measurement of this ratio provides an exact measure of the temperature. The resolution of the device is 0.1°C over the range -50 to $+250^\circ\text{C}$ and is independent of the output light intensity. However, the instrument has rather complex processing electronics and requires calibration during thermal stabilization since the sensitivities of the optical detectors, even when matched, do not track together at the two different emitted wavelengths as the temperature changes.

In general terms, wavelength modulation has the distinct advantage over intensity modulation in that such spectrally encoded sensors are not affected by intensity variations associated with the optical and optoelectronic components in the system. However, the variety of wavelength modulation techniques which have been investigated are significantly fewer in number than those for intensity modulation

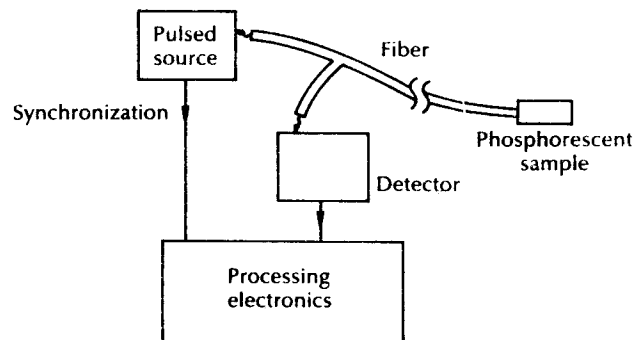


Figure 14.24 Fluoroptic temperature sensor [Ref. 102].

because the demodulation method is inherently more complex, often requiring some form of spectrometer [Ref. 95].

Extrinsic single-mode fiber sensors have been developed to provide noninvasive measurement for several physical measurands (e.g. velocity, fluid surface velocity and vibration). In particular, the all-fiber laser Doppler velocimeter (LDV) illustrated in Figure 14.25 allows the measurement of velocity in gases and fluids, as well as the velocity of objects, to be taken. The arrangement shown in Figure 14.25 employs two single-mode fibers to guide the transmitted beams to and from the probe. A fiber directional coupler is used at the probe to obtain two beams from the single incoming beam. The measurement volume is formed by the region of intersection of these two coherent optical beams which are independently scattered and Doppler shifted. A Doppler difference technique is then employed because the frequency shift is different for each beam as they are travelling in different directions. The two frequency shifts beat together to produce a frequency δf_{Do} which is proportional to the component of velocity of the scattering particle v perpendicular to the mean direction of the incident beams and in their plane, so that [Ref. 89]:

$$\delta f_{Do} = \left| \frac{2v}{\lambda} n \sin \frac{\theta}{2} \right| \quad (14.2)$$

where λ is the wavelength of the laser source, n is the refractive index of the measurement volume and θ is the angle of convergence between the two input beams.

It may be noted that Eq. (14.2) suggests an ambiguity in the direction of the velocity which may introduce serious errors. This problem can be resolved, however, through the introduction of a frequency shift into one of the transmitted beams. Hence the fiber modulator shown in Figure 14.25 produces the required frequency shift. With such a fiber LDV system, velocity can be measured with high precision in a short period of time. In addition, arrangements based on the classical

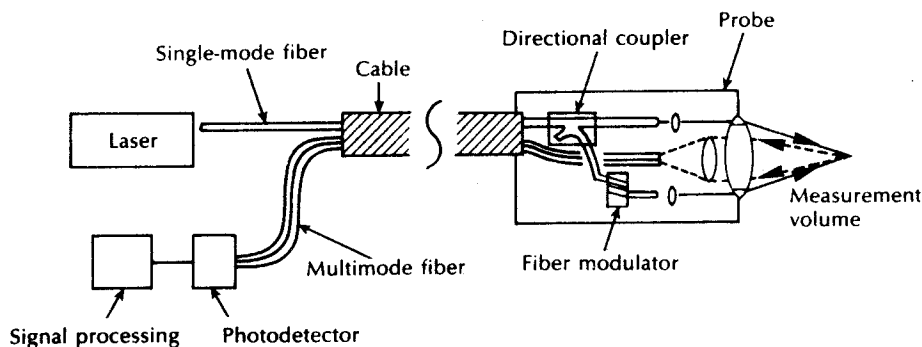


Figure 14.25 Optical fiber laser Doppler velocimeter.

interferometer configurations (e.g. Mach–Zehnder, Fabry–Perot and Michelson) have been employed to produce fiber laser vibrometers for remote vibration measurement [Ref. 89]. Finally, resonant structures, particularly those employing micromachined silicon resonators have attracted increasing interest for application within optical sensor devices in recent years [Refs. 91, 106]. In particular this work has focused upon optically actuated micromachined silicon devices in which a transmitted optical signal is partially absorbed by the resonator structure, creating thermal strain and hence mechanical excitation.* The subsequent detection of the movement of the mechanical system is based on interferometric and/or intensity modulation techniques using the remaining optical signal. For example, such devices have been demonstrated incorporating thermally absorbing surfaces on miniature (10 μm long) silicon bridges [Ref. 91]. In these devices incident optical powers of less than 20 μW (usually delivered via single-mode fiber) are sufficient to produce 10 nm displacements.

Generally, intensity modulation is preferred for use with silicon micromachined devices when the oscillation frequency is relatively low (i.e. less than 20 kHz), whilst the more complex interferometric detection tends to be employed at higher oscillation frequencies. Nevertheless, a steadily increasing number of examples of optical sensor devices using silicon as optically energized microresonators are being reported [Ref. 106], even though the potential ageing and failure mechanisms have still to be fully explored.

14.6 Computer applications

Modern computer systems consist of a large number of interconnections. These range from lengths of a few micrometres (when considering on-chip, very large scale integration (VLSI) connections) to perhaps thousands of kilometres for terrestrial links in computer networks. The transmission rates over these interconnections also cover a wide range from around 100 bit s^{-1} for some teletype terminals to several hundred Mbit s^{-1} for the on-chip connections. Optical fibers are starting to find application in this connection hierarchy where secure, interference-free transmission is required.

Although in its infancy, integrated optics has stimulated interest in connections within equipment, between integrated circuits, and even within hybrid integrated circuits, using optical techniques. Much of this work is still at the research stage and therefore was discussed in Sections 10.5 and 10.6. Moreover optical transmission techniques and optical fibers themselves have found application within data processing equipment. In addition, as indicated in Sections 10.7–10.9 investigations have already taken place into the use of optical fibers for mains isolators and digital data buses within both digital telephone exchanges and computers. Their small size,

* The mechanical excitation of these devices can be explained by photoacoustic effects [Ref. 106].

low loss, low radiation properties and freedom from ground loops provide obvious advantages in these applications.

At present, however, a primary application area for optical fiber communications remains interequipment connections. These provide noise immunity, security and removal of earth loop problems, together with increased bandwidth and reduced cable size in comparison with conventional coaxial cable computer system interconnections. The interequipment connection topology for a typical mainframe computer system (host computer) is illustrated in Figure 14.26. The input/output (I/O) to the host computer is generally handled by a processor, often called a data channel or simply channel, which is attached to the main storage of the host computer. It services all the I/O requirements for the system allowing concurrent instruction processing by the central processing unit (CPU). Each data channel contains an interface to a number of I/O control units. These, in turn, control the I/O devices (e.g. teletypes, visual display units, magnetic disk access mechanisms, magnetic tape drives and printers). When metallic cables are used, the interface between the data channel and the control units comprises a large number (often at least forty-eight) of parallel coaxial lines incorporated into cables. An attractive use of optical fiber interconnection is to serialize this channel interface [Ref. 107] using a multiplex system. This significantly reduces cable and connector bulk and improves connection reliability.

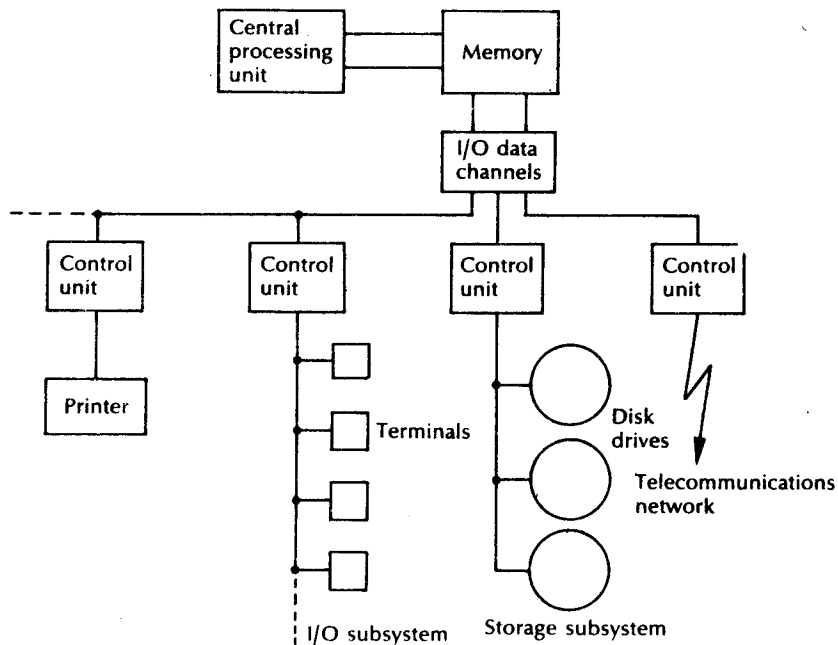


Figure 14.26 Block schematic of a typical mainframe computer system.

Optical fiber links of this type were demonstrated in 1978 by Sperry Univac [Ref. 108], and subsequently Fujitsu developed a product to perform the same function. However, neither of these systems offered enhanced channel performance as measured by the product of bit rate and link length. Developments are therefore continuing with regard to high performance channel links utilizing new protocols for data exchange. An early prototype [Ref. 107] optical fiber serial subsystem designed by IBM Research operates at 200 Mbit s^{-1} over distances of up to 1 km. This system utilized a laser chip mounted on a silicon substrate with the fiber encapsulated in a monolithic dual in line package, and a single chip, high sensitivity, silicon *p-i-n* receiver.

A more recent development to provide high speed communication on a backbone network for use in computer centres is called Datapipe [Ref. 109]. Initially, this system comprised a 275 Mbit s^{-1} single-mode fiber link which could operate over a radius of 30 km. Subsequently, the system was developed to give a 500 Mbit s^{-1} transmission rate providing a site capability of 1 Gbit s^{-1} when a redundant system was installed.

The other interconnection requirement for the mainframe computer system is between the I/O control units and the I/O terminals. Again, optical fiber systems can provide high speed, multiplexed, secure communication links to replace the multitude of coaxial cables normally required for these interconnections. An example of such a fiber system utilizes a multiplexing system on to a single optical fiber cable for connecting an IBM 3274 controller to its terminals [Ref. 110]. In this case up to thirty-two terminals and printers can be linked to the controller in either a point to point or multidrop* configuration employing a star coupler or beam splitters. This interconnection requirement is often extended due to the trend of connecting numbers of processors together in order to balance the system work load, increase system reliability and share storage and I/O devices. Hence optical fiber systems have been developed for use in local area networks.

14.7 Local area networks

A local area network (LAN), unlike the local telecommunication network, is an interconnection topology which is usually confined to either a single building or group of buildings contained entirely within a confined site or establishment (e.g. industrial, educational, military, etc.). The LAN is therefore operated and controlled by the owning body rather than by a common carrier.† Optical fiber

* The multidrop bus configuration will not allow interconnection of as many as thirty-two terminals due to the insertion losses obtained at the beam splitters or T-couplers.

† Another possible definition of a LAN, based on speed and range of operation, is that a LAN typically operates at a transmission rate of between 100 kbit s^{-1} and 100 Mbit s^{-1} over distances of 500 m to 10 km. Hence a LAN is intermediate between a short range, multiprocessor network (usually data bus) and a wide area network which has historically provided relatively low speed data transmission (up to 100 kbit s^{-1}) over very long distances using conventional communications technology. However, it must be noted that there are always exceptions to these general definitions which are already increasing in number as the technology advances.

communication technology is finding application within LANs to meet the on-site communication requirements of large commercial organizations and to enable access to distributed or centralized computing resources.

Figure 14.27 shows the Open Systems Interconnection (OSI) seven layer network model which was originally developed for wide area networks (WANs). This model, which has been developed by the International Organization for Standardization (ISO), provides a standard architecture that defines communication tasks into a set of hierarchical layers within networks. Each layer performs a related set of functions required in order that one system (nominally a heterogeneous computer) will be able to communicate with another system. The partitioning of these functions following logical methodology was undertaken by an ISO subcommittee, resulting in the reference model comprising seven layers which are listed with a brief definition in Table 14.6.

As there are fundamental differences between LANs and WANs it has been found necessary to redefine the two bottom layers of the OSI model into three layers, as displayed in Figure 14.27. The physical layer, as in the WAN, is responsible for the physical transmission of information.

The functions of data link layer, however, are separated into two layers: namely, the logical link control (LLC) layer which assembles/disassembles data frames or packets and provides the appropriate address and error checking fields, and the medium access control (MAC) layer which organizes communications over the link. The MAC layer embodies the set of logical rules or the access protocol which allow nodes to access the common communication channel, and several MAC options may therefore be provided for the same LLC layer. Furthermore, another major

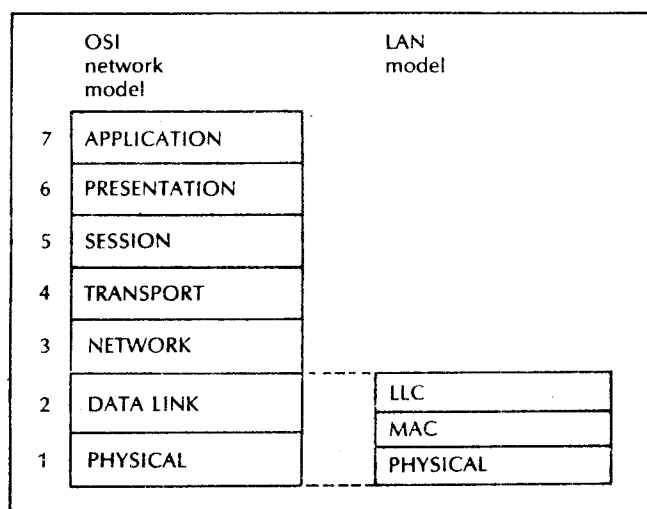


Figure 14.27 Network reference models: OSI and LAN modification.

Table 14.6 Principal functions for the seven levels of the OSI reference model.

1. PHYSICAL	-	For interfacing to the physical transmission medium. Concerned with transmission of unstructured bit stream over the physical link.
2. DATA LINK	-	Provides for the reliable transfer of data across the physical link; controls the transmission and reception of blocks with necessary synchronization, error and flow control.
3. NETWORK	-	For interworking with the underlying telecommunication network. Provides upper layers with independence from data transmission technologies.
4. TRANSPORT	-	Provides reliable transparent transfer between end points; end to end synchronization, flow control and error recovery.
5. SESSION	-	For tying terminals to applications during a session; establishes, manages and terminates connections (sessions).
6. PRESENTATION	-	Provides for manipulation of the data structure. Performs useful transformations on data (eg. encryption, text compression, reformatting).
7. APPLICATION	-	Provides services to the users of the OSI environment (eg. data base management, network management).

difference between WANs and LANs is that each node on the network can be directly connected to all others, thus eliminating the need for routing via the network layer. As a result of this high degree of connectivity, the specific topologies shown in Figure 14.28 have become commonplace [Ref. 111].

The basic optical fiber LAN topologies are the bus, ring and star [Refs. 112, 113]. In the bus topology, data generally circulate bidirectionally. Data are input and removed from the bus via four port couplers located at the nodes (see Section 5.6.1). In the ring, configuration data usually circulate unidirectionally, being looped through the nodes at each coupling point and hence repeatedly regenerated in phase and amplitude. The optical star forms a central hub to the network which may be either active or passive. In passive operation, the star coupler (see Section 5.6.2) at the hub splits the data in terms of power, so that they are available to all nodes. Line losses are therefore primarily determined by the degree of splitting. With an active hub the data are split electrically in the active star coupler and therefore the only causes of line loss are the fiber and splice/connector losses.

The design of the MAC layer is crucial in LANs because, in general, it is the efficiency of the access protocol which governs the availability of the bandwidth

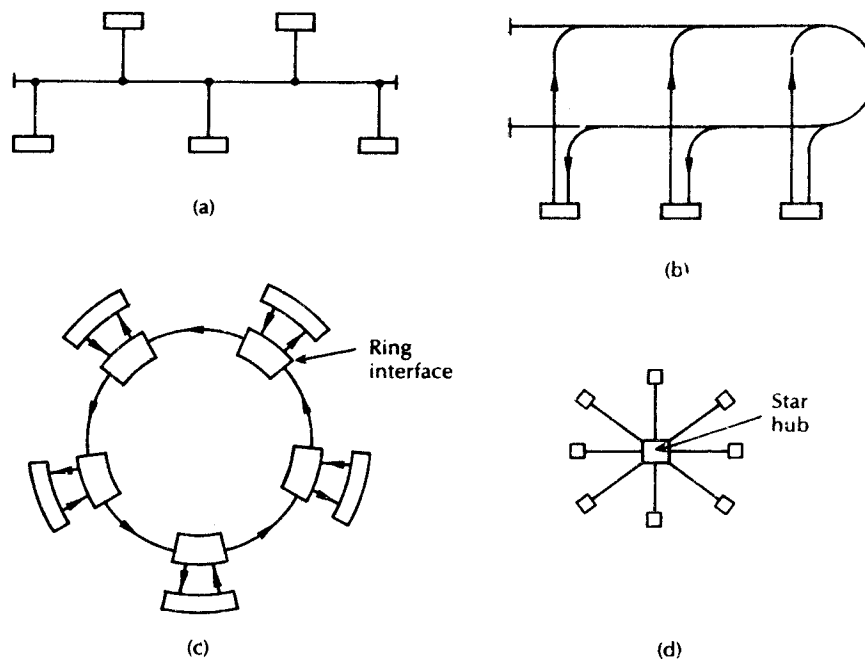


Figure 14.28 Common LAN topologies: (a) linear bus; (b) U-bus; (c) ring; (d) star.

provided by the network for the dual functions of data transmission and channel arbitration. Three specific types of access protocol have gained a fair degree of acceptance, primarily because of their simplicity. These are: (1) random access protocols, the most popular example of which is carrier sense multiple access with collision detection (CSMA/CD) used on the Ethernet LAN; (2) token passing protocols; and (3) time division multiple access (TDMA) protocols.

With CSMA/CD protocols, nodes are allowed to transmit their data as soon as the communication channel is found to be idle (i.e. carrier sense). If the transmissions from two or more nodes collide, the event is detected by the physical layer hardware and the nodes involved terminate transmission before attempting retransmission after a random time interval. Token passing protocols behave as distributed polling systems in which nodes sequentially obtain permission to use the channel. The channel arbitration is determined by the possession of a small distinctive bit packet, known as a token, which can only be held by one node (which is then permitted to use the channel) at any one time. When the data transmission from that node is completed it passes the token packet to the next node in the logical sequence. Finally, with basic (i.e. fixed assignment) TDMA protocols, each node on the network is assigned a fixed length time slot during which it may

transmit data. In this way, the protocol operates in a similar manner to that of time division multiplexing on a point to point link (see Section 11.5).

A schematic of an optical fiber regenerative repeater (see Section 11.6.1) which may be used to restore the attenuated signal power in an optical fiber LAN is displayed in Figure 14.29(a). In addition, this device may be employed as an active tap to allow the interconnection of numerous nodes within ring or linear bus topologies. The use of such repeater interfaces allows similar topologies to be realized for optical fiber LANs as their metallic counterparts, but with certain cost penalties: In order to reduce the number of repeaters required, a range of passive tapping components are available (see Section 5.6). Figure 14.29(b) shows a four port tap which allows data to be removed from and added on to a unidirectional optical fiber bus. A pair of three port passive taps which can be used to receive and transmit on to dual linear buses or U-buses are shown in Figure 14.29(c). Unfortunately, as a result of the optical power budget requirements mentioned previously there is an upper limit to the number of passive taps which can be inserted into the linear bus or ring topologies. At present commercial taps incur an excess loss of between 0.1 and 1 dB. In addition to this excess loss the tap must also divert some of the optical signal power to the tapping receiver. Even if the tap only diverts 1% of the transmitted optical signal power, this places a limit of around thirty on the number of taps which may be provided unless active electrical components are included to allow regeneration of the transmitted optical signal.

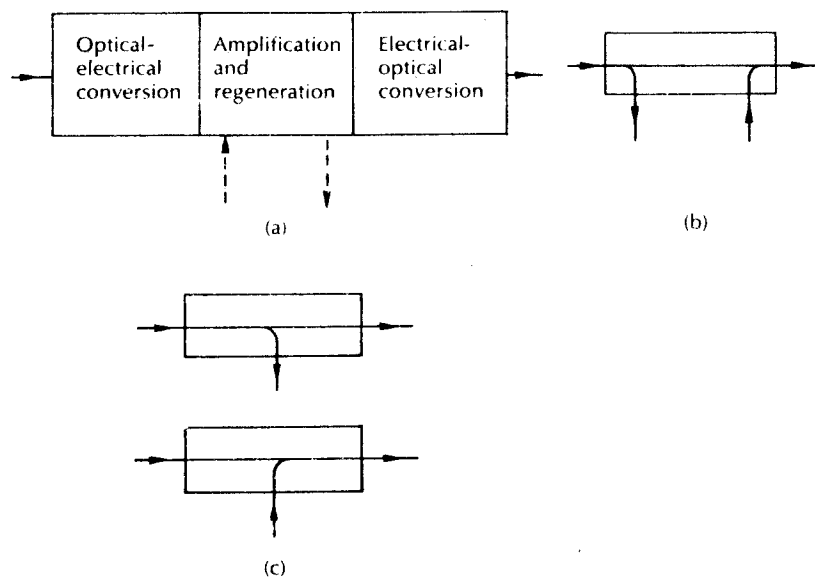


Figure 14.29 Optical fiber LAN tapping devices: (a) regenerative repeater and active tap; (b) four port passive tap; (c) three port passive taps.

Alternatively, the use of optical amplifiers to provide gain and thus enhance the power budgets in such networks is under active consideration (see Section 11.10).

One of the major problems associated with optical fiber buses which use the tapping methods discussed previously is that there is an uneven distribution of the transmitted optical power between the connected receivers. This has two distinct drawbacks, namely that the optical receivers must have a large dynamic range and that detection of the collision events required for CSMA/CD protocols becomes difficult [Refs. 114, 115]. One solution to this problem is to use the passive star couplers discussed in Section 5.6.2. Each node in the star topology has a single input and a single output fiber connected to the hub of the star. Optical power within the input fibers can be distributed more evenly between the output fibers, thus achieving more uniform reception levels. Passive star couplers are currently available using up to 100×100 ports. Typical port to port insertion losses for 32×32 and 64×64 port transmissive passive stars employing multimode fiber are around 19 dB and 23 dB respectively. Variations on the passive star topology include the use of an active star hub [Ref. 116] and the use of cascaded passive stars [Ref. 117].

Activity in the LAN area in general, and more recently in the optical fiber LAN field, has intensified over the last few years as a result of the increasing demand for information technology within commerce and industry. Optical fiber LAN or mixed-media (e.g. fiber and twisted wire pairs) LAN products are available from several equipment suppliers and a good number of networks are at varying stages of development ranging from theoretical studies, sometimes accompanied by experimental investigation, to commercial products [Refs. 118, 119].

An early experiment based on the Ethernet LAN and also developed by Xerox was Fibernet [Ref. 120]. This passive transmissive star network employing nineteen ports and multimode fiber was successfully operated at data rates of 150 and 100 Mbit s^{-1} over distances of 0.5 and 1.1 km, respectively, with zero errors. A more recent development of CSMA/CD network is Fibernet II [Ref. 116] which employs an active star repeater. Collision detection was implemented in the twenty-five port star repeater which was electrically compatible with the standard 10 Mbit s^{-1} Ethernet coaxial cable system. The network span was around 2.5 km, and using eight channel multiplexers the network is capable of handling 200 stations. Alternative passive star-based CSMA/CD networks have been developed by the Codenoll Corporation (Codenet) and Ungermann-Bass Corporation together with the Siecor Corporation to be coupled to their Ethernet compatible Net/One.

Passive bus topologies for optical fiber LANs, as mentioned previously, exhibit drawbacks in relation to optical power losses at the necessary node couplers. However, limited connection bus systems have been demonstrated. For example, Philips have developed a closed optical bus network which can accommodate eight to ten nodes on passive T-couplers. In addition, there are a number of developments by manufacturers (e.g. BICC Data Networks, Siemens) which provide an optical bus interconnection between two coaxial Ethernet segments to form a multimedia network.

Optical fibers have also been demonstrated within the Cambridge ring network [Ref. 121]. This system employing 50/125 μm graded index fiber and LED sources was demonstrated with 245 terminals with distances up to 2 km between adjacent nodes. Several examples of token ring networks have also been demonstrated. For instance the Nippon Electric Corporation Loop 6770 is a 32 Mbit s^{-1} ring which includes fault-tolerance mechanisms for a ring interface bypassing in case of an interface failure. However, more recently interest has been focused on the inclusion of optical fiber versions within specific LANs adopted for standardization. Hence, within the IEEE 802 Committee, optical fiber versions of some standard LANs have been specified. These include the optical fiber Ethernet, based on an active star topology (IEEE 802.3), the optical fiber Token bus (IEEE 802.4H) and the optical fiber Token ring operating at either 4 Mbit s^{-1} or 16 Mbit s^{-1} (IEEE 802.5). Moreover, a standardization development which has been entirely concerned with optical fiber transmission media is entitled the Fiber Distributed Data Interface.

14.7.1 Fiber distributed data interface

Standardization within optical fiber local area networking is currently centred on the Fiber Distributed Data Interface (FDDI) which has been specified by the X3T9.5 working group of the American National Standards Institute (ANSI). Although originally based on the emerging IEEE 802.5, Token ring operating at a data of 4 Mbit s^{-1} , FDDI is intended for use at the much higher data rate of 100 Mbit s^{-1} employing optical fiber transmission media [Refs. 122, 123]. Hence the facilities supported by the FDDI can be summarized as follows:

- (a) 100 Mbit s^{-1} data transfers with a 125 Mbaud transmission using a 4B5B line code;
- (b) up to 100 km of dual ring fiber;
- (c) up to 500 network nodes;
- (d) up to 2 km between nodes;
- (e) timed token passing protocol.

It is envisaged that at one extreme FDDI is suitable for real-time process control and voice applications, with its relatively high data rate, small minimum packet size (9 bytes) and low interpacket gap (8 bytes), whilst at the other extreme the maximum packet size (4500 bytes) provides for efficient large data file transfers such as bit imaged graphics.

The architecture for the FDDI has been made compatible with the OSI model and the IEEE 802 structure, as illustrated in Figure 14.30. The various blocks shown in Figure 14.30 are each the subject of specific areas within the standardization proposals. Hence the physical layer is divided into two sublayers, these being the physical medium dependent (PMD) layer and the physical layer protocol (PHY). The former specifies the required performance of the optical hardware including the optical fibers, connectors, transmitters, receivers and bypass switches [Ref. 124]. Interfacing between the PMD and the data link layer is provided by the PHY

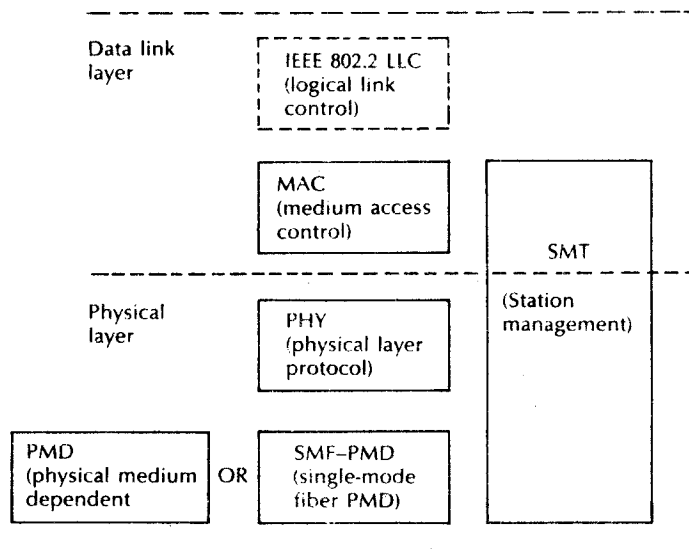


Figure 14.30 FDDI reference model and its relationship to the OSI model.

together with such functions as encoding, clock synchronization and symbol alignment [Ref. 125]. Medium access control for the data link layer is provided by the MAC layer [Ref. 126]. Finally, station management (SMT) controls processes within stations including configuration, fault tolerance and link quality [Ref. 127].

The FDDI network topology consists of stations which are logically connected into a ring. However, two contrarotating rings are employed, each of which is capable of supporting a data rate of 100 Mbits s^{-1} , as shown in Figure 14.31(a). Furthermore, the FDDI can be physically installed as a dual ring incorporating concentrators (or star points) to form a dual ring of trees. This comprises a series of duplex, point-to-point optical fiber links. On each link, the clock is recovered at the receiver from the incoming data. An elasticity buffer of ten bits is employed in each station to absorb the differences between the recovered clock and the local station clock. Jitter on the network is thus partitioned on a per link basis.

The FDDI optical fiber links are specified to use InGaAsP LED sources emitting at a wavelength of $1.3 \mu\text{m}$ to take advantage of the zero (first order) material dispersion point. Five multimode graded index fiber types have now been specified with dimensions (core/cladding) ranging from $50/125 \mu\text{m}$ to $100/140 \mu\text{m}$. However, the two primary recommendations are $62.5/125 \mu\text{m}$ and $85/125 \mu\text{m}$ graded index fibers. Each of the specified fibers has a bandwidth–distance product better than 400 MHz km^{-1} with losses of less than 2 dB km^{-1} at $1.3 \mu\text{m}$. Germanium or InGaAs *p-i-n* photodiode detectors are to be utilized to provide receivers with a sensitivity around -31 dBm at a bit error rate of 10^{-12} [Ref. 128]. The power budget over the 2 km maximum span is specified at 11 dB whilst maintaining the

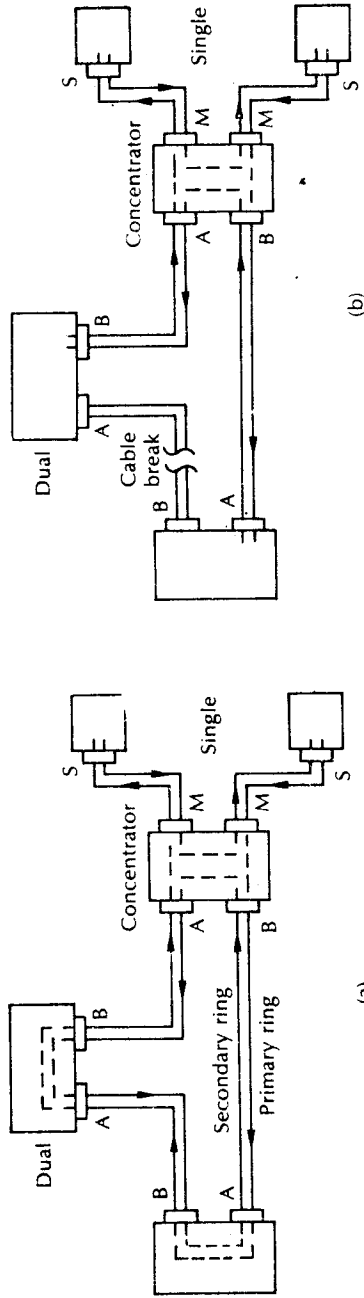


Figure 14.31 FDDI: (a) the dual ring structure; (b) ring reconfiguration on fault detection.

required bit error rate. This results in an overall bit error rate for the network of 10^{-9} .

More recently, a single-mode fiber (SMF) version of the PMD has been defined which utilizes injection laser transmitters [Refs. 123, 129]. This development is shown in Figure 14.30 as SMF-PMD. Two power level categories for the laser transmitters have been specified, the lower level of which retains the same optical receivers as the basic multimode fiber PMD. Nevertheless, it is intended that the SMF-PMD will enable individual links to be extended up to 60 or possibly even 100 km [Ref. 123]. Interestingly, however, the network data rate is set to remain at 100 Mbit s^{-1} (125 Mbaud) under this single-mode fiber standardization proposal [Ref. 129].

The FDDI has in-built recovery mechanisms to enhance its robustness. Network operation is normally designated to the primary ring (Figure 14.31(a)). However, if this ring is broken, then transmission is switched to the secondary ring. The reconfiguration of stations around a cable break, as illustrated in Figure 14.31(b), is controlled by the station management function. In addition, station failure does not affect the network operation due to the provision of optical bypass switches within all the stations. This ensures that the optical path through a station is maintained in the event of a station fault, or power down.

The token passing protocol aspects of the FDDI are somewhat similar to the IEEE 802.5 token passing ring. Each station in the scheme is allowed to transmit only when it is in possession of a token which is circulated sequentially around the stations on the ring. The basic FDDI protocol (i.e. FDDI-1) has provision for handling two priority classes of data traffic: synchronous and asynchronous. At each station, transmission under these classes is controlled by employing timers and by specifying the percentage of the ring bandwidth that can be used by synchronous traffic [Ref. 130].

In order to cater for periodic deterministic traffic, traffic with a single time reference (e.g. speech, possibly video), a circuit-switched mode of operation within the protocol has recently been defined [Refs. 123, 131, 132]. This development, which is referred to as FDDI-11, allocates the 100 Mbit s^{-1} bandwidth of FDDI to circuit-switched data increments of $6.144 \text{ Mbit s}^{-1}$ isochronous channels. These $6.144 \text{ Mbit s}^{-1}$ portions of circuit-switched data bandwidth are known as wideband channels (WBCs). Up to sixteen WBCs may be assigned using a maximum of $98.304 \text{ Mbit s}^{-1}$ of bandwidth. Each of these WBCs offers a full duplex highway which may in turn be flexibly reallocated into a variety of subhighways at modular rates of 8 kbit s^{-1} (e.g. 8 kbit s^{-1} , 64 kbit s^{-1} , 384 kbit s^{-1} , $1.536 \text{ Mbit s}^{-1}$ and $2.048 \text{ Mbit s}^{-1}$ or combinations thereof). When all sixteen WBCs are allocated, a residual token channel of 768 kbit s^{-1} capacity remains, after allowance for the preamble and cycle header. This packet bandwidth, which consists of twelve bytes every cycle ($125 \mu\text{s}$), is known as the packet data group (PDG) and is interleaved with the sixteen WBCs. Moreover, WBCs may be assigned on a real-time basis with any of the unassigned bandwidth being made available to the token passing channel. Finally, several WBCs can be combined into aggregates to satisfy the

requirements of video, or applications necessitating bandwidths in excess of $6.144 \text{ Mbit s}^{-1}$.

The above implementations of FDDI (i.e. 1 and II) incorporate the same PMD layer equipments which allow station spacings of up to 2 km for multimode fiber, or perhaps up to 100 km with single-mode fiber. The implementation of FDDI-II, however, requires an additional standard relating to the hybrid ring control (HRC) [Ref. 133]. The HRC has become the new lowest sublayer of the data link layer, being positioned below and between the MAC and PHY layers, as illustrated in Figure 14.32. It multiplexes data between the (packet) MAC and the isochronous MAC (I-MAC). This function requires that the (packet) MAC be able to transmit data on a noncontinuous basis because packet data are interleaved with isochronous data.

FDDI networks are perceived to have a range of applications within the local area, as illustrated in Figure 14.33. At present a likely application area is as a backbone network for the interconnection of other smaller, lower speed LANs. Some examples are the connection of Ethernet (IEEE 802.3), Token bus (IEEE 802.4) and the Token ring (IEEE 802.5). However, it is also suggested [Ref. 132] that the FDDI could operate as a back-end network for the interconnection of mainframes or minicomputers to peripheral controllers, communication controllers, file servers, database machines, laser printers, etc. Although FDDI networks could possibly provide a replacement for common networks utilized in this area such as Hyperchannel, it is the case that current (nonstandard) developments in this application area are targeted at transmission rates of around 500 Mbit s^{-1} [Ref. 109].

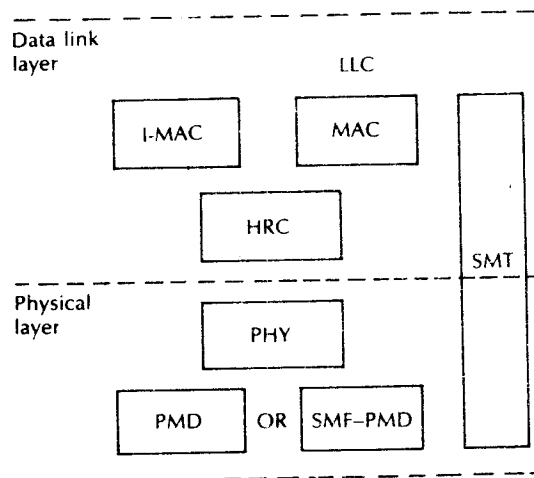


Figure 14.32 FDDI-II relationship to the OSI model.

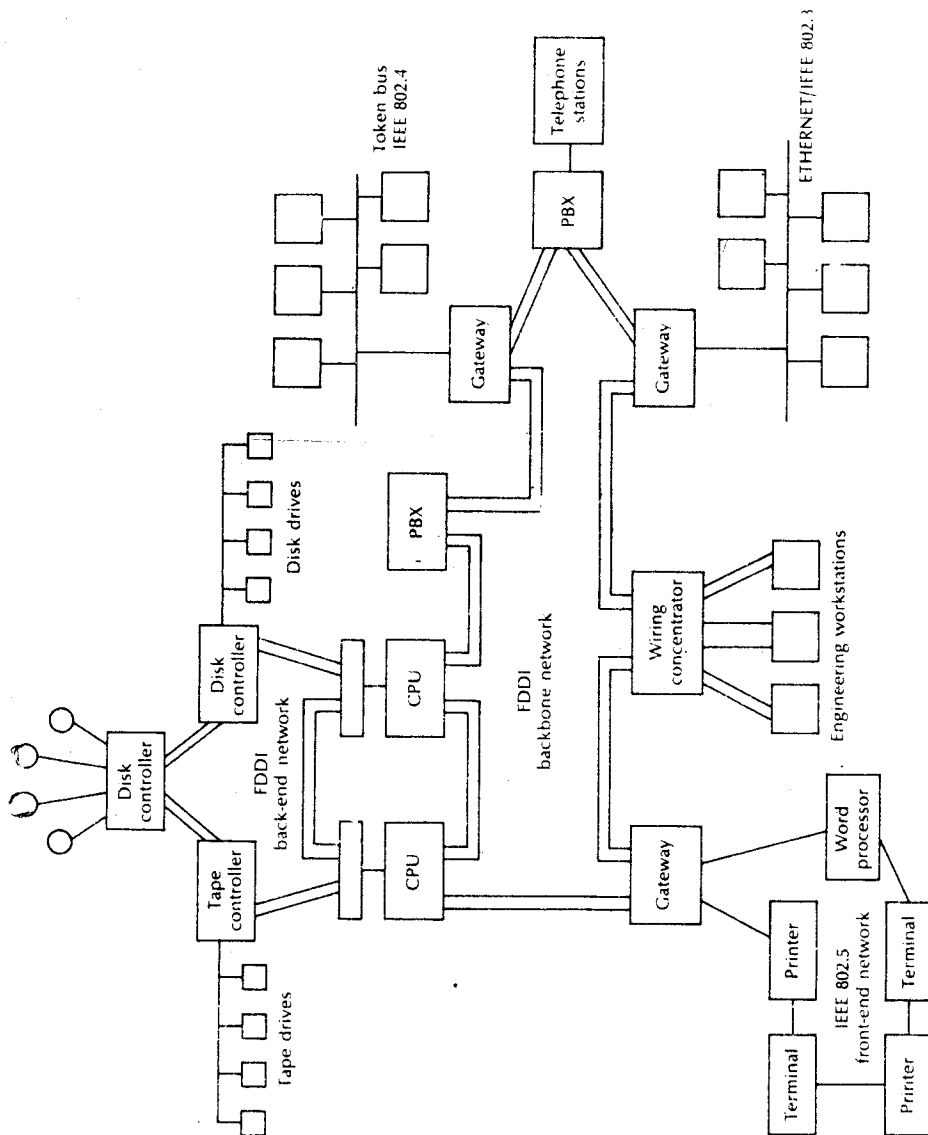


Figure 14.33 Application example for FDDI LANs.

Front-end networks are perhaps the most rapidly expanding application area for FDDI networks [Ref. 132]. Engineering work stations such as computer aided design terminals use a variety of accelerators, processors and LANs. However, it is normally the LAN which ultimately limits the useful performance of such devices. It is here that the bandwidth of FDDI networks should prove sufficient to provide real-time support. In this context it is apparent that FDDI networks (particularly FDDI-11) may well find widespread application within industrial environments. The obvious advantages of the fiber transmission media coupled with much higher bandwidth capacity in comparison with other LAN standardization proposals must assist FDDI LANs for use in such application areas. In addition, the mixed traffic capability to be offered by the FDDI-11 protocol, as well as the fault tolerant dual ring approach, must make these networks an attractive proposition for the provision of backbone and/or front-end networks on industrial sites and within manufacturing premises. It must be noted, however, that to date commercial developments of FDDI LANs have concentrated on the FDDI-1 protocol and it is not clear how quickly FDDI-11 products will become available [Ref. 134].

Notwithstanding the above comment, work is also in progress to define the next generation of LANs which will supersede the FDDI. The so-called 'FDDI follow-on LAN' (FFOL) has been discussed by an ANSI working group since 1990 [Ref. 135]. It is suggested that FFOL would act as a backbone for FDDI networks or as a higher speed front-end network. The proposed data rates for FFOL are intended to integrate with those of the future public telecommunications network under the SDH and SONET developments (see Section 14.2.5), being in the range 150 Mbit s^{-1} to 2.5 Gbit s^{-1} . Furthermore, it is envisaged that the follow-on LAN will also have a dual ring configuration employing optical fiber transmission media. It is suggested that both single-mode and multimode fibers will be put into the FFOL standardization process [Ref. 135], the former fibers providing for the higher speeds over longer distances (e.g. tens of kilometres) whilst the latter graded index fibers would be operated at data rates up to 622 Mbit s^{-1} over distances of around 300 m.

14.7.2 Industrial networks

Various models for industrial communications have been suggested [Refs. 136 to 138], including the four level hierarchical structure illustrated in Figure 14.34. In this structure the factory level (level 1) connects all systems in the plant ranging from administrative to the computer aided design/computer aided manufacturing (CAD/CAM) functions. Office services at level 2 include input/output (I/O) devices and database management. Manufacturing services at this second level include overall planning functions such as numerical-control program distribution together with materials handling and scheduling. At level 3 a cell might typically be a flexible manufacturing system or a warehouse storage unit. At the fourth, or application,

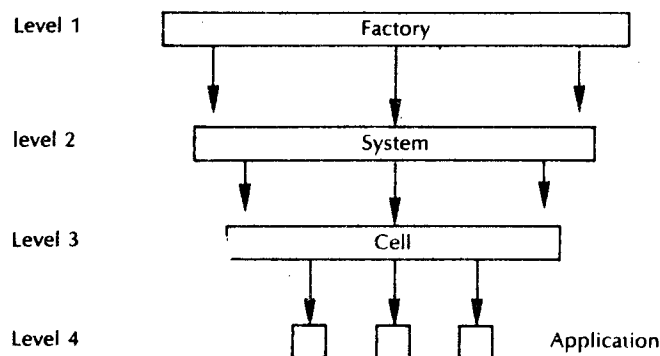


Figure 14.34 Model for industrial communications.

level, controller specific connections occur serving robots, machine tools, computer numerical controllers (CNCs) and, perhaps, advanced guided vehicles (AGVs).

As the service requirements differ from level to level an approach has been suggested [Refs. 136 to 138] whereby each level may adopt its own protocol. For example, application/cell connections generally require a real-time response for automatic monitoring and control, whereas I/O and database transactions at the system level are not critically dependent on message delays. In order to maintain flexibility without increasing complexity a more attractive approach is to employ a single access protocol solution. Hence, in this case all the offered traffic is seen by the network at the same level and the service requirements placed on the protocol for each device may be considered in this context.

A major development over the past few years in industrial local area networking is the Manufacturing Automation Protocol (MAP) activity initiated by General Motors in the United States to fulfil their future factory communication requirements [Ref. 139]. This development has broadened to include many other manufacturing concerns, together with major vendors on an international front. The MAP 3.0 specification which is compatible with the OSI reference model defines a broadband (i.e. frequency division multiplexed) coaxial cable network employing a token passing protocol which originates from the IEEE 802.4 Token bus proposals. Two adjacent 6 MHz channels on the LAN are utilized to provide a data rate for industrial traffic of 10 Mbit s^{-1} . The specification also includes a carrier band option on a single channel operating at 5 Mbit s^{-1} .

Included within the MAP 3.0 specification is an appendix on fiber optics which was written by the European Map User Group (EMUG WG2). The appendix, whose object is to allow the use of optical fiber within MAP where it is considered the appropriate medium, recommends two specific options from the IEEE 802.4 and 802.5 proposals [Ref. 140]. These are:

Token bus (IEEE 802.4H).

- (a) use of single passive star with up to thirty-two ports and excess loss less than 3 dB (Figure 14.35);
- (b) transmission rate of 10 Mbit s^{-1} ;
- (c) operating wavelength at $0.85 \mu\text{m}$;
- (d) high sensitivity power budget of 30 dB;
- (e) use of dual window multimode fiber with losses of less than 3 dB km^{-1} at $0.85 \mu\text{m}$ and 1 dB km^{-1} at $1.3 \mu\text{m}$.

Token ring (IEEE 802.5C)

- (a) use of dual ring configuration;
- (b) transmission rate of 16 Mbit s^{-1} ;
- (c) operating wavelength at $0.85 \mu\text{m}$;
- (d) the use of optical fiber bypass relays as an option;
- (e) use of dual window multimode fiber with losses of less than 3 dB km^{-1} at $0.85 \mu\text{m}$ and 1 dB km^{-1} at $1.3 \mu\text{m}$.

The above recommendations within MAP are intended to provide the basis for lower speed industrial optical fiber networks whereas FDDI will provide for some of the higher speed traffic requirements.

The Token ring recommendation within MAP has been suggested in part to cater for networks requiring in excess of thirty-two stations. However, an attractive

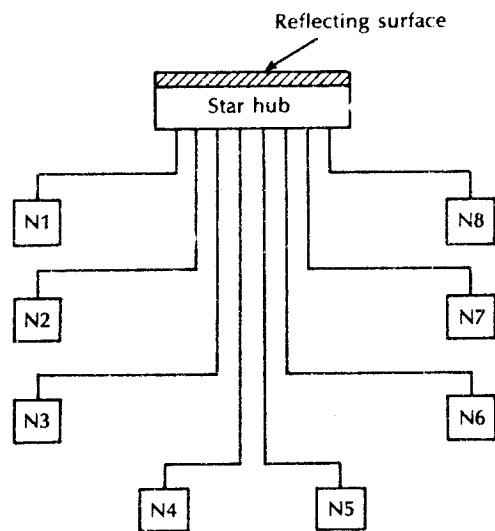


Figure 14.35 Passive star optical fiber LAN topology shown with reflective star coupler hub.

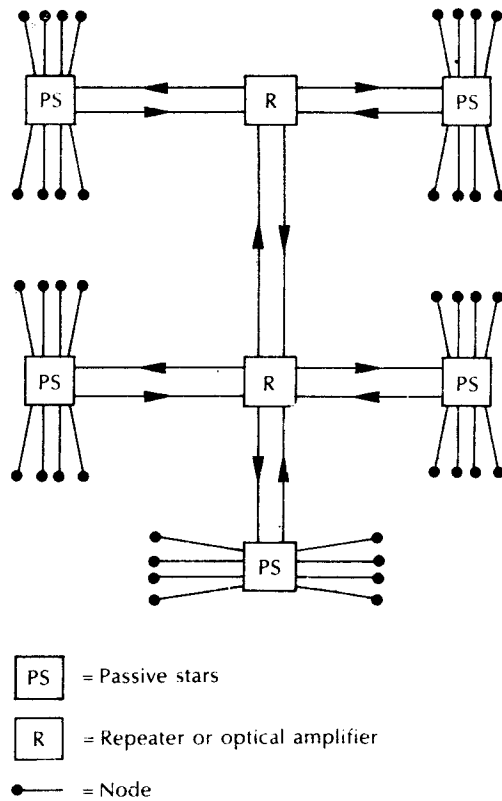


Figure 14.36 Multiple passive star optical fiber LAN topology.

alternative which has not as yet been specified is the use of a multiple star topology [Ref. 141]. Such a configuration is shown in Figure 14.36 in which the smaller passive star coupler devices (see Section 5.6.2) are interconnected by active repeaters. This topology reduces the quantity of fiber required as the large distances on a site are covered by the interstar links. Furthermore, with single-mode fiber networks the active repeaters could be provided by optical amplifiers (see Section 11.9), or even in the future by a derivative of the recently demonstrated optical regenerator [Ref. 142] so that the interstar signals remain in the optical domain. The modular configuration of the multiple star topology is also particularly appropriate to the cellular nature of modern automated production processes and flexible manufacturing systems (FMS) [Ref. 143].

Generally within FMS, a number of automated devices are grouped together to form a flexibly automated cell. A typical industrial plant would then contain a number of these cells, each of which has the capability to perform a variety of automated tasks. Communication is required for the exchange of information

between the devices which are associated with individual automated cells as well as between the various cells. Passive star couplers could therefore be located within cells with the intercellular communication being provided on the interstar links.

References

- [1] M. C. Brierley, P. W. France, R. A. Garnham, C. A. Millar and W. A. Stallard, 'Long wavelength fluoride fibre system using a 2.7 μm fluoride fiber laser, *Proc. Optical Fiber Commun. Conf., OFC'89 (USA)*, Postdeadline paper, PD-14, February 1989.
- [2] K. Iwatsuki, S. Nishi and M. Saruwatari, '2.8 Gbit/s optical soliton transmission employing all laser diodes', *Electron. Lett.*, **26**(1), pp. 1-2, 1990.
- [3] C. P. Sandbank (Ed.), *Optical Fibre Communication Systems*, Chapter X, John Wiley, 1980.
- [4] C. J. Lilly, 'The application of optical fibres in the trunk network', *Telecomm. J. (Eng. edn), Switzerland*, **49**(2), pp. 109-117, 1982.
- [5] R. S. Bergin Jr, 'Economic analysis of fiber versus alternative media', *IEEE J. on Selected Areas in Commun.*, **SAC-4**(9), pp. 1523-1526, 1986.
- [6] P. E. Radley, 'Systems applications of optical fiber transmission', *Radio Electron. Eng. (IERE J.)*, **51**(7/8), pp. 377-384, 1981.
- [7] D. R. Smith, 'Advances in optical fibre communications'. *Physics Bulletin*, **33**, pp. 401-403, 1982.
- [8] A. R. Beard. 'High capacity optical systems for trunk networks', *Proc SPIE Int. Soc. Opt. Eng. (USA)*, **374**, pp. 102-110, 1983.
- [9] P. Cockrane, R. Brooks and R. Dawes, 'A high reliability 565 Mbit/s trunk transmission system', *IEEE J. on Selected Areas in Commun.*, **SAC-4**(9), pp. 1396-1403, 1986.
- [10] P. Cockrane and M. Brain, 'Future optical fiber transmission technology and networks', *IEEE Commun. Mag.*, pp. 45-60, November 1988.
- [11] P. Cockrane, 'Future directions in long haul fibre optic systems', *Br. Telecom Technol. J.*, **8**(2), pp. 5-17, 1990.
- [12] A. Javed, F. McAllum and G. Nault, 'Fibre optic transmission systems: the rationale and application'. *Telesis 1981 Two (Canada)*, pp. 2-7, 1981.
- [13] D. C. Gloge and I. Jacobs, 'Terrestrial intercity transmission systems', in S. E. Miller and I. P. Kaminow (Eds.), *Optical Fiber Telecommunication II*, Academic Press, pp. 855-878, 1988.
- [14] P. Matthijse, 'Essential data on optical fibre systems installed in various countries', *Telecomm. J. (Eng. edn), Switzerland*, **49**(2), pp. 124-130, 1982.
- [15] O. Cottatellucci, F. Lombardi and G. Pellegrini, 'The application of optical fibres in the junction network', *Telecomm. J. (Eng. edn), Switzerland*, **49**(2), pp. 101-108, 1982.
- [16] S. S. Cheng and E. H. Angell, 'Interoffice transmission systems', in S. E. Miller and I. P. Kaminow (Eds.), *Optical Fiber Telecommunication II*, Academic Press, pp. 833-854, 1988.
- [17] R. W. Klessig, 'Overview of metropolitan area networks', *IEEE Commun. Mag.*, **24**(1), pp. 9-15, 1986.

- [18] J. F. Mollenauer, 'Standards for metropolitan area networks', *IEEE Commun. Mag.*, **26**(4), pp. 15–19, 1988.
- [19] J. O'Sullivan, 'The ICEberg project – a broadband network in Ireland', *Br. Telecommun. Eng.*, **9**, pp. 47–49, August 1990.
- [20] T.-H. Wu and M. E. Burrowes, 'Feasibility study of a high-speed SONET self healing ring architecture in future interoffice networks', *IEEE Commun. Mag.*, pp. 33–51, November 1990.
- [21] G. Schweiger and H. Middel, 'The application of optical fibres in the local and rural networks', *Telecomm. J. (Eng. edn), Switzerland*, **49**(2), pp. 93–101, 1982.
- [22] G. Lentiz, 'The fibering of Biarritz', *Laser Focus (USA)*, **17**(11), pp. 124–128, 1981.
- [23] G. A. Trough, K. B. Harris, K. Y. Chang, C. I. Nisbet and J. F. Chalmers, 'An integrated fiber optics distribution field trial in Elie, Manitoba', *IEEE International Conference on Communication, ICC 82, Philadelphia, PA, USA*, 13–17 June 1982, pp. 4D4/1–5, Vol. 2, IEEE, 1982.
- [24] J. R. Fox, D. I. Fordham, R. Wood and D. J. Ahern, 'Initial experience with the Milton Keynes optical fiber cable TV trial', *IEEE Trans. Comm.*, **COM-30**(9), pp. 2155–2162, 1982.
- [25] W. K. Ritchie, 'Multi-service cable-television distribution systems', *British Telecomm. Eng.*, **1**(4), pp. 205–210, 1983.
- [26] W. K. Ritchie, 'The BT switched-star cable TV network', *Br. Telecom Technol. J.*, **2**(4), pp. 5–17, 1984.
- [27] J. R. Fox and E. J. Boswell, 'Star-structured optical local networks', *Br. Telecom Technol. J.*, **7**(2), pp. 76–88, 1989.
- [28] J.R. Stern, J. W. Ballance, D. W. Faulkner, S. Hornung and D. B. Payne, 'Passive optical networks for telephony and beyond', *Electron. Lett.*, **23**(24), pp. 1255–1257, 1987.
- [29] D. W. Faulkner and D. I. Fordham, 'Broadband systems on passive optical networks', *Br. Telecom Technol. J.*, **7**(2), pp. 115–122, 1989.
- [30] T. R. Rowbotham, 'Plans for a British trial of fibre to the home', *Proc. Second IEE Conf. on Telecommun.*, York, UK, pp. 73–77, April 1989.
- [31] D. Clery, 'Trial makes light of cable network', *New Scientist*, p. 28, 27 October 1990.
- [32] S. Fenning and P. Rosher, 'A subcarrier multiplexed broadcast video system for the optical field trial at Bishops Stortford', *Br. Telecom Technol. J.*, **8**(4), pp. 26–29, 1990.
- [33] R. S. Bergen Jr, 'Southern Bell's fiber-to-the-home projects', *Opt. Fiber Commun. Conf. (OFC'88)*, New Orleans, USA, paper WK2, January 1988.
- [34] P. E. White and L. S. Smoot, 'Optical fibers in loop distribution systems', in S. E. Miller and I. P. Kaminow (Eds.) *Optical Fiber Telecommunications II*, Academic Press, pp. 911–931, 1988.
- [35] Y.-K. M. Lin, D. R. Spears and M. Yin, 'Fiber-based local access network architectures', *IEEE Commun. Mag.*, pp. 64–73, October 1989.
- [36] R. M. Huyler, D. E. McGowan, J. A. Stiles and F. J. Horsey, 'SLC Series 5 Carrier System fiber to the home feature', *FOCLAN'88 (USA)*, paper 10.7, 1988.
- [37] S. S. Wagner, H. Kobrinski, T. J. Robe, H. L. Lemberg and L. S. Smoot, 'Experimental demonstration of a passive optical subscriber loop architecture', *Electron Lett.*, **24**(6), pp. 344–346, 1988.
- [38] I. Gallager, J. Ballance and J. Adams, 'The application of ATM techniques to the local network', *Br. Telecom. Technol. J.*, **7**(2), pp. 151–160, 1989.

- [39] J. W. Ballance, P. H. Rogers and M. F. Halls, 'ATM access through a passive optical network', *Electron. Lett.*, **26**(9), pp. 560–588, 1990.
- [40] I. Yamashita, Y. Negishi, M. Nunokawa and H. Wakabayashi, 'The application of optical fibres in submarine cable systems', *Telecom. J. (Eng. edn), Switzerland*, **49**(2), pp. 118–124, 1982.
- [41] P. Worthington, 'Design and manufacture of an optical fibre cable for submarine telecommunication systems', *Proceedings of Sixth European Conference on Optical Communication*, York, UK, pp. 347–356, 1980.
- [42] T. R. Rowbotham, 'Submarine telecommunications', *Br. Telecom. Technol. J.*, **5**(1), pp. 5–24, 1987.
- [43] P. K. Runge and N. S. Bergano, 'Undersea cable transmission systems', in S. E. Miller and I. P. Kaminow (Eds.), *Optical Fiber Telecommunications II*, Academic Press, pp. 879–909, 1988.
- [44] R. L. Williamson, 'Submarine optical telephone cables present status and future prospects', *Proc. SPIE Int. Soc. Opt. Eng. (USA)*, **1120** (*Fibre Optics '89*), pp. 38–42, 1989.
- [45] P. W. Black, 'Undersea system design constraints', *Proc. Soc. Photo-Opt and Instrum. Eng., SPIE*, **1314** (*Fibre Optics '90*), pp. 112–115, 1990.
- [46] P. R. Trischitta and D. T. S. Chen, 'Repeaterless undersea lightwave systems', *IEEE Commun. Mag.*, pp. 16–21, March 1989.
- [47] A. F. Mitchell and W. A. Stallard, 'Application of semiconductor optical amplifiers to submarine systems', *Proc. IEEE ICC '89*, Boston, MA, USA, pp. 1546–1550, June 1989.
- [48] P. Cockrane, 'Future directions in undersea fiber optic system technology', *Proc. IOOC '89*, Kobe, Japan, paper 21B1–2, July 1989.
- [49] M. Saito, 'An over 2200 km coherent transmission experiment at 2.5 Gbit/s using erbium doped fibre amplifiers', *Proc. Opt. Fiber Commun. Conf. OFC '90*, USA, postdeadline, PD2, January 1990.
- [50] T. J. Aprille, 'Introducing SONET into the local exchange carrier network', *IEEE Commun. Mag.*, **28**(8), pp. 34–38, 1990.
- [51] R. Ballert and Y.-C. Ching, 'SONET: now It's the standard optical network', *IEEE Commun. Mag.*, pp. 8–15, March 1989.
- [52] CCITT Recommendation G.707, 'Synchronous Digital Hierarchy Bit Rates', 1989.
- [53] CCITT Recommendation G.708, 'Network Node Interface for the Synchronous Digital Hierarchy', 1989.
- [54] CCITT Recommendation G.709, 'Synchronous Multiplexing Structure', 1989.
- [55] 'American National Standard for Telecommunications-Digital Hierarchy Optical Interface Rates and Formats Specifications', ANSI T1.105 – 1988, Draft, March 1988.
- [56] M. De Block, 'The new synchronous digital hierarchy', *Frost & Sullivan Fibre Optics Conference*, London, UK, section 13, 10–11 April, 1989.
- [57] C. S. Grace and R. H. West, 'Nuclear radiation effects on fibre optics', *Proc. No 53, International Conference on Fibre Optics*, London, 1–2 March 1982, pp. 121–128, IERE, 1982.
- [58] J. G. Farrington and M. Chown, 'An optical fibre multiterminal data system for aircraft', *Fibre and Integrated Optics*, **2**(2), pp. 173–193, 1979.
- [59] J. J. Mayoux, 'Experimental "Gina" optical data bus in the Mirage 4000 aircraft', *Proc. No 53, International Conference on Fibre Optics*, London, 1–2 March 1982, pp. 147–156, IERE, 1982.

- [60] D. L. Williams, 'Military applications of fiber optics', *Proc. SPIE Int. Soc. Opt. Eng. (USA)*, **374**, pp. 138–142, 1983.
- [61] R. James, 'Fly by light for the Skyship 600', *Proc. SPIE Int. Soc. Opt. Eng. (USA)*, **1120**, pp. 217–223, 1989.
- [62] M. J. Kennett and A. E. Perkins, 'The design of a helicopter fibre optic data bus', *Proc. SPIE Int. Soc. Opt. Eng. (USA)*, **1120**, pp. 25–34, 1989.
- [63] P. T. Gardiner and R. A. Edwards, 'Fibre optic sensors (FOS) for aircraft flight controls', *Proc. Royal Aeronautical Soc., Applications of Light to Guided Flight*, London, UK, pp. 42–63, January 1987.
- [64] A. G. Gleave, 'Optical technology aspects of fibre optic guided weapon duplex links', *Proc. Royal Aeronautical Soc., Applications of Light to Guided Flight*, London, UK, pp. 25–31, January 1987.
- [65] M. K. Barnoski, 'Fiber systems for the military environment', *Proc. IEEE*, **68**(10), pp. 1315–1320, 1980.
- [66] P. H. Bourne and D. P. M. Chown, 'The Ptarmigan optical fibre subsystem', *Proc. No 53, International Conference on Fibre Optics*, London, 1–2 March 1982, pp. 129–146, IERE, 1982.
- [67] J. Gladenbeck, K. H. Nolting and G. Olejak, 'Optical fiber cable for overhead line systems', *Proceedings of Sixth European Conference on Optical Communication*, York, UK, pp. 359–362, 1980.
- [68] S. E. Miller, 'Potential applications', in S. E. Miller and A. G. Chynoweth (Eds.), *Optical Fiber Telecommunications*, pp. 675–683, Academic Press, 1979.
- [69] T. Nakahara, H. Kumanaru and S. Takeuchi, 'An optical fiber video system', *IEEE Trans. Commun.*, **COM-26**(7), pp. 955–961, 1978.
- [70] A. C. Deichmiller, 'Progress in fiber optics transmission systems for cable television', *IEEE Trans. Cable Television*, **CATV-5**(2), pp. 50–59, 1980.
- [71] S. R. Cole, 'Fiber optics for CATV applications', *International Conference on Communications*, pp. 38.3.1–4. IEEE, 1981.
- [72] E. A. Lacey, *Fiber Optics*, Chapter 1, Prentice Hall, 1982.
- [73] P. Tolstrup Nielsen, B. Scharøe Petersen and H. Steffensen, 'A trunk system for CATV using optical transmission at 140 Mb/s', *Proceedings of Sixth European Conference on Optical Communication*, York, UK, pp. 406–409, 1980.
- [74] M. Sekita, T. Kawamura, K. Ito, S. Fujita, M. Ishii and Y. Miyake, 'TV video transmission by analog, baseband modulation of a 1.3 μm -band laser diode', *Proceedings of Sixth European Conference on Optical Communication*, York, UK, pp. 394–397, 1980.
- [75] M. Kajino, K. Nishimura, F. Hayashida, T. Otsuka, K. Ito, H. Shiono and T. Yamada, 'A 4-channel WDM baseband video optical fiber system for monitoring of an automated guideway transit', *Proceedings of Sixth European Conference on Optical Communication*, York, UK, pp. 442–445, 1980.
- [76] N. Yumoto, H. Ikeda, T. Sugimoto, K. Hayashi and F. Sakamoto, 'Optical data link for automobiles', *Sumitomo Electr. Tech. Rev.*, **23**, pp. 152–158, 1984.
- [77] R. P. Page, 'A fibre optic multiplexing system for use on a motor car', *Proc. SPIE Int. Soc. Opt. Eng. (USA)*, **522**, pp. 142–147, 1985.
- [78] E. Wolsthoff, 'Ring-main wiring wing light (for cars)', *Funkschau (Germany)*, **5**, pp. 34–35, 1986.
- [79] P. Extance, R. J. Hazelden, J. W. Birch and C. P. Cockshott, 'Fibre optics for monitoring internal combustion engines', *Proc. SPIE Int. Soc. Opt. Eng. (USA)*, **734**, pp. 224–230, 1987.

- [80] C. P. Cockshott, A. J. Cook, R. J. Hazelden, S. J. Pacand, R. A. Pinnock and I. Sakai, 'Applications of optical sensors in the automobile industry', *Proc. SPIE Int. Soc. Opt. Eng. (USA)*, **1120**, pp. 210–214, 1989.
- [81] T. Sasayama and H. Asano, 'Multiplexed optical transmission system for automobiles utilizing polymer fiber with high heat resistance', *Proc. SPIE Int. Soc. Opt. Eng. (USA)*, **989**, pp. 148–155, 1988.
- [82] I. Sakai and C. Stenson, 'Optical sensors for inferring road adhesion', *Proc. SPIE Int. Soc. Opt. Eng.*, **1314**, pp. 236–243, 1990.
- [83] D. A. A. Roworth, 'Fibre optics for industrial applications', *Optics and Laser Technology*, **12**(5), pp. 255–259, 1981.
- [84] P. B. Lyons, E. D. Hodson, L. D. Looney, G. Gow, L. P. Hocker, S. Lutz, R. Malone, J. Manning, M. A. Nelson, R. Selk and D. Simmons, 'Fiber optic application in nuclear testing', *Electro Optics/Laser '79 Conf. Exposition*, Anaheim, CA, 23–25 October, 1979.
- [85] W. F. Trover, 'Fiber optics for data acquisition and control communications: case histories', *Wire Technology*, **9**(2), pp. 79–87, 1981.
- [86] D. E. N. Davies and S. A. Kingsley, 'A novel optical fibre telemetry highway', *Proceedings of First European Conference on Optical Communication*, London, UK, 16–18 September 1975, pp. 165–167, IEE, 1975.
- [87] G. B. Hocker, 'Fiber-optic sensing of pressure and temperature', *Appl. Opt.*, **18**(9), pp. 1445–1448, 1979.
- [88] T. G. Giallorenzi *et al.*, 'Optical fiber sensor technology', *IEEE J. Quantum Electron.*, **18**(4), pp. 626–666, 1982.
- [89] D. A. Jackson and J. D. C. Jones, 'Interferometers', in B. Culshaw and J. P. Dakin, (Eds.), *Optical Fiber Sensors: Systems and Applications*, Artech House, pp. 329–380, 1989.
- [90] H. C. Lefevre, 'Fibre optic gyroscope', in B. Culshaw and J. Dakin, (Eds.), *Optical Fibre Sensors: Systems and Applications*, Vol. 2, Artech House, pp. 381–429, 1989.
- [91] G. D. Pitt, 'Optical fiber sensors', in F. C. Allard, *Fiber Optics Handbook: For Engineers and Scientists*, McGraw-Hill, 1990.
- [92] A. J. Rogers, 'Optical fibre current measurement', *Proc. SPIE Int. Soc. Opt. Eng. (USA)*, **374**, pp. 196–201, 1983.
- [93] J. Wilson and J. F. B. Hawkes, *Optoelectronics: An introduction*. 2nd edn, Prentice Hall, 1989.
- [94] S. K. Yao and C. K. Asawa, 'Microbending fiber optic sensing', *Proc. SPIE Int. Soc. Opt. Eng.*, **412**, pp. 9–13, 1983.
- [95] B. E. Jones, R. S. Medlock and R. C. Spooner, 'Intensity and wavelength-based sensors and optical actuators', in B. Culshaw and J. Dakin, (Eds.), *Optical Fibre Sensors: Systems and applications*, Vol.2., Artech House, pp. 431–473, 1989.
- [96] Cambridge Consultants, 'Optics challenge electronic sensing', *Eureka*, pp. 78–80, 1983.
- [97] J. M. Senior, S. D. Cusworth, N. G. Burrow and A. D. Muirhead, 'An extrinsic optical fibre sensor employing a partially reflecting mirror', *Proc. SPIE Int. Soc. Opt. Eng. (USA)*, **522**, pp. 204–210, 1985.
- [98] B. E. Jones and R. C. Spooner, 'An optical fibre pressure sensor using a holographic shutter modulator with two-wavelength intensity referencing', *Proc. SPIE Int. Soc. Opt. Eng. (USA)*, **514**, pp. 223–226, 1984.
- [99] J. M. Senior, G. Murtaza, A. I. Stirling and G. H. Wainwright, 'Dual-wavelength

- intensity-modulated optical fibre sensor system', *Proc. SPIE Int. Soc. Opt. Eng. (USA)*, **1120**, pp. 332–337, 1989.
- [100] B. Culshaw, J. Foley and I. P. Giles, 'A balancing technique for optical fibre intensity modulated transducers', *Proc. SPIE Int. Soc. Opt. Eng. (USA)*, **574**, pp. 117–120, 1984.
- [101] A. Rogers, 'Measurement using fibre optics', *New Electronics (GB)*, pp. 29–36, 27 October 1981.
- [102] B. Culshaw, 'Optical fibre transducers', *The Radio and Electronic Eng.*, **52**(6), pp. 283–290, 1982.
- [103] S. K. Yao and C. K. Asawa, 'Fiber optical intensity sensors', *IEEE J. Selected Areas in Commun.*, **SAC-1**(3), pp. 562–573, 1983.
- [104] C. Menadier, C. Kissinger and H. Adkins, 'The fotonic sensor', *Instruments and Control Systems*, **40**, pp. 114–120, 1967.
- [105] J. A. Powell, 'A simple two-fiber optical displacement sensor', *Rev. Sci. Instrum.*, **45**(2), pp. 302–303, 1974.
- [106] B. Culshaw, 'Silicon in optical fiber sensors', in B. Culshaw and J. Dakin (Eds.), *Optical Fiber Sensors: Systems and applications*, Vol. 2, Artech House, pp. 475–509, 1989.
- [107] J. D. Crow and M. W. Sachs, 'Optical Fibers for Computer Systems', *Proc. IEEE*, **68**(10), pp. 1275–1280, 1980.
- [108] J. A. Eibner, *Fiber Optics for Computer Applications*, Connector Symp. Proc., Vol. 11, Cherry Hill, NJ, 1978.
- [109] D. Schibonski, 'A 500 megabit network: the applications and issues', *Proc. European Comp. Cqmmun. Conf.*, London, UK, pp. 257–264, June 1987.
- [110] C. P. Wyles, 'Fibre-optic multiplexing system for the IBM 3270 series', *Proc. SPIE Int. Soc. Opt. Eng. (USA)*, **374**, pp. 78–83, 1983.
- [111] D. Clark, K. Pograd and D. Reed, 'An introduction to local area networks', *Proc. IEEE*, **66**, pp. 1497–1517, 1978.
- [112] S. Y. Suh, S. W. Granlund and S. S. Hegde, 'Fiber-optic local area network topologies', *IEEE. Commun. Mag.*, **24**(8), pp. 26–32, 1986.
- [113] M. M. Nasseki, F. A. Tobagi and M. E. Marhic, 'Fiber optic configurations for local area networks', *IEEE. J. Selected Areas in Commun.*, **SAC-3**(6), pp. 941–949, 1985.
- [114] J. W. Reedy and J. R. Jones, 'Methods of collision detection in fiber optic CSMA/CD networks', *IEEE. J. Selected Areas in Commun.*, **SAC-3**(6), pp. 890–896, 1985.
- [115] S. D. Personick, 'Protocols for fiber-optic local area networks', *Journal of Lightwave Technology*, **LT-3**, pp. 426–431, 1985.
- [116] R. V. Schmidt, E. G. Rawson, R. E. Norton, S. B. Jackson and M. D. Bailey, 'Fibernet II: a fiber optic ethernet', *IEEE. J. Selected Areas in Commun.*, **SAC-1**(5), pp. 702–710, 1983.
- [117] T. Tamura, M. Nakamura, S. Ohshima, T. Ito and T. Ozeki, 'Optical cascade star network – a new configuration for a passive distribution system with optical collision detection capability', *Journal of Lightwave Technology*, **LT-2**(1), pp. 61–66, 1984.
- [118] M. R. Finley, 'Optical fibers in local area networks', *IEEE. Commun. Mag.*, **22**(8), pp. 22–23, 1984.
- [119] D. Rosenburger and H. H. Witte, 'Optical LAN activities in Europe', *Journal of Lightwave Technology*, **LT-3**(3), pp. 432–437, 1985.
- [120] E. G. Rawson and R. M. Metcalfe, 'Fibernet: multimode optical fibers for local computer networks', *IEEE. Trans-Commun.*, **COM-26**(7), pp. 983–990, 1978.

- [121] G. W. Lichfield, P. Hensel and D. J. Hunkin. 'Application of optical fibers to the Cambridge ring system', *Proc. 6th Int. Conf. on Computer Commun.*, Sept. 1982, pp. 513-517, 1982.
- [122] F. E. Ross, 'FDDI - a tutorial', *IEEE Commun. Mag.*, **24**(5), pp. 10-17, 1986.
- [123] F. E. Ross, 'An overview of FDDI: the Fiber Distributed Data Interface', *IEEE J. Selected Areas in Commun.*, **7**(7), pp. 1043-1051, 1989.
- [124] FDDI Token Ring Physical Layer Medium Dependent (PMD), American National Standard, ANSI \times 3.166, 1990: ISO Standard 9314-3, 1990.
- [125] FDDI Token Ring Physical Layer Protocol (PHY), American National Standard, ANSI \times 3.138, 1988: ISO Standard 9314-1, 1989.
- [126] FDDI Token Ring Media Access Control (MAC), American National Standard, ANSI \times 3.139, 1987: ISO Standard 9314-2, 1989.
- [127] FDDI Token Ring Station Management (SMT), Draft proposed American National Standard, Rev. 6.2, 15 May 1990.
- [128] T. King, 'Fiber optic components for the Fiber Distributed Data Interface (FDDI) 100 Mbit s⁻¹ local area networks'. *Proc. SPIE Int. Soc. Opt. Eng. (USA)*, **949**, pp. 2-13, 1988.
- [129] FDDI Token Ring Single-Mode Fiber Physical Layer Medium Dependent (SMF-PMD), Draft proposed American National Standard, Rev. 4, April 1989.
- [130] F. E. Ross, 'FDDI - an overview', *IEEE COMPCOM Conf.*, pp. 434-440, 1987.
- [131] K. Caves, 'FDDI - 2: a new standard for integrated services high speed LANs', *Proc. European Computer Commun. Conf.*, (London), pp. 245-256, June 1987.
- [132] S. D. Rigby, 'FDDI speeds networks', *Commun. Int.*, **15**(4), pp. 67-69, 1988.
- [133] FDDI Hybrid Ring Control (HRC), Draft proposed American National Standard, Rev. 6; 11 May 1990.
- [134] A. R. Hills, 'FDDI-II - An implementor's perspective', *The Ninth Annual Europ. Fibre Optic Commun. and Local Area Network Conf.* (London), LAN Proc. pp. 194-200, June 1991.
- [135] G. E. Mityko, 'The FDDI follow-on LAN', *The Ninth Annual Europ. Fibre Optic Commun. and Local Area Network Conf.* (London), LAN Proc. pp. 201-205, June 1991.
- [136] A. Leach, 'Distributing PCs via local area networks', *Control and Instrumentation*, **17**(1), pp. 51-55, 1985.
- [137] J. Keogh, 'Real-time control', *Systems Int.*, **14**(9), pp. 79-81, 1986.
- [138] J. Pingrie, 'MAP users speak out at Satech', *FMS Magazine*, **5**(1), pp. 26-30, 1987.
- [139] P. Cheshire, 'MAP & TOP in perspective: the role of communications', *Proc. European Computer Commun. Conf.* (London), pp. 361-368, June 1987.
- [140] N. C. L. Beale, 'Standard fiber optic LANs and options for MAP', *Proc. European Computer Commun. Conf.* (London), pp. 387-400, June 1987.
- [141] J. M. Senior, W. M. Walker and A. Ryley, 'Topology and MAC layer access protocol investigation for industrial optical fiber LANs', *Computer Networks and ISDN Systems*, **13**, pp. 275-289, 1987.
- [142] C. R. Giles, T. Li, T. H. Wood, C. A. Burrus and D. A. B. Miller, 'An all optical regenerator', *Optical Fiber Commun. Conf., OFC '88, (USA)*, Postdeadline PD22, January 1988.
- [143] J. Chandler and D. Hobson, 'Connecting for FMS - experiences in building of an educational system', *Computer-Aided Engineering Journal*, pp. 13-20, February 1985.

Appendices

A. The field relations in a planar guide

Let us consider an electromagnetic wave having an angular frequency ω propagating in the z direction with propagation vector (phase constant) β . Then as indicated in Section 2.3.2 the electric and magnetic fields can be expressed as:

$$\mathbf{E} = \text{Re}\{\mathbf{E}_0(x, y) \exp j(\omega t - \beta z)\} \quad (\text{A1})$$

$$\mathbf{H} = \text{Re}\{\mathbf{H}_0(x, y) \exp j(\omega t - \beta z)\} \quad (\text{A2})$$

For the planar guide the Cartesian components of \mathbf{E}_0 and \mathbf{H}_0 become:

$$\frac{\partial E_z}{\partial y} + j\beta E_y = -j\mu_r\mu_0\omega H_x \quad (\text{A3})$$

$$j\beta E_x + \frac{\partial E_z}{\partial x} = j\mu_r\mu_0\omega H_y \quad (\text{A4})$$

$$\frac{\partial E_y}{\partial x} - \frac{\partial E_x}{\partial y} = -j\mu_r\mu_0\omega H_z \quad (\text{A5})$$

$$\frac{\partial H_z}{\partial y} + j\beta H_y = j\omega\epsilon_r\epsilon_0 E_x \quad (\text{A6})$$

$$-j\beta H_x - \frac{\partial H_z}{\partial x} = j\omega\epsilon_r\epsilon_0 E_y \quad (\text{A7})$$

$$\frac{\partial H_y}{\partial x} - \frac{\partial H_x}{\partial y} = j\omega\epsilon_r\epsilon_0 E_z \quad (\text{A8})$$

If we assume that the planar structure is an infinite film in the y - z plane, then for an infinite plane wave travelling in the z direction the partial derivative with respect to y is zero ($\partial/\partial y = 0$). Employing this assumption we can simplify the above equations to demonstrate fundamental relationships between the fields in

such a structure. These are:

$$j\beta E_y = -j\mu_r\mu_0\omega H_x \quad (\text{TE mode}) \quad (\text{A9})$$

$$j\beta E_x + \frac{\partial E_z}{\partial x} = j\mu_r\mu_0\omega H_y \quad (\text{TM mode}) \quad (\text{A10})$$

$$\frac{\partial E_y}{\partial x} = -j\mu_r\mu_0\omega H_z \quad (\text{TE mode}) \quad (\text{A11})$$

$$j\beta H_y = j\omega\epsilon_r\epsilon_0 E_x \quad (\text{TM mode}) \quad (\text{A12})$$

$$-j\beta H_x - \frac{\partial H_z}{\partial x} = j\omega\epsilon_r\epsilon_0 E_y \quad (\text{TE mode}) \quad (\text{A13})$$

$$\frac{\partial H_y}{\partial x} = j\omega\epsilon_r\epsilon_0 E_z \quad (\text{TM mode}) \quad (\text{A14})$$

It may be noted that the fields separate into TE and TM modes corresponding to coupling between E_y , H_x , H_z , ($E_z = 0$) and H_y , E_x , E_z ($H_z = 0$) respectively.

B. Gaussian pulse response

Many optical fibers, and in particular jointed fiber links, exhibit pulse outputs with a temporal variation that is closely approximated by a Gaussian distribution. Hence the variation in the optical output power with time may be described as:

$$P_o(t) = \frac{1}{\sqrt{2\pi}} \exp - \left(\frac{t^2}{2\sigma^2} \right) \quad (\text{B1})$$

where σ and σ^2 are the standard deviation and the variance of the distribution respectively. If t_e represents the time at which $P_o(t_e)/P_o(0) = 1/e$ (i.e. $1/e$ pulse width), then from Eq. (B1) it follows that:

$$t_e = \sigma\sqrt{2}$$

Moreover, if the full width of the pulse at the $1/e$ points is denoted by τ_e then:

$$\tau_e = 2t_e = 2\sigma\sqrt{2}$$

In the case of the Gaussian response given by Eq. (B1) the standard deviation σ is equivalent to the rms pulse width.

The Fourier transform of Eq. (B1) is given by:

$$\mathcal{P}(\omega) = \frac{1}{\sqrt{2\pi}} \exp - \left(\frac{\omega^2\sigma^2}{2} \right) \quad (\text{B2})$$

The 3 dB optical bandwidth B_{opt} is defined in Section 7.4.3 as the modulation frequency at which the received optical power has fallen to one half of its constant

value. Thus using Eq. (B2):

$$\frac{[\omega(3 \text{ dB opt})]^2}{2} \sigma^2 = 0.693$$

and

$$\omega(3 \text{ dB opt}) = 2\pi B_{\text{opt}} = \frac{\sqrt{2} \times 0.8326}{\sigma}$$

Hence

$$B_{\text{opt}} = \frac{\sqrt{2} \times 0.8326}{2\pi\sigma} = \frac{0.530}{\tau_e} = \frac{0.187}{\sigma} \text{ Hz}$$

When employing return to zero pulse where the maximum bit rate $B_T(\text{max}) = B_{\text{opt}}$, then:

$$B_T(\text{max}) \approx \frac{0.2}{\sigma} \text{ bit s}^{-1}$$

Alternatively, the 3 dB electrical bandwidth B occurs when the received optical power has dropped to $1/\sqrt{2}$ of the constant value (see Section 7.4.3) giving:

$$B = \frac{0.530}{\tau_e\sqrt{2}} = \frac{0.375}{\tau_e} = \frac{0.133}{\sigma} \text{ Hz}$$

C. Variance of a random variable

The statistical mean (or average) value of a discrete random variable X is the numerical average of the values which X can assume weighted by their probabilities of occurrence. For example, if we consider the possible numerical values of X to be x_1, x_2, \dots, x_i , with probabilities of occurrence $P(x_1), P(x_2) \dots P(x_i)$, then as the number of measurements N of X goes to infinity, it would be expected that the outcome $X = x_1$ would occur $NP(x_1)$ times, the outcome $X = x_2$ would occur $NP(x_2)$ times, and so on. In this case the arithmetic sum of all N measurements is:

$$x_1 P(x_1)N + x_2 P(x_2)N + \dots + x_i P(x_i)N = N \sum_i x_i P(x_i) \quad (\text{C1})$$

The mean or average value of all these measurements which is equivalent to the mean value of the random variable may be calculated by dividing the sum in Eq. (C1) by the number of measurements N . Furthermore, the mean value for the random variable X which can be denoted as \bar{X} (or m) is also called the expected value of X and may be represented by $E(X)$. Hence:

$$\bar{X} = m = E(X) = \sum_{i=1}^N x_i P(x_i) \quad (\text{C2})$$

Moreover, Eq. (C2) also defines the first moment of X which we denote as M_1 . In a similar manner the second moment M_2 is equal to the expected value of X^2 such that:

$$M_2 = \sum_{i=1}^N x_i^2 P(x_i) \quad (C3)$$

M_2 is also called the mean square value of X which may be denoted as $\overline{X^2}$

For a continuous random variable, the summation of Eq. (C2) approaches an integration over the whole range of X so that the expected value of X :

$$M_1 = E(X) = \int_{-\infty}^{\infty} x p_X(x) dx \quad (C4)$$

where $p_X(x)$ is the probability density function of the continuous random variable X . Similarly, the expected value of X^2 is given by:

$$M_2 = E(X^2) = \int_{-\infty}^{\infty} x^2 p_X(x) dx \quad (C5)$$

It is often convenient to subtract the first moment $M_1 = m$ prior to computation of the second moment. This is analogous to moments in mechanics which are referred to the centre of gravity rather than the origin of the coordinate system. Such a moment is generally referred to as a central moment. The second central moment represented by the symbol σ^2 is therefore defined as:

$$\sigma^2 = E[(X - m)^2] = \int_{-\infty}^{\infty} (x - m)^2 p_X(x) dx \quad (C6)$$

where σ^2 is called the variance of the random variable X . Moreover, the quantity σ which is known as the standard deviation is the root mean square (rms) value of $(X - m)$.

Expanding the squared term in Eq. (C6) and integrating term by term we find:

$$\begin{aligned} \sigma^2 &= E[X^2 - 2mX + m^2] \\ &= E(X^2) - 2mE(X) + E(m^2) \\ &= E(X^2) - 2m^2 - m^2 \\ &= E(X^2) - m^2 \end{aligned} \quad (C7)$$

As $E(X^2) = M_2$ and $m = M_1$, the variance may be written as:

$$\sigma^2 = M_2 - (M_1)^2$$

D. Variance of the sum of independent random variables

If a random variable $W = g(X, Y)$ is a function of two random variables X and Y , then extending the definition in Eq. (C4) for expected values gives the expected

value of W as:

$$E(W) = \int_{-\infty}^{\infty} \int_{-\infty}^{\infty} g(x, y) p_{XY}(x, y) dx dy \quad (D1)$$

where $p_{XY}(x, y)$ is the joint probability density function. Furthermore the two random variables X and Y are statistically independent when:

$$p_{XY}(x, y) = p_X(x) p_Y(y) \quad (D2)$$

Now let X and Y be two statistically independent random variables with variances σ_X^2 and σ_Y^2 respectively. In addition we assume the sum of these random variables to be another random variable denoted by Z such that $Z = X + Y$, where Z has a variance σ_Z^2 . If the mean values of X and Y are zero, employing the definition of variance given in Eq. (C6) together with the expected value for a function of two random variables (Eq. (D1)) we can write:

$$\sigma_Z^2 = \int_{-\infty}^{\infty} \int_{-\infty}^{\infty} (x + y)^2 p_{XY}(x, y) dx dy \quad (D3)$$

As X and Y are statistically independent we can utilize Eq. (D2) to obtain:

$$\begin{aligned} \sigma_Z^2 &= \int_{-\infty}^{\infty} \int_{-\infty}^{\infty} (x + y)^2 p_X(x) p_Y(y) dx dy \\ &= \int_{-\infty}^{\infty} x^2 p_X(x) dx + \int_{-\infty}^{\infty} y^2 p_Y(y) dy \\ &\quad + 2 \int_{-\infty}^{\infty} x p_X(x) dx \int_{-\infty}^{\infty} y p_Y(y) dy \end{aligned} \quad (D4)$$

The two factors in the last term of Eq. (D4) are equal to the mean values of the random variables (X and Y) and hence are zero. Thus:

$$\sigma_Z^2 = \sigma_X^2 + \sigma_Y^2$$

E. Closed loop transfer function for the transimpedance amplifier

The closed loop transfer function $H_{CL}(\omega)$ for the transimpedance amplifier shown in Figure 9.9 may be derived by summing the currents at the amplifier input, remembering that the amplifier input resistance is included in R_{TL} . Hence,

$$i_{det} + \frac{V_{out} - V_{in}}{R_f} = V_{in} \left(\frac{1}{R_{TL}} + j\omega C_T \right) \quad (E1)$$

As $V_{in} = -V_{out}/G$, then

$$i_{det} = -V_{out} \left(\frac{1}{R_f} + \frac{1}{GR_f} + \frac{1}{GR_{TL}} + \frac{j\omega C_T}{G} \right) \quad (E2)$$

Therefore,

$$\begin{aligned}
 H_{CL}(\omega) &= \frac{V_{out}}{i_{det}} = \frac{-R_f}{1 + (1/G) + (R_f/GR_{TL}) + (j\omega C_T R_f/G)} \\
 &= \frac{-R_f(1 + 1/G + R_f/GR_{TL})}{[1 + j\omega C_T R_f(1 + R_f/R_{TL} + G)]} \quad (E3)
 \end{aligned}$$

Since,

$$G \gg \left(1 + \frac{R_f}{R_{TL}}\right) \quad (E4)$$

then Eq. (E3) becomes,

$$H_{CL}(\omega) \approx \frac{-R_f}{1 + (j\omega R_f C_T/G)} \text{VA}^{-1}$$

Index

- Absorption, 88–91, 284–286, 423–426
 - glass, 88–91
 - semiconductors, 421–426, 430–435
- Absorption coefficient, 423–425
- Absorption losses in fiber, 88–91
 - extrinsic, 89–91
 - intrinsic, 88–89
 - measurement, 783–787
- Acceptance angle, 16–23
 - meridional rays, 16–19
 - skew rays, 20–23
 - solid, 19–20
- Acceptance cone, 16
- Acceptor impurity, 297, 303–304
- Acousto-optic devices, 535, 541
- Acousto-optic effect, 535, 541
- Activation energy of homogeneous degradation (LED), 410–411
- Advanced guided vehicles (AGVs), 892
- AlGaAs injection laser, 319–320
 - single-mode, 323, 325, 327
- AlGaAs LED, 396, 399
- Alternative test methods (ATMs), 775
- Amplification, optical, 512–572
- Amplifier noise, 478–480
- Amplifiers
 - fiber, 524–30
 - optical, 514–530
 - semiconductor laser, 515–524
- Amplitude shift keying, 672, 702–711, 723–724
 - heterodyne detection, 742–745
 - homodyne detection, 748–749
- Analog modulation (*see also* Modulation, analog), 6, 413, 591–594, 646–652, 655–665
 - injection laser, 584
 - LED, 375, 399, 584
 - pulse, 662–665
- Analog signals, 613, 645–646, 663
- Analog systems (*see also* Optical fiber systems, analog), 6, 643–665, 846
- Analog to digital (A–D) conversion, 613–618, 644
- Antiresonant reflecting optical waveguide (ARROW), 555
- anti-Stokes component, 146
- APD (*see* Avalanche photodiode)
- APD-FET receiver, 498, 500
- APON system, 852
- Applications, 835–895
 - civil, 862–864
 - computer, 877–879
 - consumer, 864–865
 - industrial, 865–866
 - military, 859–862
 - public network, 837–859
 - submerged systems, 852–854
 - synchronous networks, 854–859
 - television, 863–864
- Asynchronous transfer mode (ATM) multiplexing, 844, 851–852
- Atmospheric transmission, 1
- Attenuation
 - coaxial cable, 4, 5
 - fiber, 4, 9, 13, 85–99
 - differential mode, 115
 - joints, 210–227
 - microbending, 197
 - measurements, 779–789
 - radiation-induced, 196–197
- Attenuation coefficient (radiation), 97
- Attenuation measurements, 779–789, 820–827
 - absorption loss in fiber, 783–787
 - cut-back method, 779–783
 - optical time domain reflectometry (OTDR), 822–827
 - portable test set, 820–821
 - scattering loss in fiber, 787–789
 - total fiber, 779–783
- Auger current, 363–364
- Automatic gain control (AGC) of receiver, 500, 604–607
- Avalanche photodiode (APD) detectors, 6, 7, 426, 441–454, 481–486, 627–632, 826
 - asymmetric pulse shape, 443
 - benefits, 451
 - carrier multiplication, 442
 - drawbacks, 451–453
 - excess noise factor, 482–487
 - germanium (Ge), 445–457
 - III–V alloy, 447–451
 - impact ionization, 441
 - microplasmas, 442
 - multiplication factor, 447–448, 453–454
 - optimum, 482–486
 - reach-through structure (RAPD), 443–445
 - receiver noise, 481–488, 627–632
 - speed of response, 442–443
- Bandgap
 - direct, 299–303
 - energy, 297–304, 313–314, 425
 - indirect, 301–303
 - tailoring, 314, 426
- Bandtail states, 307
- Band to band recombination, 303–304
- Bandwidth, 2, 4, 5, 8, 50, 104, 106, 128, 480–481, 490–491, 636–638, 654, 658–662
 - analog system, 653–654, 658–662
 - digital system, 636–638
 - electrical, 104, 404–407

910 Index

- Bandwidth (*continued*)
 - fiber types, 179–186
 - modulation, 375, 404–412
 - optical, 104, 106, 404–407
 - receiver, 481, 491
- Bandwidth-length product, 106, 179–185, 586
- Beam
 - expansion, 244–249
 - splitters, 249–270, 537–542
- Beat length, 137–138
- Bend loss (fiber), 97–99
- Bessel functions, 39–41, 67
 - modified, 67
- Biarritz project (France), 237, 846
- Biconical connector, 240–241
- BIGFON project (Germany), 846
- Bimolecular recombination (LED), 408–409
- Birefringence (modal), 136–141
- Birefringent fibers, 142–145
- Bistable laser diode, 562
- Bistable optical device (BOD), 557–562, 568
- Bit error rate (BER), 344, 471–472, 620, 626–632
- Bit rate, 104, 616–617
 - hierarchies, 617–618, 854–855
- Block codes, 643
- Boltzmann statistics, 286–289
- Bose–Einstein distribution, for incoherent light, 470
- Bragg
 - condition, 333, 546
 - diffraction, 546
 - reflection, 332
 - regime, 545
- Bragg wavelength, 332, 334, 336, 547
 - detuning, 336
- Brillouin fiber amplifiers, 528–530
- Brillouin scattering, 95–96, 146–147, 514
- Broadband Integrated Distributed Star (BIDS), 846–847, 849
- Broadband Integrated Services Digital Network (BISDN), 849
- Broadband passive optical network (BPON), 848–849
- Broadened laser transition, 292
- Buffer jacket, 184–185, 196–198, 200–203
- Buried heterostructure laser (BH), 393
- BURSCHT functions, 849
- Bus networks, 665–669, 849–850, 881, 883–884
- Burrus type LED, 386–389
- Butt jointed connectors, 238–244
- Cable strength members, 202–203
- Cable television, 673, 762–763, 846, 663–864
- Cables, 160–204
 - core, 198–199
 - design, 196–204
 - examples, 199–204
 - fiber buffering, 196–197, 199–204
 - function of, 186
 - sheath and water barrier, 199
 - structural and strength members, 197–198
- Cambridge ring network, 885
- Carrier, 296, 422–423
 - diffusion, 301, 311–313, 385, 431, 443
 - drift, 385, 422–423, 432–435
 - injection, 299–301, 305, 307, 406
 - majority, 297, 299
 - minority, 299–301
 - multiplication in APD, 442, 453–454
 - recombination, 300, 301, 304
- Carrier recovery synchronous demodulator, 733
- Carrier to noise ratio (CNR), 644
- Carson's rule, 658, 661
- Cascaded optical amplifiers, 680–682
- Caustic surfaces (graded index fiber), 50
- Central processing unit (CPU), 564
- Ceramic ferrule, 239
- Chalcogenide glass, 100
- Characteristic length, for fiber, 116
- Chemical vapour deposition (CVD), 169, 171–175, 178
- Chemical vapour purification, 177
- Chopper (optical), 779
- Chromatic dispersion (*see* Intramodal dispersion)
- Civil applications, 862–864
- Cladding of fiber, 14, 35, 58–59, 165, 173, 180–185, 810–812
 - Cladding mode stripper, 779
- Cleaving of fiber, 227–228, 238
- Close circuit television (CCTV) applications, 863–864
- Coaxial cable system
 - attenuation, 4
 - local area networks, 644–645
- Coding (digital), 104–105, 611–612, 641–643
 - coded mark inversion (CMI), 643
 - Manchester (biphase), 611, 642
 - nonreturn to zero (NRZ), 104
 - return to zero (RTZ), 104
- Coherence of laser light, 282, 286
- Coherence length, 120
- Coherence time, 119, 120
- Coherent detection, 412, 703–711
- Coherent optical fiber systems, 700–764
 - basic system, 703–706
 - demodulation schemes, 729–741
 - detection principles, 706–711
 - modulation formats, 723–728
 - practical constraints, 711–723
 - receiver sensitivities, 741–757
 - single and multicarrier systems, 758–764
- Coherent radiation, 286 469–470
- Common antenna television (CATV) applications (*see* Cable TV)
- Communication system
 - coaxial (*see* Coaxial cable system)
 - electrical, 5, 612–617
 - general, 5–7
 - optical fiber (*see* Optical fiber systems)
- Companding (pulse code modulation), 613–614
- Computer
 - applications, 877–879
 - optical, 564–572
- Computer aided design/computer aided manufacturing (CAD/CAM), 891
- Computer architecture, 564
- Computer numerical controllers, 892
- Confinement
 - of carriers, 311–313, 317, 319
 - of photons, 311–313, 317, 319
- Conduction band, 296
- Connection Machine, 567
- Connectors, 237–249
 - biconical, 240–241

- Connectors (*continued*)
 butt jointed, 238–244
 ceramic capillary, 239–240
 double eccentric, 241
 duplex, 242–244
 expanded beam, 244–249
 ferrule, 238–241
 multiple, 242–244
 single-mode, 245–246
 triple ball, 2, 246
- Consumer applications, 864–865
- Contact stripe, 394
- Continuous phase frequency shift keying (CPFSK), 725
- Core (fiber), 165, 173
 diameter measurement, 56–57, 180–185, 812
 diameter mismatch, 222
- Costas loop, 731–732, 737
- Couple cavity laser, 330–331
- Couplers, 249–270
 star, 258–262
 three and four port, 251–257
 wavelength division multiplexing, 262–270, 612
- Coupling length (mode), 776
- Crack velocity (fiber), 191
- Critical angle, 15, 18, 20, 22
- Critical radius of curvature, 74–76
- Crosstalk, 254, 264, 267
- Crystal momentum, 301
 polarization, 144–145
- Cutoff condition (mode)
 graded index fiber, 52–53
 for LP, 121
 step index fiber, 41, 46–47
- Cutoff wavelength
 photodiode, 430
 single-mode fiber, 61–62
- Dark current
 noise, 468, 469, 504
 optical detector, 425–426, 432–433, 445–457
- Dark line defects
 injection laser, 347
 LED, 410–411
- Data channel, of computer, 879
- Datapipe network, 879
- Decibel (dB), 85, 86–88
- Decision
 threshold level (regenerative repeater), 618–621, 623
 time, 618–621
- Degeneracy in atom, 286–289
- Degenerative doping, 306
- Degradation
 LED, 410–412
- Demodulation, 1, 5, 581, 654–662
- Depletion layer (region), 299, 306, 422–423, 431–438, 442–443
- Depletion width, 422–443, 431
- Detectors (*see* Optical detectors)
- DH lasers, 364–365
- Dielectric thin film (DTF) interference, 265–267
- Differential phase shift keying, 727, 728, 733
- Diffraction (Bragg), 546
- Diffraction grating, 263
- Diffusion
 carrier, 299, 311–313, 431, 443
- Digital modulation, 7, 613–618, 642–643
- Digital optics, 557–564
- Digital signals, 104–105, 613–617, 618, 641–643, 846
- Digital transmission (*see also* Optical fiber systems, digital)
 bit error rate (BER), 344, 471–472, 620, 626–632
 error probability, 471
 hierarchies, 618
 intersymbol interference, 102, 620
 regenerative repeater, 618–621, 633
- Direct badgap, 299–303
- Direct detection, 412, 475
- Directional couplers, 249, 251–257
- Dispersion, 46–47, 49, 102–121
 full width pulse broadening, 633
 intermodal, 46–47, 49, 110–119
 graded index fiber, 49, 116–119
 step index fiber, 46–47, 111–116
 intramodal, 107–110, 122–130
 material, 107–110, 123–130
 waveguide, 110, 123–130
 measurements, 789–796, 820–821
 overall fiber, 121–130
 multimode, 121–122
 single-mode, 121–130
 waveguide, 110, 123–130
- Dispersion-equalization penalty, 110, 633–634, 639
- Dispersion flattened fiber (DF), 5, 77, 130, 134–135
- Dispersion modified fiber, 130–135
- Dispersion shifted fiber, 5, 77, 130, 131–135
- Dispersion slope, 129
- Distributed Bragg reflector (DBR) laser, 332–336, 548, 762
- Distributed feedback laser (DFB), 332–336, 341, 355, 548, 684
- Distributed queue dual bus (DQDB) MAN architecture, 843, 844
- Distribution systems, 665–670
- Dome LED, 385–386
- Donor impurity, 297, 303–304
- Donor to acceptor recombination, 304
- Doping
 fluorine, 60
 of semiconductor, 299
- Doppler broadening in laser, 292
- Double-channel planar buried heterostructure (DCPBH) laser, 327, 338
- Double-clad (DC) fiber, 135
- Double eccentric connector, 241–242
- Double heterojunction (DH)
 injection laser, 312–313, 316–321, 364–365
 LED, 384, 385, 387, 389–393, 398
- DPSK field demonstration system, 758–759
- Drift of carriers, 422–423, 431
- Dual fiber cables, 200
- Duplex connectors, 242–244
- Dynamic range, 489
 of receiver, 489, 493, 496, 601–602, 604
- Dynamic single-mode (DSM) laser, 330
- Edge-emitting LED (ELED), 389–393, 675
- Effective group index, 66
- Efficiency
 injection laser, 317–318
 LED, 377–385, 386–387, 396–398, 675

912 Index

- Eigenvalue, 65
- Eigenvalue equation
 - graded index fiber, 54
 - step index fiber, 40-41, 65
- Einstein coefficients, 287-289
- Elastomeric splice, 232
- Electrical bandwidth, 104, 404-407
- Electrical signal to noise ratio, 625-628
- Electroluminescence, 300-302
- Electromagnetic carrier, 2
- Electromagnetic mode theory, 23-36
- Electromagnetic spectrum, 2, 3
- Electromagnetic waves, 2, 23-26
- Electro-optic coefficient, 538
- Electro-optic devices, 535
- Electro-optic effect, 535
- Electro-optical transducers, 866-867
- Electronic repeaters, 677
- Elie rural field trial (Canada), 846
- Emission (see Optical emission)
- Energy band structure
 - $p-n$ junction, 296-299, 306-307
 - semiconductor, 297-299
- Energy gap (see Bandgap energy)
- Energy level systems (lasers)
 - four level, 291
 - three level, 290-291
 - two level, 290
- Energy states (atom), 284-286
- Equalizer, 7, 487-488, 599, 601, 607-609, 618
 - adaptive, 609
 - transversal, 609
- Equilibrium mode distribution, 776-778, 781
- Equilibrium mode simulation, 778
- Equivalent step Index (ESI) fiber, 73-77
- Equivalent step index methods, 73-77
- Error detection, 619-620, 643
- Error function, 624-627
- Error probability (digital), 623-628
- Errors (regenerative repeater), 621
- Ethernet (LAN), 882, 884-885, 889
- Evanescence field, 34-35, 52-53, 73
 - bend loss, 97
- Excess avalanche noise factor, 486-487, 628-629
- Excess loss
 - port coupler, 254
 - star coupler, 259-262
- Excited state absorption (ESA), 526-7
- Expanded beam connectors, 244-249
- External photoemission, 421
- Extinction ratio penalty, 586
- Extrinsic fiber sensors, 872-877
- Extrinsic semiconductor, 297
- Eye pattern, 620

- Fabry-Perot amplifier, 515-517
- Fabry-Perot cavity, 291, 307, 316, 329, 332, 334, 336, 341, 353, 355, 392
 - injection laser, 839
 - resonance 395
- Far field intensity distribution
 - fiber, 777-778, 807-810
 - injection laser, 319, 813
 - LED, 813-814
- Far-infrared transmission, 99-102

- Faraday effect (see Magneto-optic effect)
- Fault location in fiber link, 824
- FDDI (see Fiber distributed data interface)
- FDDI follow-on LAN (FFOL), 891
- Feedback control for injection laser, 595-598
- Fermi-Dirac distribution, 296
- Fermi level, 297-299
 - quasi, 305-306
- Ferrule, 233
 - connector, 238-241
- Fiber amplifiers, 524-530
 - Brillouin fiber, 528-530
 - Raman fiber, 528-530
 - rare earth doped, 526-528
- Fiber distributed data interface (FDDI), 243, 665, 885-891
- Fiber drawing, 162, 165-167
- Fiber fused biconical taper coupler, 253, 254
- Fiber gyroscope, 868
- Fiber lasers, 360-362
- Fiber microbending sensor, 870-871
- Fiber Optic Test Procedures (FOTPs), 775
- Fiber ribbons, 199
- Fiber waveguide (see Optical fiber)
- Fibernet (optical LAN), 884
- Fibrevision network, 846
- Field effect transistor (FET) preamplifiers for receiver, 493-497
- Field measurements on fiber, 817-827
- Filters
 - interference, 782
- First order dispersion parameter, 123, 126
- Flame hydrolysis, 169-171, 176
- Flat cables, 200
- Flexible manufacturing systems (FMS), 894
- Fluoride glass, 14, 100, 176-178
- Fluoride-chloride glass, 100
- Fluorine doping, 60
- Fluorohafnate glass, 100, 176
- Fluoroptic temperature sensor, 875
- Fluorozirconate fiber, 351-352, 364-365
- Fluorozirconate glass, 100, 176-178, 527-528
- Forward biased $p-n$ junction, 299
- Four port couplers, 250, 251-257
- Four-wave mixing 146
- Free space transmission (see Atmospheric transmission)
- Frequency chirping, 340-341
- Frequency division multiplexing (FDM), 612, 655, 760
- Frequency division switching, 540
- Frequency modulation of subcarrier, 612, 658-660, 662-665
- Frequency shift keying, 672, 702-711, 724-726
 - heterodyne detection, 745-746
- Frequency translators, 549-551
- Fresnel reflection, 212-214, 225, 425, 823, 824
- Fringes (interference), 797-798
- Full width half power (FWHP) points, 401, 586
- Fused biconical taper (FBT) coupler, 253-256, 258
- Fusion splices, 228-230

- GaAlAs (see AlGaAs)
- GaAlAsSb/GaSb, 314
- GaAlSb/GaSb, 314-315
- GaAs, 310, 314-315, 330, 410-411, 430
 - adsorption coefficient, 424

- GaAs (*continued*)
 injection laser, 316
 LED, 385–386, 412
 MESFETs, 495–496, 595
- GaAs/AlGaAs, 314–315, 323, 375, 551, 554
 injection laser, 319, 320
 LED, 385, 387, 410–411
- Gain-guided laser, 322–325
- Galile fiber, 102
- Gaussian
 approximation (single-mode fiber), 67–73, 223
 for digital receiver, 622–628
 distribution, single-mode step index fiber, 62, 67
 noise, 623
 probability density function, 623
 pulse response, 903–904
- Germanium (Ge)
 absorption, 424–425
 photodiodes, 422, 425, 432–433, 445–457, 481, 487
- Glass, 14, 88–91, 99–102
- Glass fiber laser, 351–355
- Goos-Haenchen shift, 35
- Graded index fiber, 47–55, 105–106, 116–119, 181–183, 283
 caustic surfaces, 50
 intermodal dispersion, 49, 116–119
 mode cutoff, 52–53
 mode volume, 55
 normalized frequency, 55
 numerical aperture, 50
 optimum profile, 117–119
 parabolic profile, 49–50, 116–117
 partially graded, 183
 propagation constant, 52–54
 Wertz, Kramers, Brillouin (WKB) approximation, 50–55
- Griffith equation for fracture stress of a crack, 188
- Griffith theory for surface flaws in glass, 187–188
- GRIN-rod lens, 252–253, 264–265, 267, 268, 330, 349, 356–357
 tapered, 398
- Group
 delay, 65–67, 107
 index, 30
 velocity, 28–30, 107, 110
- Group-velocity dispersion, 148
- Guard ring structure (APD), 442
- Guide (*see* Waveguide)
- Heavy metal oxide glass, 100
- Helium-neon laser, 290–291, 810
- HEMT preamplifier, 499
- Heterodyne detection, 710
 amplitude shift keying, 742–745
 frequency shift keying, 745–746
 phase shift keying, 746–748
- Heterodyne nonsynchronous detection, 734–735
- Heterodyne synchronous detection, 730–734
- Heterojunction bipolar transistor (HBT), 498
- Heterojunctions, 311–313, 316–317
 anisotype, 313
 double, 312–313, 316–320
 isotype, 311
- Heterostructure (*see also* Heterojunctions), 311
- Hi-birefringence couplers, 256
- Hi-OVIS project (Japan), 863
- High birefringence fibers, 142
- High density bipolar (HDB3) code, 617
- High performance receivers, 497–505
- Holes, 296–297
- Hollow core glass fiber, 102
- Homodyne detection, 708, 710–711, 735–738
 amplitude shift keying, 748–749
 phase shift keying, 748–749
- Homojunction, 311, 314, 316, 433
- Hybrid
 modes (HE, EH), 36–37
 PIN-FET receiver, 495–497
- Hyperchannel, 889
- Impact ionization in APD, 441–443
- Impurity semiconductor, 297, 303–304
- Index-guided laser, 325–328
- Index matching
 fiber joint, 213–219, 241
 light emitting diode, 387
 optical detector, 779–780, 787–788
- Indirect bandgap, 301–303
- Indium antimonide, 561
- Indoor cables, 200
- Industrial applications, 865–866
- Industrial networks, 891–895
- InGaAs/GaSb, 314, 641
- InGaAsP/InP, 315, 334, 433–434, 447, 451, 454, 455–457, 550, 551
 APD, 447–450
 injection laser, 552–553
 LED, 4, 397, 399, 342
 photodetectors, 434, 447–478, 451, 456–457
 $p-i-n$ photodiode, 432, 436, 444–445
 phototransistor, 456–457
- Injection efficiency, 311
- Injection laser diode (ILD), 4, 283, 315 (*see also* Laser, semiconductor)
- Injection locked semiconductor laser, 712
- InP, 447
- InP/InGaAsP, 315
- Insertion loss
 port coupler, 254
 star coupler, 259–262
 WDM coupler, 263
- Integrated optics, 531–537
 devices, 537–551
 beam splitters, 537–542
 bistable optical devices (BOD), 557–562, 568
 COBRA, 539–540
 directional couplers, 537–542
 filters, 546–548
 length (typical), 538
 modulators, 542–546
 stepped delta β reversal coupler, 540
 switches, 537–542
 planar waveguide, 532–537
- Integrated Services Digital Network (ISDN), 849
- Intensity modulation
 analog, 6, 412, 646–647
 digital, 6, 412, 611, 618
- Interference filters, 253, 782
- Interference fringes, 797–798
- Interference microscopes, 796–798

914 Index

- Interferometric sensors, 796–798
- Integrated external cavity laser, 357–360
- Intermediate frequency, 705
- Intermodal dispersion, 46–47, 49, 110–119
 - graded index fiber, 116–119
 - mode coupling, 115–116
 - rms pulse broadening, 113–115, 117–119
 - step index fibers, 46–47, 111–116
- Interoffice network applications, 841–844
- Intersymbol interference (ISI), 102, 619, 620, 633, 638–641
- Intramodal dispersion, 107–110, 123, 128
 - material, 107–110, 123
 - total rms pulse broadening, 121–122
 - waveguide, 110
- Intrinsic fiber sensors, 870–872
- Intrinsic semiconductor, 297, 305
- Ionization coefficients, ratio of, 443, 487
- Isoelectronic impurity, 303–304
- ITT seven fiber external strength member cable, 202
- Jitter, 619, 840
- Johnson noise, 461
- Joint losses, 212–226
 - measurement, 824
 - multimode fiber, 216–223
 - single-mode fiber, 223–226
- Joints, 210–227
 - angular coupling efficiency, 220–221
 - connectors, 237–249
 - lateral coupling efficiency, 217–219
 - signal distortion, 226
 - splices, 227–237
- Junction capacitance, 457, 585
- Junction network applications, 841–844
- Kerr nonlinearities, 147–148
- Kristen 5 (KRS-5) fiber, 102
- Ladder coupler, 260–263
- LAMBDA NET network, 675–676, 851
- Lambertian integrity distribution, 380
- Laplacian operator, 24, 25
- Laser, 2, 4, 6, 281–365, 582–586
 - broadened transition, 292
 - cavity, 291–294
 - double-channel planar buried heterostructure (DCPBH), 327
 - dynamic single-mode (DSM), 330
 - gain-curve, 292, 294
 - gain-guided, 322–325
 - helium-neon, 290–291, 810
 - index-guided, 325–328
 - injection (see semiconductor)
 - modes, 293–295
 - multiquantum-well (MQW), 328–329
 - Nd:YAG, 349–350
 - nonsemiconductor, 290, 349–355
 - nonzero extinction ratio, 586
 - operation of, 284–296
 - oscillation, 291–296, 310
 - threshold condition, 295–296
 - threshold gain, 295–296, 310
 - plano-convex waveguide, 325–326
 - population inversion, 289–291, 295, 305, 307
 - quantum-well, 328–329
 - rib waveguide, 325–326
 - ridge waveguide, 325–326
 - ruby (crystal), 290–291
- semiconductor, 4, 6, 281–284, 306–311, 315–349, 582–586, 621–622
 - analog transmission, 317
 - broad-area device, 318–319
 - buried heterostructure, 327, 347, 393
 - carrier confinement, 311–313, 317, 319
 - characteristics, 336–347
 - coherence, 282, 286
 - continuous wave (CW) operation, 317
 - coupling to fiber, 347–349, 584, 621
 - current confinement, 318–321
 - dark line defects, 347
 - dark spot defects, 347
 - distributed Bragg reflector (DBR), 332–336
 - distributed feedback (DFB), 332–336, 341, 355
 - double heterojunction (DH), 312–313, 316–321
 - drive circuits, 594–598
 - dynamic response, 339–340
 - efficiency, 317–318
 - emission pattern, 319
 - external power efficiency, 318
 - far field intensity distribution, 319
 - feedback control, 595–598
 - frequency chirp, 340–341
 - heterojunctions, 311–313
 - homojunction device, 311, 314, 316
 - kinks, 311, 315, 324
 - light output against current characteristic, 583
 - linearity, 584
 - linewidth, 355–362, 712–713
 - logic interface, 595
 - materials, 313–315
 - mode hopping, 345–346
 - modes, 293–295, 321
 - multimode, 294, 319–321
 - noise, 341–345
 - nonlinearities, 322, 584
 - operational limitations, 583–586
 - output spectrum, 321
 - partition noise, 345
- periodic structures, 546–548
 - radiation confinement, 311–313, 317, 319
 - relaxation oscillations (RO), 341
 - reliability, 346–347
 - rise time, 585
 - single-mode, 283, 321–322
 - stripe geometry, 318–320, 336–339
 - temperature dependence, 584–585
 - threshold current, 309, 313–318
 - threshold current density, 310, 316
 - threshold gain coefficient, 310
- single frequency, 329–336
- single-mode, 321–322, 329–336
- single quantum-well (SQW), 328–329
- Lasing, 291, 294–295, 305–311
 - from semiconductor, 305–311
- Lateral offset fabrication, 251, 252
- Lattice
 - constant (see parameter)
 - matching, 313–315

- Lattice (*continued*)
 parameter, 313-315
- Layered cable, 201
- Leaky modes, 41, 54
- LED (*see* Light emitting diode)
- Light emitting diode, 4, 6, 282-284, 374-413, 503, 582-586, 675
- advantages, 375
 - analog modulation, 375, 399
 - characteristics, 399-412
 - coupling (to fiber), 382-384
 - dark line defects, 410-411
 - drawbacks, 375
 - degradation, 410-412
 - dome, 385-386
 - double heterojunction (DH), 384-385, 387, 389-393
 - drive circuits, 586-594
 - edge emitter, 389-393
 - efficiency, 377-385, 386-387, 396-398
 - injected carrier lifetime, 406
 - Lambertian intensity distribution, 380
 - lens coupling to fiber, 395-398, 584
 - light output against current characteristic, 399-400, 583
 - linearization schemes, 592-594
 - linewidth, 375, 401-404
 - longer wavelength operation, 297, 396, 400, 409-411
 - materials, 375-376
 - modulation, 412-413
 - modulation bandwidth, 375, 404-412
 - nonlinearities, 399-400, 583-584
 - operational limitations, 583-586
 - output, 399-404
 - output spectrum, 401-404
 - planar, 385
 - power, 377-385
 - power coupled (into fiber), 387-389, 620-622
 - quantum efficiency (external), 379
 - quantum efficiency (internal), 378-380, 400
 - radiance, 382-388
 - rise time, 585, 637-638, 654
 - speed of response, 406-411
 - stripe geometry, 389
 - structures, 385-398
 - superluminescent, 393-395
 - surface emitter (Burrus type), 386-389
 - temperature dependence, 404, 584-585
 - transmission factor, 381
- Lightpack cable, 203-204
- Line coding, 617, 641-643
- Linear encoding, 613
- Linearly polarized (LP) modes, 36-43, 56
- Linear retardation (single-mode fiber), 136-138
- Linewidth (optical source), 283, 311, 315, 375, 401-404, 586
- injection laser, 355-362, 712-713
- Liquid phase epitaxy (LPE), 433
- Liquid-phase (melting) techniques, 162-167
- Lithium niobate (LiNbO₃), 535, 536-537, 538
- Littrow mounted grating, 263-265
- Local access network applications, 844-852
- Local area network (LANs), 243, 843, 879-895
- applications, 844-852
 - fiber distributed data interface, 885-891
 - industrial networks, 891-895
- Local oscillator power, 719-721
- Loigic
- emitter coupled (ECL), 590, 595
 - interface (receiver), 588-590, 595
 - transistor-transistor (TTL), 588-590
- Long external cavity lasers (LEC), 356-357, 712-713
- Loose buffer tubes, 199, 201
- Loose tube cable, 201
- Losses (*see* Attenuation)
- Low birefringence fibers, 142
- Macrobanding, 191
- Mach-Zehnder interferometer, 544, 550-551, 684, 726
- Magneto-optic devices, 535
- Magneto-optic effect, 715, 869
- Manchester (biphase) code, 611, 642
- Manufacturing Automation Protocol (MAP), 892-5
- Material absorption losses
- glass, 88-91
 - measurement, 783-787
- Material dispersion, 107-110
- parameter, 108-110, 126
 - rms pulse broadening, 107-109
 - zero point (ZMD), 124-127, 130, 131
- Maxwell's equations, 24, 31, 36, 68
- MCVD technique, 142, 143
- Mean (mean square value) of random variable, 113
- Mean power feedback control (injection laser), 596
- Mechanical splices, 227, 230-235
- Meridional rays, 15-20, 36, 48, 111, 112, 116-117
- MESFET (metal Schottky field effect transistor), 494-495, 497, 551, 552, 554
- Metropolitan area networks (MANs), 844
- Microbend type coupler, 257
- Microbending, 134
- Microbending loss, 99, 191, 192-193, 197
- Microbending fiber sensor, 870-871
- Microcracks in fiber, 187-190
- Microplasmas in APD, 442
- Mid-infrared lasers, 362-365
- Mid-infrared photodiodes, 454-455
- Mid-infrared transmission, 99-102
- Mid-infrared wavelengths, 351
- Mie scattering losses, 94
- Military applications, 859-862
- Miller capacitance in FET preamplifier, 601
- Minority carrier lifetime
- injected, 406-407
 - radiative, 302-303, 311
- MISFET (metal integrated semiconductor field effect transistor), 551, 552
- Mixer-rod coupler, 258
- Modal birefringence (*see* Birefringence)
- Modal noise, 119-121, 141
- Mode
- boundary, 54-55
 - coupling, 43-44, 115-116, 634-635, 775-776
 - in intermodal dispersion, 115-116, 634-635
 - coupling length, 776
 - dispersion (*see* Intermodal dispersion)
 - hopping (injection laser), 345-346
 - mode filters, 776-778
 - patterns, 43
 - planar guide (concept of), 26-29
 - scrambler, 776-778

916 Index

- Mode (continued)**
stripper (cladding), 779
volume, 46, 55
- Mode cutoff**
graded index fiber, 52–53
step index fiber, 41, 46–47
- Mode delay factor**, 67
- Mode-field diameter**, 812–816
- Mode number**, 27–28, 36, 51–55
- Mode partition noise**, 336, 345
- Modes**
cylindrical fiber, 36–43
differential attenuation of, 115
electric field distributions, 27–29, 43
equilibrium distribution, 776–778
exact (step index fiber), 36–38
guided, 26–29, 37, 39–42, 51–55
hybrid (HE, EH), 36–37
laser, 293–295, 321
leaky, 41, 46, 54
LED, 282–283
linearly polarized (LP), 36–43, 121
radiation, 41, 54
second-order, 121
steady-state distribution, 776
transverse electric (TE), 27, 28, 32–43
transverse magnetic (TM), 27, 28, 32–43
- Modified chemical vapor deposition (MCVD)**, 168, 171–174
- Modified Hankel function**, 73
- Modulation**
analog, 6, 413, 611–612, 643–665
direct detection (DD), 412
direct intensity (D-IM), 645–651
double sideband suppressed carrier (DSBSC), 657–658
intensity (IM), 412
pulse, 662–665
pulse amplitude (PAM), 613–615, 662
pulse frequency (PFM), 662–665
pulse position (PPM), 662–663
pulse width (PWM), 662
subcarrier double sideband (DSB-IM), 657–658
subcarrier frequency (FM-IM), 658–660
subcarrier intensity, 654–656
subcarrier phase (PM-IM), 660–662
digital, 6, 613–618, 641–642
index, 646
- Modulation bandwidth**
LED, 375, 404–412
- Modulators**
integrated optical, 542–546
- Moiré fringe modulator**, 874
- Molecular beam epitaxy (MBE)**, 449
- Moments of random variable**, 113
- Monochromator**, 779
- Monolithic integrated optoelectronic repeater chip**, 556
- Monomode fiber (see also Single-mode fiber)**, 45
- MOSFET**, 497
- Multicarrier network concepts**, 760–764
- Multicarrier system**, 760–764
- Multifiber cables for outside plant applications**, 201–202
- Multilayer interference filter**, 266
- Multilevel codes**, 641
- Multilevel frequency shift keying**, 726
- Multimode fibers**
graded index, 47–55, 105–106, 116–119, 121, 181–183, 184, 283
mode equilibrium, 776
modes, 36–43
step index, 36–50, 105–106, 111–116, 121–122, 179–181, 184–185, 283
- Multimode laser**, 294, 319–321
- Multimode propagation effects (fiber)**, 775–776
- Multiple connectors**, 242–244
- Multiplexing**, 413, 612, 616
frequency division (FDM), 612, 655
optical time division (OTDM), 670–671
space division (SDM), 612
subcarrier, 672–674
time division (TDM), 413, 612, 620
wavelength division (WDM), 262–270, 612, 674–677
- Multiplication factor in APD**, 447–448, 453–454, 482–487, 628
- Multiport fiber couplers**, 249
- Multiquantum-well (MQW) laser**, 328–329, 448–450
- Narrow linewidth lasers**, 355–362
- Nd:YAG laser**, 351–352
- Near field intensity distribution**, 799–800, 813
- Near travelling wave (NTW)**, amplifier, 515
- Neodymium laser**, 351–352
- Network terminating equipment**, 846
- Networks**
bus, 849–850, 881, 883–884
industrial, 891–895
local area, 243, 843, 879–895
ring, 844, 883–891
star, 844–847, 883–884
tree, 844
- n-n* heterojunction**, 311–312
- Noise**, 498
dark current, 439–440, 461, 468, 469
figure (amplifier), 478–479
generation-recombination, 461
injection laser, 341–345
Johnson, 461
modal, 119–121, 141
mode partition, 336, 345
polarization modal, 121
quantization, 614
quantum, 469–470
analog transmission, 473–475, 643–646
digital signalling, 471–473, 630–632
injection laser, 627–632
receiver, 475–487, 644–645
APD, 481–486, 627–632
p-i-n photodiode, 440–441, 476–480
p-n photodiode, 476–480
relative intensity (RIN), 343
shot, 469, 473, 476–477, 630
sources in receiver, 476
thermal, 468–469, 477–478, 632, 649–651
- Noise equivalent power (NEP)**, 439–440
- Noise model for travelling wave optical amplifier**, 679
- Nonlinear encoding**, 613–615
- Nonlinear optics**, 94–96
- Nonlinear phenomena**, 145–149
- Nonradiative recombination**, 300, 302, 313

- Nonreturn to zero signalling (NRZ), 104
 Nonzero extinction ratio, 586
 Normalized film thickness, 533
 Normalized frequency, 40-43, 46-47, 55
 Normalized phase change coefficient, 63
 Normalized propagation constant, 41, 42, 64-65, 66
 123
n type semiconductor, 323
 Numerical aperture (NA), 17-20, 22-23, 40, 50, 112,
 180-186, 221-223, 224, 776, 807-810
 definition, 18
 equilibrium mode distribution, 776
 graded index fibers, 50, 807-808
 measurement of, 807-810
 practical fibers, 180-186
 Nyquist rate (sampling), 613
- Open Systems Interconnection (OSI), 880
 Optical amplification, 512-572, 562-563
 Optical amplifiers, 514-572, 563
 applications, 677-686
 Optical attenuation meter, 820-821
 Optical bandwidth, 404-408
 Optical bistability, 557-564
 Optical chopper, 779
 Optical computation, 564-572
 Optical continuous wave reflectometer (OCWR),
 816-817
 Optical detection, 285-286
 Optical detectors, 419-461
 avalanche photodiode (APD), 6, 7, 441-454,
 627-632
 capacitance, 826
 dark current, 425-426, 432-433, 445-447
 device types, 421-422
 germanium (Ge), 422, 425, 432-433
 heterodyne, 710
 homodyne, 708, 710-711
 mid-infrared, 454-455
 noise equivalent power (NEP), 439-440
 photoconductive, 458-461
 phototransistors, 455-458
p-i-n photodiode, 4, 6, 432-435
p-n photodiode, 6, 422-423, 431-432
 quantum efficiency, 426, 433-434, 444-445, 457-458
 responsivity, 427-429
 sensitivity, 423
 silicon (Si), 424, 425
 Optical displacement sensors, 873
 Optical emission
 semiconductors, 296-315
 spontaneous, 284-286, 299-301, 309-310, 374, 385,
 585
 stimulated, 284-295, 305-311, 585
 Optical feedback technique, 503
 Optical fiber
 advantages of, 7-10, 835
 alignment, 212-226
 angular momentum barrier, 41
 attenuation, 4, 9, 13, 85-99
 bandwidth-length product, 106, 179-186, 586
 bend loss, 97-99
 bow tie, 142
 buffer jacket, 180-184, 196-198, 200-203
 cables (*see also* Cables), 186-191
 characteristics (practical), 178-186
 cladding of, 14, 35, 165, 173, 180-185, 810-812
 cleaving, 227-228, 238
 core of, 165, 173, 812
 crack velocity, 191
 critical radius of curvature, 97-99
 dispersion flattened, 5, 77, 130, 134-135
 dispersion shifted, 5, 77, 130, 131-135
 drawing (*see* Fiber, drawing)
 end preparation, 227-228
 far field intensity distribution, 777-778, 807-810
 fracture stress, 187-191
 Fresnel reflection, 212-214
 graded index (*see also* Graded index fiber), 47-55,
 105-106, 116-119, 181-183, 283
 impulse response, 607
 joint losses (*see also* Joint losses), 212-226
 joints, 210-227
 losses (*see also* Attenuation), 179-186
 measurements, 774-827
 mechanical properties of, 187-191
 microbending, 99, 191, 192-193
 multicomponent glass, 163, 167, 179-180
 multimode, cutoff wavelength measurements,
 802-807
 near field intensity distribution, 799-800
 PANDA, 142
 plastic, 185-186
 plastic clad, 184-185
 polarization, 136-145
 polarization maintaining, 716-719
 polarization state, 713-719
 preform, 162, 168-173
 preparation, 161-176
 proof testing, 191
 ray model, 13-23, 27, 44-47, 49-50, 111-117
 requirements of, 161
 scattering losses, 91-96
 signal distortion at joint, 226
 silica rich glass, 167-169, 171-176
 single-mode, 45-46, 183-184, 283
 sizes, 180-185
 splices, 227-237
 spun, 143
 stability of transmission characteristics, 191-196
 step index
 multimode, 36-50, 105-106, 111-116, 121-122,
 179-181, 184-185, 283
 single-mode, 45-46, 57-58, 59-60, 105-106,
 183-184, 283
 strength and durability, 187-191
 stress corrosion, 189-191
 structure, 12-13
 theoretical cohesive strength, 187
 transmission cohesive strength, 187
 transmission characteristics, 191-196
 transmission loss factor (transmissivity), 92
 triangular profile, 47
 types currently available, 178-186
 W, 58-59, 134, 135
 Optical fiber flow meter, 872
 Optical fiber-laser Doppler velocimeter (LDV), 876
 Optical fiber systems, 5-7, 580-686
 Optical fluid level detector, 872-873
 analog, 6, 643-665

918 Index

- Optical fluid level detector (*continued*)
 - block schematic (intensity modulation) 646–647
 - direct intensity modulation (D-IM), 645–651
 - optical power budgeting, 652–653
 - pulse techniques, 662–665
 - quantum noise limit, 650
 - rise time budgeting, 654, 664
 - signal to noise ratio, 644–645
 - subcarrier double sideband modulation (DSB-IM), 657–658
 - subcarrier frequency modulation (FM-IM), 611, 658–660
 - subcarrier intensity modulation (PM-IM), 654–656
 - subcarrier phase modulation (PM-IM), 660–662
 - system planning, 652–654
 - thermal noise limit, 650–651
 - coherent (*see* Coherent optical fiber systems)
 - design considerations, 609–612
 - digital, 6, 613–643
 - bit error rate (BER), 619–620, 626–632
 - coding, 104–105, 611, 641–643
 - dispersion-equalization penalty, 638–641, 643
 - error monitoring, 619–621, 633
 - error probability, 623–627
 - eye pattern, 620
 - information capacity, 641–642
 - intersymbol interface (ISI), 619, 633
 - pulse code modulation (PCM), 611, 613–618
 - regenerative repeater, 618–621
 - redundancy, 641–649
 - safety margin, 638–641
 - synchronization, 616, 641
 - timing, 616, 643
 - digital planning considerations, 618–643
 - channel losses, 632–633
 - line coding, 641–643
 - optical power budgeting, 638–641
 - receiver, 622–632
 - rise time, 635–638
 - signal to noise ratio, 628–632
 - temporal response, 633–638
 - transmitter, 621–622
 - in Europe, 616–617
 - fault location, 822–827
 - generations of, 836
 - modulation choice, 612
 - networks (*see* Networks)
 - in North America, 617
 - repeater, 5, 610, 618–621, 638–639
 - video, 648–650
- Optical mixer, 705–706
 - Optical power meters, 818–820
 - Optical return loss, 816–817
 - Optical sensor systems, 866–877
 - extrinsic fiber, 872–877
 - intrinsic fiber, 870–872
 - phase and polarization fiber, 868–870
 - Optical signal to noise ratio, 626–627
 - Optical sources (*see also* specific types), 2, 4, 6, 281–365, 583–586
 - generations of, 282
 - laser, 2, 4, 6, 281–365, 583–586
 - nonsemiconductor, 349–355
 - semiconductor, 2, 4, 6, 281–284, 306–311, 315–349, 583–586
 - light emitting diode (LED), 4, 6, 282–284, 314, 374–413
 - limitations, 583–586
 - Optical time division multiplexing (OTDM), 670–671
 - Optical time domain reflectometry (OTDR), 822–827
 - Optical transistor (transphosor), 563
 - Optimum profile (graded index fiber), 117–119
 - Optoelectronic devices, 513
 - Optoelectronic integration, 513, 551–557
 - Outside vapor phase oxidation (OVPO), 168, 169–171, 176
 - Overall dispersion in single-mode fibers, 122–130
 - Oxide isolation, 319
 - Packet
 - data group (PDG), 888
 - wave, 29
 - Parabolic profile fiber, 47–49, 54–55, 116–117
 - Parabolic refractive index profile, 71
 - Paraxial ray equation, 247
 - Parity checking, 643
 - Passive optical network (PON), 846, 852
 - Passive Photonic Loop (PPL), 851
 - Peak detection feedback control for ADP, 605
 - Permeability, 25
 - Permittivity, 25
 - Petermann II definition (MFD for single-mode fiber), 63
 - Phase diversity reception, 738–741
 - Phase fiber sensors, 868–870
 - Phase index, 63
 - Phase locked loop techniques, 739
 - Phase propagation constant, 63–64, 65
 - Phase sensitive detection, 779–783, 799–800
 - Phase shift keying, 672, 702–711, 726–728
 - heterodyne detection, 746–748
 - Phase shift on reflection, 26–27, 30–35
 - Phase velocity, 25, 28–30
 - Phonon, 95, 99
 - Photoconductive detectors, 458–461
 - Photoconductive gain, 459–450
 - Photoconductors, 6, 458–461
 - Photocurrent, 427–429
 - Photodetectors (*see* Optical detectors *and* Photodiodes)
 - Photodiodes (*see also* Optical detectors), 4, 6
 - avalanche operation, 441–443
 - capacitance, 437
 - cutoff (long wavelength), 430
 - dark current, 425–426, 432–433
 - depletion layer (region), 422–423, 431–438
 - depletion width, 431
 - detection principles, 285–286, 422–423
 - diffusion of carriers, 436–437
 - drift of carriers, 435–436
 - germanium (Ge), 424, 425, 445–447
 - mid-infrared, 454–455
 - p-i-n* structure, 432–435, 436–437
 - quantum efficiency, 426, 444–445
 - responsivity, 427–429
 - sensitivity, 423
 - silicon (Si), 424, 425, 443–445
 - time constant, 437
 - with internal gain 441–454
 - without internal gain, 430–441
 - Photoelastic pressure sensor, 874

- Photon, 284, 302–303
 Photon density, 309
 Phototransistor, 4, 6, 455–458
p-i-n photodetector, 503
p-i-n photodiode, 6, 432–435, 451–452, 497–8, 503
 operation of, 432
 speed of response, 435–438
 structures, 432–435
 PIN-FET receiver, 719–720
 hybrid receiver, 495–497, 554
 optimization, 497–8, 500
 Planar LED, 385
 Planar waveguide, 26–36, 532–537
 field relations, 902–903
 integrated optics, 532–537
 slab, 532–534, 535
 strip, 535–536
 Planck's constant, 284, 343
 Plano-convex GRIN-rod lens, 398
 Plano-convex waveguide (PCW) laser, 325–326
 Plasma-activated chemical vapor deposition (PCVD),
 168, 174–175
 Plastic-clad fibers, 184–185
 Plastic fibers, 185–186
p-n heterojunction, 311–312, 447
p-n junction, 296–299, 311, 323, 393–400, 434–435
p-n photodiode, 6
 operation of, 434–435
 Polarization crosstalk, 144–145
 Polarization diversity reception, 718–719
 Polarization fiber sensors, 868–870
 Polarization in single-mode fiber, 56, 136–145
 Polarization maintaining fibers, 5, 141–145, 703,
 716–717
 Polarization modal noise, 121
 Polarization mode dispersion, 140–141
 Polarization noise, 827
 Polarization optical time domain reflectometer
 (POTDR), 827
 Polarization scrambler, 718–719, 827
 Polarization shift keying, 705
 Polarization state, 713–719
 Polarization-state control, 715–717
 Polarization transformers, 549–551
 Polymethyl methacrylate fabricated fiber, 185
 Population inversion, 289–291, 295, 305–307
 semiconductors, 305–307
 Port couplers, 251
 Power law refractive index profile, 124
 Power meters (optical), 818–820
p-p heterojunction, 311–312, 385
 Preform (fiber), 162, 168–173, 177–178
 Probability density function (PDF), 623
 Profile dispersion, 118–119, 124
 Profile parameter (graded index fibers), 47
 Proof testing of fiber, 191
 Propagation constant, 25, 37–43, 52–54, 63–64, 65,
 72, 122–123, 136
 normalized, 41–43
 vacuum, 25
 Propagation vector for wave, 25
 Proton bombardment, 319
p type semiconductor, 297–299, 323
 Public network applications, 837–859
 PuEuTe/PbTe DH laser, 363–364
 Pulse amplitude modulation (PAM), 613–616, 662
 Pulse broadening, 102–130
 rms, 107–110, 114–115, 117–130
 temporal moments, 113
 variance, 109, 113
 Pulse code modulation (PCM), 611, 613–621
 30 channel system, 616–617
 Pulse delay from material dispersion, 107–108
 Pulse dispersion, 122–130, 790–794
 Pulse frequency modulation (PFM), 662–665
 Pulse position modulation (PM), 662
 Pulse width (rms), 102–104
 Pulse width modulation (PWM), 662
 Pumping (laser), 290–291
 Quadruple clad (QC) fiber, 135
 Quantization, 614–615
 Quantum efficiency
 injection laser, 303, 311, 313–314, 317–318
 LED, 378–379, 385
 photodiode, 426, 433–434, 444–445
 phototransistor, 457–458
 Quantum limit to detection, 630–632, 650
 Quantum noise, 630–632, 644–645
 analog transmission, 644–645
 digital signalling, 630–632
 Quantum theory, 284
 Quantum-well laser, 328–329, 341
 Quaternary semiconductor alloys, 314–315
 Radiance, 382–388
 Radiation modes, 41, 54
 Radiation-resistant fibers, 195–196
 Radiative recombination, 300–301, 302–304, 313
 Radius of the fundamental mode, 69
 Raised cosine (pulse shape), 629
 Raman fiber amplifier, 514, 528–530, 683–684
 Raman scattering, 95–96, 146–147, 514
 Raman-Nath regime, 545
 Rare earth doped fiber amplifiers, 526–528, 686
 Ray model, 13–23, 27, 45–47, 49–50, 111–117
 Rayleigh scattering, 92–94, 96, 99, 100, 101, 128, 138,
 177, 822, 824
 Raynet fiber bus system, 849–850
 Rays
 meridional, 15–20, 36, 48, 111, 112, 116, 117
 skew, 20–23, 36, 49
 Reach through avalanche photodiode (RAPD),
 443–445
 Reactive atmosphere processing (RAP), 177
 Receiver, 598–609
 analog, 647–652, 656–665
 automatic gain control (AGC), 604–607
 avalanche photodiode (APD), 481–488, 627–632
 block schematic, 598
 capacitance, 480–481
 digital, 622–633
 dynamic range, 601–603, 604
 equalization, 599, 601, 607–609, 618
 high impedance front end, 489, 600–601
 high performance, 497–505
 linear channel, 599
 low impedance front end, 488–489, 600
 main amplifier, 599, 605–606
 noise (*see also* Noise, receiver), 627–632, 644–645

920 Index

- Receiver (*continued*)
 - PIN-FET, 719-720
 - preamplifier circuits, 599-604
 - sensitivity, 638-641, 701, 741-758
 - comparison of, 749-758
 - structures, 487-493
 - transimpedance front end, 489-493, 601-604
- Recombination (carrier), 300, 301-304
- Redundancy in digital transmission, 617, 641-643
- Reference test methods (RTMs), 775, 781, 803-805
- Reflectance, 816-817
- Reflection coefficient, 32-33
- Refracted near field method (RNF), 800-802
- Refraction, 13
- Refractive index
 - definition, 13
 - profile, 45, 48, 118, 180-186, 223, 796-802
 - profile measurement, 796-802
- Regenerative baseband recovery (PFM), 663-664
- Regenerator circuit, 618-619
- Relative intensity noise (RIN), 343-344
- Relative refractive index difference, 18, 40, 47, 112, 114, 220
- Relaxation oscillation (ROs), 339
- Repeater, 5, 610, 618-621
 - analog, 619
 - regenerative (digital), 618-621, 883
 - spacing, 620, 633
- Responsivity (optical detector), 427-429
- Return to zero (RZ), signalling, 104
- Rib waveguide laser, 325-326
- Ribbon fiber cable, 203, 235
- Ridge waveguide laser, 325-326
- RIN value, 344
- Ring networks, 844, 883-891
- Rise time
 - APD, 654
 - injection laser, 585
 - LED, 585, 637-638, 654
 - $n-i-n$ photodiode, 432-435, 633-638
- rms impulse response
 - graded index fiber (multimode), 116-119
 - step index fiber (multimode), 114-115
- rms pulse broadening
 - intermodal dispersion, 112-115, 117-119
 - intramodal, 119, 121-122
 - material dispersion, 107-110
 - total, 121-122, 123
- Sagnac interferometer, 354, 868
- Sampling (of analog signal), 613
- Scalar wave equation, 68-71
- Scattering
 - Brillouin, 95-96, 514, 722-723
 - linear, 91-95
 - Raman, 514, 722
- Scattering loss, 100-102
 - measurement, 787-790
 - Mie, 94
 - nonlinear, 94-96
 - Raman, 95-96
 - Rayleigh scattering, 92-94, 96, 99, 100, 101, 128, 138, 177, 822, 824
- Schottky photodiode, 553-556
- Scrambler (mode), 718-719, 776-778
- Self-electro-optic effect device (SEED), 560, 569-571
- Self phase modulation, 146, 148
- SELFOC, GRIN-rod lens, 248
- Semiconductor
 - alloys (III-V), 314-315
 - APD (*see also* Avalanche photodiode), 6, 7, 826
 - injection laser (*see also* Laser semiconductor), 4, 6, 7, 281-284, 306-311, 315-349
 - LED (*see also* Light emitting diode), 6, 282-284, 374, 413
 - n type, 297-299
 - $p-i-n$ photodiode, 6, 432-435
 - $p-n$ photodiode, 6, 431-432
 - phototransistor, 4, 6
 - p type, 297, 299
- Semiconductor laser amplifier (SLA), 504, 515-524
 - performance, 522-4
 - theory, 518-522
- Semitransparent mirror fabrication, 251, 252
- Shift keying, 672, 702-711
 - amplitude, 702-711, 723-724
 - frequency, 702-711, 724-726
 - phase shift, 702-711, 726-728
- Short and coupled cavity laser, 330-331
- Shot noise, 710
- Signal to noise ratio (SNR) at receiver, 102, 701
- Signals
 - analog, 613, 645-646, 654-663
 - digital, 104-105, 613-617, 618
- Silicon grating, 265
- Silicon junction FET (JFET), 497
- Single frequency laser, 329-336
- Single-mode fiber, 56-77
 - advantages, 59
 - bend losses, 98
 - cross-section, 58
 - cutoff wavelength, 56, 57, 61-62, 76, 98-99
 - depressed-cladding (DC), 60, 61
 - dispersion-flattened, 135
 - dispersion-shifted, 131-135
 - dispersion modified, 130-135
 - dispersion optimization, 60
 - effective refractive index, 63-65
 - equivalent step index (ESI), 73-77
 - Gaussian approximation, 67-73
 - graded index, 57-58, 183-184
 - joint losses, 223, 226
 - matched-cladding (MC), 60
 - material dispersion parameter, 123
 - mode-field diameter (MFD), 60, 61, 62-63, 131, 132
 - mode-field radius, 63
 - overall dispersion, 122-130
 - polarization, 56
 - propagation constant, 63-64, 65, 72, 110
 - rotary splice, 233-234
 - spot size, 62-63
 - step index, 45-46, 57-58, 59-60, 105-106, 183-184, 283
- Single quantum-well (SQW) laser, 328-329
- Single-mode laser, 321-322
 - nonsemiconductor, 349-355
 - semiconductor, 283, 321-322
 - structures, 321-322
- Skew rays, 20-23, 36, 49
- Slotted core cable, 202

- Slotted core ribbon cable, 203
- Snell's law, 13
- Soliton propagation, 149
- SONET, 855-856
- Sources (see Optical sources)
- Space division multiplexing (SDM), 612
- Spatial light modulator, 568
- Speckle patterns, 119-120
- Spectral slicing, 677
- Spectral width (see Linewidth)
- Spectrum
 - electromagnetic, 2
 - extrinsic absorption in silica, 90-91
 - LED (output), 401-404
- Speed of response
 - LED, 406-411
 - photodiode, 435-441
- Splices, 133, 227-237
- Splitting loss (star coupler), 259-262
- Spontaneous emission, 284-286 299-301, 309-310, 374, 385
- Spontaneous lifetime, 287
- Spot size, 69, 71, 72, 223, 806-807
- Springgroove splice, 232, 233
- Star
 - coupler, 250, 251, 258-262, 761, 895
 - network, 665-670, 844-847, 881
- Step index fiber
 - mode cutoff, 41, 46-47
 - modes, 36-43
 - multimode, 36-50, 105-106, 111-116, 121-122, 179-181, 184-185
 - intermodal dispersion, 46-47, 49, 110-119
 - mode volume, 46
 - rms impulse response, 114-115
 - propagation constant, 37-43
 - single-mode (see also Single-mode fiber), 45-46, 105-106, 183-184, 283
- Stimulated Brillouin scattering (SBS), 95, 722
- Stimulated emission, 284-295, 305-311
- Stimulated Raman scattering (SRS), 95-96, 722
- Stokes component, 146
- Stokes shift, 738
- Stress corrosion of fiber, 189-191
- Stripe geometry, 322
- Stripper (cladding mode), 779
- Subcarrier multiplexing, 672-674
- Submerged systems, 852-854
- Surface acoustic wave (SAW), 545
- Surface-emitting LED (Burrus type), 386-389
- Switch delay feedback control (injection laser), 399-340, 585
- Switched star network (SSN), 846
- Switches (integrated optic), 537-542
- Synchronous digital hierarchy, 857
- Synchronous optical network (SONET), 851
- Synchronous payload envelope (SPE), 856-857
- Synchronous transport module (STM), 857-858
- Tapered fiber lenses, 395
- Telephone exchange, 877
- Ternary semiconductor alloys, 314-315
- TE-TM mode conversion, 549-550
- Terbium doped fiber amplifier, 514
- Thermal equilibrium, 289, 296
- Three port couplers, 250, 251-257
- Threshold current density (injection laser), 310, 316
- Time division multiple access (TDMA), 882
- Total internal reflection, 13-16, 30-35
 - critical angle, 15, 18, 20, 22
- Transducers (see Sensors)
- Transfer function, 906-907
- Transimpedance amplifier, 906-907
- Transition rates (between atomic energy levels), 286-287
- Transmission coefficient (fields), 32-33
- Transmission distance, 702
- Transmission factor (LED), 381
- Transmission medium limitations, 721-723
- Transmissivity (fiber), 92
- Transmitted near field, 799-800
- Transmitter, 582-598
- Transverse electric (TE) modes, 27-28, 32-43
- Transverse electromagnetic (TEM) waves, 28
- Transverse magnetic (TM) modes, 27-28, 32-43
- Travelling wave amplifier (TWA), 515-516
- Travelling wave semiconductor laser amplifier (TWSLA), 514, 522-524, 683
- Tree coupler, 260-263
- Tree network, 844
- Triangular profile fiber, 47, 133, 134
- Triple clad (TC) fiber, 135
- Trunk network applications, 837-841
- Unguided modes, 41, 54
- Unguided systems, 2
- V-groove flat chip, 237
- V-groove multiple splice, 236
- V-groove splices, 227, 231-232
- V-grooves, 256
- V number, 41, 57, 58
- Valence band, 296-297
- Vapour axial deposition (VAD), 134, 168, 171, 176
- Vapour phase deposition, 167-176
- Variance
 - pulse broadening, 113
 - random variable, 113, 904-906
 - sum of independent random variables, 119, 905
- Voltage controlled oscillator (VCO), 672, 736
- Von Neumann bottleneck, 564
- W fiber, 58-59, 134, 135
- Wave
 - interference, 26-30
 - plane, 26-28
 - standing, 27
 - transverse electromagnetic (TEM), 28
- Wave equation, 25-26, 30, 37-41
- Wave packet, 29
- Wave propagation vector, 25
- Wave vacuum propagation constant, 25
- Wavefront, 29
- Waveguide
 - cylindrical, 36-47, 47-55
 - planar, 26-36, 532-537
 - propagation losses, 537
 - Waveguide dispersion, 110
 - parameter, 124-126, 130
- Wavelength demultiplexers, 262, 263

www.srinivasitech.com
@srinivasitech

Srinivas Institute of Technology
Acc. No.:14760.....
Call No.:

So,